TNIP1 regulates myddosome dynamics during IL-1β signaling

DISSERTATION
zur Erlangung des akademischen Grades

Doctor rerum naturalium
(Dr. rer. nat.)

eingereicht an der
Lebenswissenschaftlichen Fakultät der Humboldt-Universität zu Berlin

von
Fenja Helga Ursel Gerpott, M. Sc.

Präsidentin
der Humboldt-Universität zu Berlin

Prof. Dr. Julia von Blumenthal

Dekan der Lebenswissenschaftlichen Fakultät
der Humboldt-Universität zu Berlin

Prof. Dr. Dr. Christian Ulrichs

Gutachter/innen

1. Prof. Arturo Zychlinsky, PhD
2. Prof. Dr. Simone Reber
3. Prof. Dr. David Mick

Tag der mündlichen Prüfung: 12.01.2023

Zusammenfassung

Entzündungen sind ein mehrstufiger Prozess des Immunsystems von Säugetieren zur Aufrechterhaltung der Homöostase, der durch das komplexe Zusammenspiel verschiedener Zytokine wie Interleukin 1β (IL-1β) vermittelt wird. Die IL-1β-Signaltransduktion ist für die akute Entzündung von entscheidender Bedeutung, muss aber gleichzeitig streng reguliert werden, da eine veränderte IL-1β-Signalübertragung entweder zu einer Hypo- oder Hyperinflammation führt. Die Bindung von IL-1β an seinen Rezeptor induziert die sequentielle Rekrutierung des myeloiden Differenzierungsgenes 88 (MyD88) und der IL-1-Rezeptor-assoziierten Kinasen (IRAKs) 4 und 1. Zusammen bilden sie einen makromolekularen Komplex, das Myddosom. Daraufhin aktiviert das Myddosom den NF-κB- und den MAPK-Signalweg. Diese Aktivierung wird durch die räumliche und zeitliche Dynamik der nachgeschalteten Signalwegnetze kodiert. Wie setzt das intrazelluläre IL-1β-Signalnetzwerk den extrazellulären Nachweis von IL-1β effizient in eine präzise und angemessene zelluläre Reaktion um? Welche Kontrollmechanismen kommen zum Einsatz, um eine angemessene Antwort zu gewährleisten und eine Hypo- oder Hyperantwort zu verhindern?

Diese Arbeit charakterisiert die IL-1β-vermittelte Signalwegdynamik mithilfe der Immunpräzipitations-Massenspektrometrie (IP-MS). Dazu verwendete ich endogen gen-editierte EL4-Zelllinien mit Fluorophorproteinen an allen Myddosom-Proteinen MyD88, IRAK4 und IRAK1. Mittels statistischer Analysen identifizierte ich das Interaktom dieser Proteine nach 15-, 30- und 60-minütiger IL-1β-Stimulation und untersuchte, wie sich dieses Interaktom im Laufe der Zeit veränderte. Anschließend identifizierte ich mithilfe von Signalwegannotationsanalysen Proteine, die potentiell an der Runterregulierung des IL-1β-Signalwegs beteiligt sind.

Um zu verstehen, wie das IL-1β-Signalwegnetzwerk die Translationsmaschinerie in EL4 Zellen beeinflusst, um eine angemessene Reaktion zu gewährleisten, untersuchte ich außerdem den IL-1β-abhängigen Proteinumsatz. Konkret wandte ich gepulste stabile Isotopenmarkierung durch Aminosäuren in der Zellkultur (pSILAC) in Kombination mit Azidohomoalanin (AHA)-Klickchemie und MS nach 30-, 60-, 120- und 240-minütiger IL-1β-Stimulation an

Das Ergebnis dieser Proteomik-Untersuchungen war die Identifizierung des TNFα-induzierten Proteins 3 (Tnfaip3) interagierendes Protein 1 (TNIP1) als potenziellen Kandidaten für die Herunterregulierung des IL-1β-Signalwegs. Nach IL-1β-Stimulation kolokalisiert TNIP1 mit allen Myddosomen-Proteinen sowie mit Tnfaip3. Diese Deubiquitinase wird ebenfalls zum Myddosom rekrutiert. Mittels CRISPR/Cas9 erzeugte ich eine TNIP1-KO-EL4 Zelllinie. Nach IL-1β-

Stimulation zeigten TNIP1-KO-Zellen vermehrt phosphoryliertes p65, aber verringertes phosphoryliertes JNK sowie eine langfristig verringerte IL-2-Sekretion. Daher ist TNIP1 nicht nur an der Herunterregulierung des NF-κB-Signalwegs beteiligt, sondern aktiviert auch den MAPK-Signalweg.

Summary

Inflammation is a multistep process of the mammalian immune system to maintain homeostasis, mediated by the complex interplay of different cytokines such as interleukin 1β (IL-1β). IL-1β signal transduction is crucial for acute inflammation, but at the same time needs tight regulation as altered IL-1β signaling results in either hypo- or hyperinflammation. IL-1β binding to its receptor induces the recruitment of myeloid differentiation primary response gene 88 (MyD88), IL-1 receptor associated kinases (IRAKs) 4 and 1 sequentially, resulting in a macromolecular complex, called the myddosome. The formed myddosome triggers activation of NF-κB signaling and the MAPK pathways. This response is encoded by the spatial and temporal dynamics of downstream signaling networks. How does the intracellular IL-1β signaling network efficiently convert the extracellular detection of IL-1β into a precise and proportionate cellular response? What control mechanisms apply in order to ensure a proportionate response and prevent a hypo- or hyper response?

This study characterizes the IL-1β mediated signaling dynamics using immunoprecipitation purification mass spectrometry (IP-MS). I used endogenously gene-edited EL4 cell lines that expressed myddosome proteins MyD88, IRAK4 and IRAK1 tagged with genetically encoded fluorescent proteins. Using statistical analysis, I identified the interactome of these proteins, and assayed how this interactome remodeled in time by comparing interactomes generated after 15-, 30- and 60-min of IL-1β stimulation. Next, I identified proteins potentially involved in IL-1β signaling downregulation using pathway annotation analysis.

Further, in order to understand how the IL-1β signaling network affects the translational machinery to ensure a proportionate response, I investigated IL-1β-dependent protein turnover in EL4 cells. Specifically, I applied pulsed stable isotope labeling by amino acids in the culture (pSILAC) combined with azidohomoalanine (AHA)-click chemistry and MS after 30-, 60-, 120- and 240-min of IL-1β stimulation.

The result of these proteomics approaches was the identification of TNFα induced protein 3 (Tnfaip3) interacting protein 1 (TNIP1) as a potential candidate in IL-1β signal downregulation. TNIP1 co-localizes with all myddosome proteins after IL-1β stimulation. TNIP1 also colocalized with the deubiquitinase Tnfaip3, which was also recruited to myddosomes. I generated a TNIP1 KO EL4 cell line using CRISPR/Cas9. After IL-1β stimulation, TNIP1 KO cells show increased levels of phosphorylated p65, but decreased levels of phosphorylated JNK as well as decreased levels of long-term IL-2 secretion. Therefore, TNIP1 is not only involved in downregulatory NF-κB signaling, but activates MAPK pathway.

Content

Figures

Abbreviations

ABIN	A20-binding inhibitor of NF-κB
ACN	Acetonitrile
AHA	Azidohomoalanine
AHD	ABIN homology domain
ATP	Adenosintriphosphate
BMDC	Bone marrow-derived dendritic cell
BMDM	Bone marrow-derived macrophage
bp	Base pair
BSA	Bovine serum albumin
CAA	Chloroacetamide
CAPS	Cryopyrin-associated periodic syndrome
CD	Cluster of differentiation
CHX	Cycloheximide
CRISPR	Clustered regularly interspaced short palindromic repeats
C_t	Cycle of threshold
Cyld	Cylindromatosis
DAMP	Danger associated molecular pattern
dH2O	Distilled water
DMSO	Dimethyl sulfoxide
DNA	Deoxyribonucleic acid
DTT	Dithiothreitol
DUB	Deubiquitinating enzyme
EtOH	Ethanol
EDTA	Ethylenediaminetetraacetic acid
e.g.	Exempli gratia, latin for *for example*
ERK	extracellular-signal regulated kinase
FACS	Fluorescence activated cell sorting
FBS	Fetal Bovine Serum
fwd	forward
gRNA	Guide RNA
EGFR	Epidermal growth factor receptor
GPCR	G protein-coupled receptor
GSDMD	Gasdermin
HEK	Human embryonic kidney
HIV	Human Immunodeficiency virus
HP	High Performance
HRP	Horse Radish Peroxidase
IFS	Immunofluorescence staining
IκB	Inhibitor kappa B
IKK	IκB kinase
i.e.	id est, latin for *that is*
IFS	Immunofluorescence staining
IL…	Interleukin
IL-1RA	IL-1 Receptor agonist
IL-1RAcP	IL-1R accessory protein
IL-1R	IL-1 receptor type
IP	Immunoprecipitation
IRAK	IL-1R associated kinase
JNK	c-Jun-N-terminale kinase

kDa	Kilo Dalton
KO	Knockout
LC	Liquid Chromatography
LPS	Lipopolysaccharide
LUBAC	Linear ubiquitin chain assembly complex
MAPK	Mitogen-activated protein kinase
mAB	Monoclonal antibody
mRNA	Messenger RNA
MS	Mass spectrometry
MyD88	Myeloid differentiation primary response gene 88
NBD	NEMO binding domain
NEMO	NF-κB essential modulator
NF-κB	nuclear factor 'kappa-light-chain-enhancer' of activated B-cells
NLRP3	Leucine rich repeat-containing protein 2
PBMC	Peripheral blood mononuclear cell
PBS	Phosphate-buffered saline
PCR	Polymerase chain reaction
PFA	Paraformaldehyde
PIP2	Phosphatidylinositol 4,5-bisphosphate
PI3K	Phosphoinositide-3-kinase
PMSF	Phenylmethylsulfonyl fluorid
PPAR	Peroxisome proliferation activator receptor
PPI	Protein-protein interaction
PRR	Pattern recognition receptor
pSILAC	Pulsed stable isotope labeling by amino acids in the culture
RAR	Retinoic acid receptor
rev	reverse
RNA	Ribonucleic acid
RIPK1	Receptor-interacting serine-kinase 1
RPMI 1640	Roswell Park Memorial Institute (Cell Culture Medium)
SDS	Sodium dodecyl sulfate
SDS-PAGE	SDS-polyacrylamide gel electrophoresis
SLB	Supported lipid bilayer
ssODN	single stranded oligodeoxynucleotides
TAB	TAK binding protein
TAK	TGFβ activated kinase
Tax1bp1	Tax-1 binding protein 1
TBS	Tris-buffered saline
TFA	Trifluoroacetic acid
TGF-β	Transforming growth factor β
TIR	Toll/IL-1 receptor
TLR	Toll-like receptor
TNF	Tumor necrosis factor
TNFAIP	TNFα induced protein
TNIP	Tnfaip3 interacting protein
TOLLIP	Toll-interacting protein
TRAF6	TNF-receptor associated factor
UBAN	UBD in ABIN proteins and NEMO
UBD	Ubiquitin binding domain
WT	Wildtype

1 Introduction

1.1 Inflammation and the inflammatory cascade

Every day, we are continuously exposed to harmful stimuli such as pathogenic invaders, toxic compounds and tissue injury. To overcome these insults, the mammalian body evolved a complex network of specialized cells and proteins that comprise the immune system. The immune system is a multilayered network that is broadly organized into two branches termed the innate and the adaptive immune system. The innate system comprises germline encoded pattern recognition receptors (PRRs) with the capability to rapidly recognize and respond to alterations in homeostasis by sensing an endogenous or exogenous threat. The adaptive system, on the other hand, relies on unique receptors that are generated via genetic recombination leading in theory to limitless T cell and B cell receptor repertoires that can recognize antigens culminating in the formation of long-term immunological memory[1,2]. Importantly, the functions of both the innate and adaptive system is interdependent. One feature that is connects the innate and adaptive system is the ability to produce proinflammatory mediators. Together, they form a complex immune cascade consisting of harmful stimuli recognition and resolution, a process called inflammation[3]. Within this process, inflammatory cytokines act as important chemical messengers, regulating the inflammatory response by transferring instructions and mediating communication among immune and non-immune cells[4,5].

Inflammation is a multistep process to maintain physiological homeostasis and is essential for mammalian health. Phenotypically, inflammation is accompanied by the following cardinal signs namely *calor* (fever)*, rubor* (redness)*, tumor* (swelling and oedema)*, dolor* (pain) and potentially *function laesa* (loss of function)[6]. Controlled and localized inflammation protects the host and allows for the return to homeostasis by coordinating immune function. However, uncontrolled and chronic inflammation is a major driver of a variety of disease[7]. Therefore, inflammation requires tight spatial and temporal regulation[8].

The inflammatory response is comprised of four universal components: inducer, sensor, mediator and effector. The inducer of inflammation is either exogenous such as pathogens or endogenous such as danger signals from necrotic cells[9]. Specifically, the immune system does not (exclusively) distinguish between self- and non-self, but also recognize whether a given exo- or endogenous signal is pathogenic or non-pathogenic[10]. Exogenous inflammatory inducers of pathogenic origin are termed pathogen-associated molecular patterns (PAMPs). Damage-associated molecular patterns (DAMPs) are of endogenous origin. Both types of stimuli are recog-

nized by corresponding PRRs (sensors). Pattern recognition initiates corresponding PRR intracellular signaling cascades, like the nuclear factor κappa Beta (NF-κB) pathway, or triggers activation of interferon regulatory factors (IRFs), resulting in production and release of mediators[2,11]. Based on biochemical properties mediators are classified into seven groups: (1) vasoactive amines, (2) vasoactive peptides, (3) fragments of complement components, (4) lipid mediators, (5) cytokines, (6) chemokines and (7) proteolytic enzymes. These mediators convey specific cues to the effectors of inflammation, innate and adaptive immune cells. The response to certain mediators such as the (pro-)inflammatory cytokines tumor necrosis factor α (TNFα) or interleukin 1 (IL-1)) are nearly ubiquitous with the most obvious effect: resisting the inflammatory effect and signal elimination. Other mediators elicit adaptive inflammatory effects such as regulation of metabolic functions or homeostasis[3,11,12].

Assessing the four components of the inflammatory response emphasizes that controlled inflammation is dependent on the cooperation of the innate and adaptive immune response[11]. Specifically, this cooperative work is enabled by immune cells 'communicating' with one another most importantly through cytokines[4]. Cytokines are small soluble proteins secreted by all immune cells, with their secretion best characterized for T cells and macrophages[4,13]. Binding to their specific cell surface receptors initiates a broad range of signaling pathways with effects including cell recruitment and differentiation, subsequent waves of cytokine production and healing responses[14]. Based on their ability to drive or inhibit inflammation in the different phases of inflammation, cytokines are categorized as pro- and anti-inflammatory cytokines (Fig. 1)[4,13,15,16]. However, cytokines such as interferon-α, interleukin (IL-) 6 and transforming growth factor (TGF) β show both pro- and anti-inflammatory capacities[4,13]. These contradictory capacities are e.g., due to concentration dependency of the cytokine, cross talk with other signaling pathways activated at the time and available receptors to initiate signal transduction[17,18].

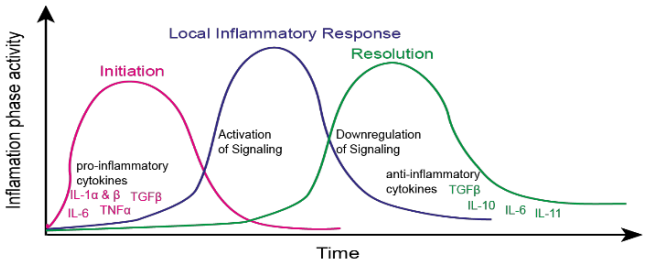

Fig. 1: Acute inflammation consists of three specific phases: initiation, local inflammatory response and resolution. The different phases are accompanied by secretion of distinct pro- and anti-inflammatory cytokines and activation or downregulation of signaling pathways (based on Sugimoto et al., 2016; Schwartz & Baruch, 2014[15,16]).

A complex interplay between cytokines at specific phases of inflammation modulates the corresponding response[4,13]. Accordingly, an imbalance, especially excessive levels of upregulated cytokines and dysregulation in cytokine initiated signaling may lead to significant negative

health impact[5]. Members of the IL-1 cytokine family are highly potent inflammatory modulators with immune-amplifying effects that certainly are necessary for acute inflammation but also require tight regulation to prevent disease development[19,20]. IL-1 is fundamental to initiate inflammation in response to both infection and injury (Fig. 1)[21,22]. Consistent with its pathological association when dysregulated, IL-1 cytokine family member IL-1β has been described as the 'gatekeeper' of inflammation[22].

1.2 The IL-1 cytokine family

The IL-1 cytokine family includes seven pro-inflammatory members (IL-1α, IL-1β, IL-18, IL36α, IL-36β, IL-36y) and four members with anti-inflammatory capacities, namely two receptor agonists (IL-37, IL-38) and two receptor antagonists (IL-1 Receptor antagonist (IL-1Ra), IL-36Ra)[23,24]. However, next to their fundamental properties during inflammation, the IL-1 members are further closely linked to harmful inflammation, more than any other cytokine family. Given the strong inflammatory effect and the link to mediating autoinflammatory diseases IL-1β is the most studied IL-1 family member[23,25].

1.2.1 IL-1: origin and function

IL-1 comprises two forms, IL-1α and IL-1β, which are encoded by different genes, but share biological activities, because they bind the same receptor, IL-1 type receptor (IL-1R1). This receptor binding characteristic is intriguing since the IL-1α and IL-1β only have 27 % of amino acid sequence homology. However, structural resolution of these cytokines revealed a high level of structural similarity[24].

IL-1 activates both innate and adaptive immune cells. IL-1α and IL-1β cause some differing but also overlapping effects, together coordinating local inflammation. While a variety of cell types such as keratinocytes, fibroblasts, hepatocytes, epithelial and endothelial cells produce IL-1α, IL-1β is mostly expressed by myeloid cells. IL-1α induces the early phase of inflammation because of its release by dying cells. In contrast, IL-1β is produced directly at the direct site of inflammation[21,26,27].

1.2.2 IL-1 signal transduction

A variety of different cells express IL-1R1 at the plasma membrane to recognize extracellular IL-1[28]. At first, the IL-1R1 binds IL-1 with nM affinity, and recruits the co-receptor IL-1RAcP to initiate signaling, summarized in Figure 2[19].

Myddosome formation

Upon ligand binding the adaptor protein myeloid differentiation primary response gene 88 (MyD88) interacts with the cytoplasmic Toll/Interleukin-1 receptor (TIR) domain of the IL-1R1, and its subsequent oligomerization recruits and co-assembles interleukin-1 receptor associated kinases (IRAKs) 4 and 1. Together, these oligomerization and interaction events result in a macromolecular complex, called the myddosome[29]. MyD88 interaction with IRAK4 and IRAK1/2 triggers their *trans*-autophosphorylation[30,31].

Formation of the TAB-TAK1-TRAF6 complex

Autophosphorylation of the IRAKs results in the recruitment and activation of the tumor necrosis factor (TNF)-receptor-associated factor 6 (TRAF6). TRAF6 mediated polyubiquitination of IRAK1 recruits TGF-β activated kinase (TAK) binding protein (TAB) 2 or 3, which then activates TAK1. The formed TAB-TAK1-TRAF6 complex transmits the IL-1 signal through two different pathways: IKK-IκB and/or MAPK-JNK/ERK[32–34].

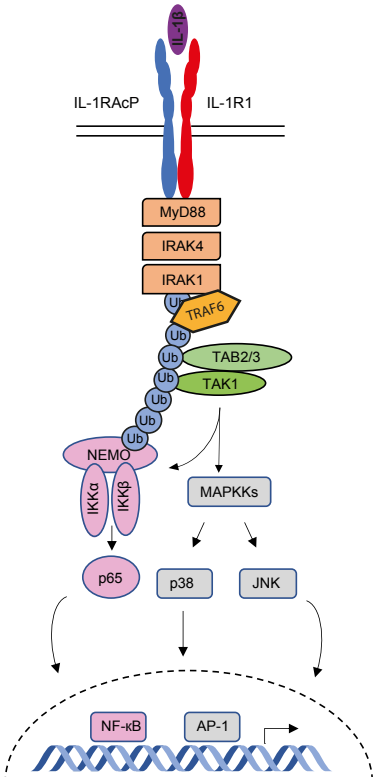

Fig. 2: Overview of IL-1β signal transduction. IL-1β mediated signal transduction is characterized by fast, transient and reversible protein assemblies accompanied by phosphorylation and ubiquitination (based on Courtois et al., 2018[37]).

The IKK-IκB pathway

In the first pathway, TRAF6 ubiquitinates, and thereby activates the NF-κB essential modulator (NEMO, IKKγ) to support the formation of the NF-κB (IκB) kinase (IKK) complex. TAK1 activates the formed IKK complex, consisting of IKKα, IKKβ and NEMO, by serine phosphorylation[35–37]. In turn, the activated IKK-complex phosphorylates IκB[38]. As a consequence, IκB is degraded and NF-κB is released so that it can bind DNA. For nuclear translocation of NF-κB, the IKKβ subunit phosphorylates the NF-κB subunit p65 (also known as RelA) and its associated inhibitory protein IκBα, which is subsequently degraded. The resulting p65-p50 complex translocates into the nucleus for corresponding (NF-κB) gene activation[27,30].

The MAPK-JNK/ERK pathway

In the second pathway, the TAB-TAK1-TRAF6 complex activates the mitogen-activated protein kinase (MAPK) signaling pathway. This conserved signaling pathway consists of three-

tiered kinase cascade, in which one kinase sequentially phosphorylates another. The MAPK kinase kinase (MAPKKK) phosphorylates MAPK kinases (MAPKK), which in turn phosphorylate MAPKs[39]. During IL-1 signal transmission, TAK1 functions as a MAPKKK phosphorylating MAPKKs (MAPKK3, -4, -6, -7) specific for MAPKs p-38, c-Jun N-terminal kinase (JNK) and extracellular signal-regulated kinase (ERK). These MAPKs in turn activate nuclear translocation of c-Jun, c-Fos, and activating transcription factor 2 (ATF-2), turning on transcription of corresponding genes (such as IL-6 and IL-8)[27].

Interplay of the IKK-IκB and MAPK/JNK pathway

Together, these pathways drive the expression of IL-1 target genes including Cox-2, IL-1α & -1β, IL-6, IL-8, IκBa, Mcp-1 and Mkp-1 through post-translational and transcriptional events[27,40]. Yet, the expression of IL-1 target genes cannot always be ascribed to either the IKK-IκB or MAPK-JNK/ERK pathway, because the different signaling routes converge with one another. For example, MAPPK3, usually described as a MAPK-JNK/ERK pathway mediating protein, transmits the IL-1 signal through both signaling routes[41]. Similarly, the IKK complex is not restricted to mediating signal transmission in the IKK-IκB pathway but is also involved in the MAPK-JNK/ERK signaling cascade[42]. Yet, if further proteins are involved in mediating between the different routes is unknown. Do cells receive IL-1 signals through only one route or the other at any given time, or are both routes simultaneously involved? An interesting parallel can be seen in TLR4 activation, where increasing ligand concentration above a threshold leads to a switch from NF-κB to MAPK signaling, but whether this dichotomy also applies to IL-1 stimulation is unknown [43]. Given the myddosome's role as a signaling hub, are those proteins involved in both signaling routes getting recruited to the myddosome? And how do they evolve over time?

In addition, most intracellular components of IL-1 signaling also mediate other cytokine (IL-18, IL-33), Toll-like-receptor (TLR) and cytotoxic stress responses in the same manner. What factors are specific for one pathway is just starting to be investigated[27,44].

Taken together, the IL-1 mediated signaling pathway consists of sequential and reversible post-translational and degradation events that include phosphorylation and ubiquitination of specific proteins resulting in the activation of NF-κB signaling as well as MAPK pathways[27,40]. The ubiquitin system is especially versatile with the capacity for both signal activation and attenuation, and is thus highly important for controlled IL-1 signal transduction[45,46].

1.2.3 Dysregulation of IL-1β signal transduction is associated with the development of severe diseases

Altered IL-1β signaling results in either hypo- or hyperinflammation and is linked to the development of various acute and chronic inflammatory diseases[25,26]. Most of these diseases are accompanied by an overproduction of IL-1β. Therefore, inhibition of IL-1β and the associated signaling pathway are potential therapeutic treaments[47]. For example, blocking IL-1β activity through IL-1β neutralizing antibodies has been shown to reduce disease severity (e.g., Cryopyrin-associated periodic syndrome (CAPS)) with limited side effects[25]. However, for the treatment of other diseases (e.g., myocardial infraction), the application of IL-1β neutralizing antibodies certainly reduced severity but at the same time has further been linked to serious undesirable effects, namely a significantly higher risk for fatal infection and sepsis[48,49]. Why only some patients show severe side effects and others is an open question. Nevertheless, the benefits of IL-1β blockade outweigh the risk and is therefore applied for disease treatment regardlessly[50]. Further, the example of myocardial infraction treatment emphasizes that both excessive and insufficient amounts of IL-1β are deleterious. Besides, the exact mechanisms of IL-1β functions are not completely resolved and thus, methods to rectify dysfunctional IL-1β signaling within distinct inflammatory conditions are of current interest[51]. Elucidating the regulatory mechanisms of IL-1β signal transduction in non-disease conditions would aid the development of drugs that target IL-1β signaling associated diseases or other diseases where inflammation drives pathology such as arthritis or even infectious disease.

1.2.3.1 Molecular regulation of the IL-1β signaling network

Given the high potency of IL-1α and IL-1β (referred to as IL-1 in the following text) to activate inflammation IL-1 activity is regulated at three distinct levels: (1) cellular IL-1 synthesis and release, (2) activation of IL-1 receptors and (3) IL-1 mediated signal transduction downstream the activated receptor[27].

Regulation of cellular IL-1 synthesis and release

The processing and release of IL-1 is tightly controlled and regulated at multiple level. Due to a lack of signaling peptide, IL-1 synthesis occurs in the cytoplasm in contrast to most other cytokines[52]. Pro-IL-1β needs proteolytic maturation for subsequent cellular release and to exert its pro-inflammatory properties. However, proteolytic maturation of pro-IL-1α is not necessarily required to pursue its inflammatory effects. IL-1β maturation is dependent on the canonical inflammasome. The inflammasome is a multiprotein complex and functions as a activation

platform for caspase-1. Inflammasome activation through PAMPs or DAMPs initiates autoproteolytic activation of caspase-1, which then proteolytically cleaves the polybasic motif of pro-IL-1β resulting in mature IL-1β. Thus, mature IL-1β differs from pro-IL-1β in charge, which allows mature IL-1β to localize to phosphatidylinositol 4,5-bisphosphate (PIP2) in the plasma membrane. However, IL-1β secretion requires pores in the plasma membrane. Specifically, active caspase-1 generates Gasdermin-D (GSDMD) pores are generated in PIP2-rich regions of the plasma membrane. Therefore, to facilitate IL-1β secretion active caspase-1 exhibits two different functions: proteolytic maturation of IL-1β and generation of GSDMD pores[26]. Pro-IL-1α does not require proteolytic maturation for activation and subsequent secretion. However, IL-1α maturation results in higher extracellular release and bioactivity[53]. Specifically, the proteases calpain, chymase, elastase, granzyme B or also caspase-1 may cleave pro-IL-1α into IL-1α[54]. While caspase-1 activity is not necessary for IL-1α maturation, caspase-1 dependent GSDMD formation is required for both IL-1α maturation and IL-1α secretion[53].

The importance of regulating IL-1 processing and release is highlighted by the development of autoinflammatory disease in case of both gain and loss of function mutations in inflammasome proteins. As such, CAPS (section 1.2.3) is caused by a mutation in nucleotide-binding oligomerization domain (NOD), leucine rich repeat (LRR)-containing protein 3 (NLRP3) causing an overactivation of caspase-1 and subsequent IL-1β maturation and release[55]. Besides, upon inflammasome activation bone marrow-derived macrophages (BMDMs) or dendritic cells (BMDCs) from caspase-1 deficient mice are not able to secrete IL-1β or undergo pyroptosis[56]. Similarly, IL-1α & -β is not released in cells that lack GSDMD pores[53,57]. Taken together, processing and release of especially IL-1β is dependent on several different steps to ensure a controlled IL-1 release[26]. However, given caspase-1 involvement in other processes than IL-1β release, such as cell death, cytoskeleton organization and metabolism, therapeutic targeting of caspase-1 or its activators for the treatment of IL-1β mediated disease is controversial[58].

Regulation of IL-1R1 activation

The second level of IL-1 regulation occurs at IL-1R1 activation. Firstly, another ligand IL-1 receptor antagonist (IL-1RA) also binds to IL-1R1 with comparable affinity and specificity but without receptor activating properties. Therefore, IL-1RA competes with IL-1 for IL-1R1 binding, restricting IL-1R1 activation. Secondly, for sufficient IL-1 signaling initiation, IL-1R1 must dimerizes with IL-1RAcP (section 1.2.2)[27,59]. However, this co-receptor is shared with other IL-1 family receptors, and is specifically necessary for IL-18 and IL-33 signal initiation. Therefore, competition with other IL-1 receptors (IL-18R & IL-33R) for the co-receptor re-

stricts its availability to IL-1R1 for subsequent dimerization and intracellular IL-1 signal initiation[60]. Thirdly, IL-1 also binds to type II IL-1 receptor (IL-1R2). This receptor acts as a decoy receptor, sequestering IL-1 without transmitting IL-1 mediated signaling. IL-1R2 bound to IL-1 results into a non-active ligand-receptor complex, thereby sequestering IL-1 away from IL-1R1. Together, these features regulate IL-1 activity through competition with other ligands, receptors or inefficient signal transduction[27,59].

Lastly, endocytosis of the IL-1 receptor complex following activation regulates IL-1R activation[61]. Endocytosis is the cellular process of macromolecule uptake by plasma membrane invagination[62–64]. Endocytosis of the signaling receptor limits the available number of receptors on the cell surface that can be activated. Examples of this regulatory property come from studies on TGFβ or G protein-coupled receptor (GPCR) mediated signaling pathways where receptor endocytosis terminates signaling[65]. IL-1R1 is also internalized within 60-120 min after IL-1 stimulation for signal termination[61]. Intracellularly, ubiquitin receptor Toll-interacting protein (Tollip) recognizes ubiquitinated IL-1R, targeting IL-1R1 to endosomes that fuse with lysosomes, where IL-1R1 is subsequently degraded[27,61]. However, IL-1R1 degradation in fibroblasts and the T cell lymphoma line EL4 only starts as late as 4 h post stimulation, suggesting that other regulatory signaling events may be occurring at the endosome level before IL-1R1 is degraded[61]. Further, signaling events at the endocytosed ligand-receptor complex may not be exclusively signal terminating but also propagating. For example, the endocytosed epidermal growth factor receptor (EGFR) improves cell survival by activating the phosphoinositide-3-kinase (PI3K) serine/threonine kinase (Akt) pathway[66]. Whether signaling events at the endocytosed IL-1R1-ligand complex are signal activating or attenuating remains unknown. Taken together, endocytosis of activated IL-1R1 is involved in signal termination, but both receptor endocytosis and subsequent degradation occur long after stimulation and at different time points while its signaling capacity within endosomes remains unknown. These observations emphasize that other, more rapid regulatory mechanisms must apply in order to negatively regulate IL-1β signal transduction.

Regulation of IL-1 mediated signal transduction downstream the activated receptor

The third and last level of IL-1 activity regulation is IL-1 mediated intracellular signal transduction. Different proteins that negatively regulate IL-1b signal transduction at the post translational level have been identified [27,28]. As such, Tollip does not only direct the IL-1R1-ligand complex to the endosome, but is also believed to inhibit IRAK1's kinase activity, consequently blocking further IL-1β signal transduction [67]. However, Tollip's inhibitory function only applies

under strong inflammatory conditions. Under low dose conditions, Tollip translocates to mitochondria, thus precluding its mediation of IL-1R1 fusion with lysosomes[68]. In an IL-1β stimulation setting, Tollip deficient mice did not show a difference in NF-κB and MAPK activation compared to WT mice, but had a reduced production of proinflammatory cytokines[69]. In light of these different phenotypes, I summarize that Tollip modulates inflammation, but does not necessarily negatively regulate Il-1β signal transduction[68,69].

Furthermore, IL-1β signaling is negatively regulated via specific types of proteins and their enzymatic activity. Specifically, alternative splice variants of MyD88 and IRAK1 are shorter, and are recruited to the activated receptor, but are not able to transmit further signaling events, which may serve to dissipate pathway activation. Another IRAK, IRAK-M, is kinase dead and competes with IRAK1 during myddosome formation during TLR4 activation[27,28]. IRAK-M may additionally play an important scaffolding role in recruiting other proteins that might be involved in signal downregulation[27,28].

IL-1β signaling also initiates its own negative feedback. For example, MAPK p38 phosphorylates TAB1, which in turn inactivates TAK1 leading to a disruption of the TAB-TAK1-TRAF6 signaling complex thereby preventing further IL-1β signal transducing protein recruitment. As described in 1.2.2 MAPK p65 induces the transcription of NF-κB genes. These genes include the IκBa gene, which in turn gets transcribed and translated. Synthesized IκBa binds NF-κBα subunit p65, preventing NF-κB complex formation and signaling. Another NF-κB induced gene is MAPK phosphatase 1 (MPK1). MPK1 inactivates MAPKs through dephosphorylation[27].

To conclude, this signal system is based on conserved mechanisms that include fast, transient or stable and reversible multiprotein complex assembly governed by posttranslational modifications that can lead to stabilization or degradation of proteins and protein complexes[27,32]. Its activation in line with different phosphorylation (section 1.2.2) and ubiquitination events (section 1.2.3.2) has been extensively studied. However, compared to signal activation negative regulation of IL-1 signal transduction remains largely understudied.

1.2.3.2 The ubiquitin system is a master regulator in IL-1β signal transduction

Ubiquitin is an approximately 8.5 kDa protein post-translationally added to target proteins, thereby affecting a variety of cellular processes such as cell division, movement, apoptosis and different signaling pathways[33,45]. The process of adding ubiquitin to target proteins is termed ubiquitination and is mediated by the ubiquitin system. This intracellular protein modification pathway for cytosolic, membrane localized and nuclear proteins consists of three specific biochemical steps, requiring ubiquitin and the three ubiquitin enzymes E1, E2 and E3. First, the

ubiquitin activating enzyme E1 catalyzes the ATP-dependent transfer of ubiquitin to itself, thereby activating ubiquitin. In the next step, the ubiquitin thioester-linked ubiquitin to E1 is transferred to a cysteine residue of the ubiquitin conjugating enzyme E2. Finally, this E2-bound ubiquitin is transferred to the target protein, mediated by the ubiquitin ligase E3[33,46].

A variety of proteins are ubiquitinated including ubiquitin itself, generating poly- and linear ubiquitin chains. Polyubiquitin chains are linked by at least one of the seven ubiquitin lysine residues (K6, K11, K11, K27, K29, K33, K48, K63). This results in a variety of possible linkages in polyubiquitin chain formation. K63 polyubiquitin chains are especially important in cell signal transduction independent of the proteasomal pathway and are further involved in DNA repair as well as protein trafficking[33,45,46]. In contrast, linear ubiquitin chains are linked at the N terminus of ubiquitin and also referred to as M1-linked ubiquitin chains[45,46]. Linear ubiquitin chains are involved in NF-κB activation and cell survival[70].

E3 ligases hydrolyzing K63- and M1-ubquitin chains are essential activators IL-1β signal transduction

Both M1 and K63-ubiquitin chains assembled by different E3 ligases mediate IL-1β signal transduction (Fig. 3). After myddosome formation, the E3 ubiquitin protein ligase TRAF6 together with the E2 ubiquitin-conjugating enzyme complex consisting of ubiquitin-conjugating enzyme 13 (Ubc13) and ubiquitin-conjugating enzyme variant 1A (Uev1a) catalyzes the formation of K63-chains on itself and phosphorylated IRAK1. IRAK1 and 4 phosphorylate, and thereby activate, the E3 ubiquitin ligases Pellino 1 and 2, which in turn also bind K63-ubiquitin chains to the myddosome[71,72]. K63-chains are bound by NEMO and TAB2/3, leading to IKK-complex and MAPKK4 and -7 activation[72]. Further, K63-chains are bound by the linear ubiquitin chain assembly complex (LUBAC). This heterotrimeric complex exerts a unique E3 ubiquitin ligase function, catalyzing M1-ubiquitin chain formation. K63- and M1-chains are covalently attached to each other, resulting in K63/M1-linked hybrid chains[73]. M1-chains are also recognized by NEMO, with a 100x higher binding affinity than the K63-chains, but do not ac-

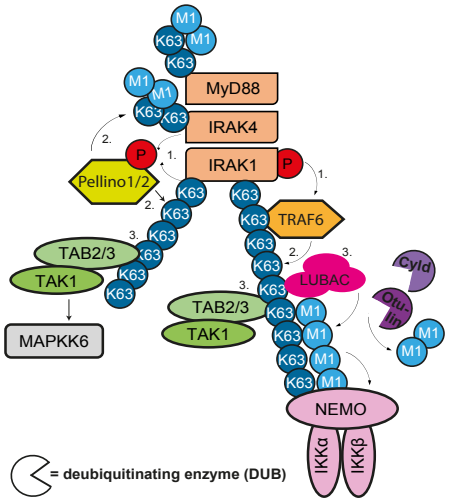

Fig. 3: Addition and cleavage of IL-1β mediated ubiquitination occurs in a distinct stepwise manner and is tightly regulated. TRAF6, Pellino1/2 and LUBAC ubiquitinate the IL-1β mediated signaling machinery. Deubiquitinases (DUBs) cylindromatosis (Cyld) and Otulin hydrolyze M1-linked ubiquitin chains.

tivate p38 and JNK activation[72]. Therefore, the proceeding signaling events formed via K63/M1-linked hybrid chains prevent TAK1 and NEMO recruitment to the same complex, since TAB2/3 binds K63-chains thereby recruiting and activating TAK1 and NEMO binds M1-chains. Prevention of corecruitment of TAK1 and the IKK complex facilitates TAK1-dependent activation of IKKα and -β[73].

Taken together, IL-1β signaling induced ubiquitination of different moieties is mandatory for controlled IL-1β signal transduction[46,72]. Nevertheless, the different ubiquitin chains only mediate the signal. The actual signal transmitting function is executed by ubiquitin binding proteins, binding to the specific binding surface of ubiquitin chains[45]. Several ubiquitin binding proteins involved in IL-1β signal transduction have been identified[46,72]. Yet, especially given the highly dynamic nature of ubiquitination in the myddosome, the recruitment kinetics of ubiquitin binding proteins remain mostly unknown[74]. Which ubiquitin binding proteins come first and when are they getting recruited? Do they bind to all myddosome proteins or to just one? A precise characterization of ubiquitin binding proteins recruited to the myddosome might reveal unknown functional links between IL-1β signaling and the ubiquitin system.

Degradation of ubiquitin chains can limit or terminate IL-1β signal transduction

M1-linked ubiquitin chains do not exclusively trigger signal transduction, but also facilitate signal inhibition. Specifically, the deubiquitinases (DUBs) cylindromatosis (Cyld) and Otulin bind to formed LUBAC. They hydrolyze M1-linked ubiquitin chains from their substrates, which limits or terminates IL-1β signal transduction (Fig. 3). Therefore, one single multi-enzyme complex catalyzes M1-linked ubiquitin chain formation and destruction[72].

While Cyld and Otulin activities are dependent on IL-1β induced LUBAC formation, the DUB TNFα induced protein 3 (Tnfaip3), also known as and further referred to A20, is dependent on A20-interacting proteins (Fig. 4). These accessory proteins are ubiquitin-binding proteins, thereby linking A20 to its substrate by acting as a binding domain that recruits A20. Linked to its substrates, A20 hydrolyzes IL-1β induced activating K63- and M1-linked ubiquitin chains[75]. In IL-1β mediated signaling, A20 cleaves signal activating ubiquitin chains from TRAF6 and/

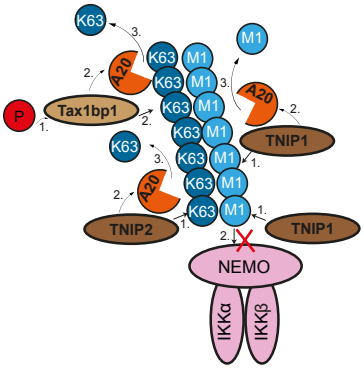

Fig. 4: A20 deubiquitinating function is facilitated through interaction with phosphorylated Tax1bp1, TNIP1 and TNIP2.

or NEMO, thereby restricting initiation of further downstream NF-κB signaling. A20's importance in regulating NF-κB signaling is underpinned by the fact that A20 deficiency in mice and various cell types results in exaggerated NF-κB signaling[76]. Therefore, characterizing the different mechanisms of how the different A20 accessory proteins regulate A20's function will shed light on A20's substrate specificity and regulation[77]. Accordingly, the different characteristics of A20's accessory proteins and A20 will be addressed in the next section.

1.2.3.3 A20's deubiquitinating activity is dependent on and regulated by different accessory proteins

The exact molecular mechanism of how A20 facilitates NF-κB inhibition is unknown. Nevertheless, characterization of A20's different accessory proteins has shed some light on A20's mechanism[76,78]. As such, phosphorylated Tax-1 binding protein 1 (Tax1bp1) facilitating A20 binding to K63-ubiquitinated substrates (Fig. 4)[78]. Specifically, the IKKα subunit of the IKK complex phosphorylates Tax1bp1 thereby initiating A20 binding [79]. Therefore, IL-1β signal transduction induces its own regulation by inducing Tax1bp1 phosphorylation for subsequent K63-deubiquitination by A20[78,79].

Further, given their ability to bind A20 and promote A20-dependent NF-κB inhibition Tnfaip interacting protein 1, -2 and -3 (TNIP1, -2 and -3) comprise the A20 binding inhibitor of NF-κB (ABIN) protein family[80]. Tnip2, also known as ABIN2, mediates NF-κB inhibition through binding to K63-linked ubiquitin chains and A20[78,81,82]. Intriguingly, Tnip2 is also able to activate Ikkα-mediated NF-κB transcriptional activity and thus exhibits dual functionality by acting as both a positive and negative regulator of the myddosome[83]. A20's deubiquitinating function is further promoted by Tnip3, also known as ABIN3. However, Tnip3's interacting mechanism and specific function with A20 in IL-1β mediated signaling remains elusive[84]. TNIP1, also known as ABIN1, facilitates A20 binding to M1-ubiquitinated proteins like NEMO[85]. In this setting, TNIP1 also binds to NEMO, bringing ubiquitinated NEMO and A20 in direct proximity to promote A20 mediated de-ubiquitination. Another model for TNIP1-dependent NF-κB inhibition is A20-independent and implies that TNIP1 competes with other proteins binding ubiquitinated NEMO, therefore preventing the recruitment of signal transmitting proteins downstream of NEMO[84]. To summarize, the exact mechanisms on how TNIP1 (1) regulates A20 activity and (2) inhibits NF-κB activation is not clear. The current knowledge of the relationship between A20 and TNIP1 are based on TNF-R and TLR signaling[84,86]. Therefore, TNIP1's function in IL-1β mediated signaling requires further clarification.

1.2.3.4 TNIP1 is a hub protein that is associated with autoimmune diseases

Compared to TNIP1's protein family members TNIP2 and TNIP3, TNIP1 is involved in various different contexts, dependent and independent from A20[86]. Investigation of TNIP1 mRNA expression levels identified a largely global expression profile in human tissues with high TNIP1 expression levels in skeletal muscle, peripheral blood, lymphocytes, hematopoietic cells and spleen. A long with the association of identified TNIP1 mutations and autoimmune diseases as well as inflammatory disorders, TNIP1 is thought to exert an important function in immune homeostasis[84,87].

Expression of TNIP1 results in two main isoforms (TNIP1α and TNIP1β), encoding 72 and 68 kDa proteins respectively. While the human isoforms differ at their C-termini, the N-termini in murine isoforms differ[88]. The differences in C- and N-termini have not been investigated. The dominant expressed TNIP1 isoform in peripheral blood mononuclear cells (PBMCs) of healthy donors is TNIP1α[89].

TNIP1 is mostly known and characterized for its NF-κB inhibitory function in T-cell receptor (TCR)/CD28, TLR, CD40, TNF-, IL-17 and partly in IL-1α mediated signaling[87,90–93]. However, our knowledge about its specific function and characteristics in IL-1β mediated signaling is limited. Initially, TNIP1 was identified as a Human Immunodeficiency virus type 1 (HIV-1) protein Nef interacting protein, therefore first named Nef-associated factor 1 (Naf1)[94] and further interacts HIV matrix[95]. These interactions suppress HIV-1 replication[96]. In the following years, TNIP1 was described as cytoplasmic and nuclear protein further interacting with a variety of different proteins such as ERK2, ligand-bound peroxisome proliferation activator receptors (PPARs), retinoic acid receptors (RARs), NEMO, HDAC1, NLRP10, Tax1bp1, OPTN and others[87,97–103]. Given TNIP1's diverse, not necessarily A20-dependent nature, TNIP1 has been defined as a hub protein, because of its number of protein interactions (≥ 10 proteins) and its involvement in protein-protein interaction (PPI) networks[104,105]. TNIP1's importance is emphasized by its inhibitory function on NF-κB and receptor-interacting serine-kinase 1 (RIPK1)-mediated necroptosis upon TNFα stimulation. TNIP1 may also be involved in a variety of cellular processes and is further emphasized by high lethality of TNIP1$^{-/-}$ mice[87,106].

So far, five functional domains of TNIP1 have been described (Fig. 5). Four of these are shared homology regions with the two other A20 binding proteins Tnip2 and Tnip3 (section 1.2.2.2), namely the 'A20 binding inhibitor of NF-kB (ABIN) homology domains' (AHD) 1-4. While AHD1 directs A20 binding and AHD2 NF-κB inhibition, AHD3's and AHD4's functions remain elusive. Based on AHD2's ubiquitin binding capabilities, this domain is also referred to

as ubiquitin binding domain (UBD). In close proximity of AHD2, TNIP1 further contains a C-terminal NEMO binding domain (NDB). Together, AHD2 and the NBD comprise the 'UBD in ABIN proteins and NEMO' (UBAN). Together, the AHD1 and UBAN are involved in TNIP1's NF-κB inhibitory function[87,88].

The mechanistic understanding of TNIP1 in signal transduction is based on studies investigating TNFα mediated signaling. TNFα stimulation induces the formation of the TNF-R-signaling-complex (TNF-R-SC), which then recruits RIPK1. Both, the TNF-R-SC complex and bound RIPK1 are ubiquitinated. First, the formed TNF-R-SC activates the E3 ubiquitin ligases cellular inhibitor apoptosis protein 1 and 2 (cIAP1/2), subsequently mediating K63-ubiquitination of RIPK1. K63-linked ubiquitin chains are then recognized by LUBAC, catalyzing M1-linked ubiquitin chain formation[107]. TNIP1 binds M1-linked ubiquitin chains, specifically through AHD2. Next, TNIP1's AHD1 mediates A20 recruitment. Subsequently, A20 deubiquitinates K63-linked ubiquitin chains bound to RIPK1, permitting further downstream signal activation[106].

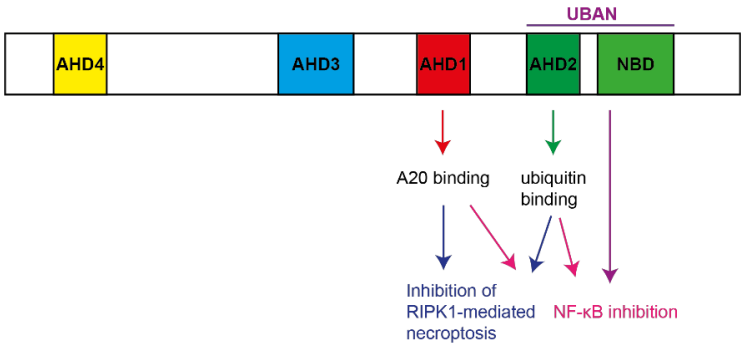

Fig. 5: Gene domains of TNIP1 comprises A20 binding inhibitor of NF-κB homology domains 1-4 (AHD1-4) and a NEMO binding domain (NBD). AHD1 directs A20 binding. AHD2 binds ubiquitin. AHD2 and NBD comprise the 'UBD in ABIN proteins and NEMO' (UBAN), involved in NF-κB inhibition (based on G'sell et al., 2015[87]).

TNIP1 mutations strongly correlate with the development of psoriasis, psoriatic arthritis, systematic lupus erythematosus (SLE) and systemic sclerosis (SSc). Intriguingly, most disease-associated TNIP1 mutations are not located in its ubiquitin binding domain (UBD), but in intronic regions, up- or downstream of TNIP1 coding regions, implying an interference with TNIP1 transcription or alterations at the RNA level. This observation raises the hypothesis that a threshold of TNIP1 expression level is required to prevent autoimmunity[87,88].

Interestingly, TNIP1 expression varies between cell types and is also differently regulated depending on the stimulated receptor[87]. While TNIP1 mRNA level is increasing after IL-36-, IL-1β-, TNF- and CD40-stimulation, TNIP1 protein is degraded upon TLR4 and IL-17 stimula-

tion[90,92,108–110]. However, investigations of changing mRNA expression levels do not necessarily reflect actual protein level changes[111]. Therefore, TNIP1's actual protein levels upon IL-36-, IL-1β-, TNFα- and CD40-stimulation is not based on evidence at the protein level[84,87]. Yet, changes in protein level are directly required for its ability to regulate signaling transduction [112]. Taken together, given TNIP1's link to autoimmune diseases, its important NF-κB inhibitory role, but differing regulatory features of TNIP1 depending on the stimuli, further characterization of TNIP1 might enable to develop more selective therapeutic strategies by understanding the basic biology of this protein[84,87].

1.3 Feedback mechanisms of IL-1β mediated signaling

In IL-1β signaling, most research has focused on IL-1β mediated signaling events as a series of more or less linear interaction responses[19]. However, cell signaling is more complex[113]. Cell signaling enables a cell to react to its environment by receiving and processing intra- and extracellular information to execute a precise response[114]. These signaling pathways influences different cellular systems including the transcriptional, translational as well as metabolic networks, mechanotransduction and others[111,115,116]. Thus, disruptions in cell signaling can affect many other systems within the cell indirectly. The cell must therefore be able to reset or readapt after stimulation, which is necessary to react or not react to subsequent receptor engagement events. Specifically, signaling feedback control mechanisms allow the adaptation to changing conditions and re-achieving homeostasis[117].

Conclusively, an understanding of IL-1β mediated signaling as a stepwise process ignores the high interaction complexity with other interaction networks[19,113]. As such, investigated control mechanisms are limited to endocytosis of the activated receptor and negative-feedback loops (section 1.2.3.5)[27,32]. How IL-1β mediated signaling influences other cellular system and in how far this influence affects the cell as a whole remain unknown. However, understanding the connection of IL-1β signal transduction and with different cellular systems might help to elucidate further (more systems wide) IL-1β signaling feedback mechanisms, which might influence the design of therapeutic strategies to target IL-1β signaling associated diseases.

For example, numerous investigations highlight how immune cell activation connects to alterations in intracellular metabolism. Immune cell activation through TLRs, TCR/BCR or IL-2 receptor (IL-2R) results in a drastic increased energy demand to fulfill immune cells' functions (e.g. cell proliferation or migration). These functions require a metabolic switch in immune cells, which is provided by receptor activation induced reprogramming towards glycolytic gene expression. Specifically, receptor-based initiation of kinase signaling maintains glucose uptake

and glycolysis, promotes *de novo* synthesis of lipids, cholesterol, fatty acids, as well as proteins and lastly induces anaplerosis. Characterizing the connection between cell signaling and immunometabolism allowed the design of anti-inflammatory therapies targeting the metabolism, e.g. the development of metformin for the treatment of type 2 diabetes[115].

Immunometabolism is only one example how immune cell activation connects to other cellular networks. Understanding these connections may lead to the development of disease treating therapies. In the context of inflammation, IL-1β mediated signaling has been shown to enhance skin wound healing after re-experiencing inflammation in mice, empathizing the importance of IL-1β mediated signaling in trained immunity[118,119]. Contradictory, re-stimulating cells (murine fibroblasts) after 3 h with IL-1β results in lower NF-κB activation[120]. Both observations emphasize that IL-1β mediated signaling influences other cellular systems, but further IL-1β dependent extents and molecular mechanisms remain elusive.

1.4 Aims of the study

This thesis aims to characterize the temporal IL-1β signaling dynamics using non-biased approaches. Specifically, this thesis consists of three aims: (1) temporally resolving the interactome of the IL-1β activated myddosome to subsequently identify potential proteins down-regulating IL-1β signal transduction, (2) investigating degraded and *de novo* synthesized proteins that occur in response to IL-1β stimulation followed, again, by the identification of potential proteins down-regulating IL-1β signal transduction and (3) characterizing TNIP1, identified in both previous approaches and previously linked to signaling downregulating capacities, at the different temporal steps in IL-1β signal transduction.

2 Results

2.1 Temporal resolution of the myddosome protein network upon IL-1β stimulation

This part of the project sought to characterize the myddosome interactome using an immunoprecipitation and mass spectrometry (IP-MS) approach. To gain a complete picture of this interactome, I assayed interactors of all three myddosome proteins (MyD88, IRAK4 and IRAK1) at different time points post IL-1β stimulation. I hypothesize that analysis of this interactome will generate a data set that will 1) reveal new myddosome associated signaling effectors, and 2) reveal when, relative to know effectors, these new interactors are recruited to the myddosome. Finally, I predict this approach will generate time-resolved system-wide interactomes of IL-1β-myddosome signaling, which will lead to new insights and hypotheses and mechanistic details for how this critical signaling transduction pathways is temporally regulated.

2.1.1 Development of a workflow of immunoprecipitation (IP) coupled to MS for identifying the temporal dynamics of proteins interacting with the myddosome following IL-1β stimulation

In order to determine the temporal dynamics of myddosome interacting proteins, I choose EL4.NOB1 cells (further referred to as EL4 cells), being highly responsive to IL-1. EL4 cells are murine T lymphocytes selected for high expression of IL-1R. Given their high responsiveness to IL-1 using EL4 cells allows to resolve the myddosome interaction network with high resolution[121].

To immunoprecipitate all three myddosome components, I used CRISPR/Cas9 edited EL4 cell lines expressing C-terminal tagged MyD88, IRAK4 and IRAK1 from the endogenous gene loci (described in Deliz-Aguirre et al., 2021). We had previously determined that these fluorescent proteins form myddosomes. Specifically, MyD88 was tagged with enhanced GFP, IRAK4 and IRAK1 were tagged with red fluorescent protein mScarlet-I. While the MyD88-GFP cell line was single edited, the IRAK4/1-mScarlet cell lines were double edited also expressing MyD88-GFP[122]. I choose fluorophore tags over shorter epitope tags, because fluorescent proteins can be used for both IP-MS and microscopy.

To generate an IL-1β-dependent-myddosome interactome, I used the experimental workflow outlined in Fig. 6. The different gene edited EL4 cells were either left untreated as ‘a vehicle control’ (0 min) or stimulated with IL-1β for 15-, 30- and 60-min or. The chosen timepoints represent an appropriate time frame of signaling events to characterize the IL-1β signaling dynamics based on previous published reports[123–125].

Precise optimization of the developed workflow is described in 4.2.2.1.

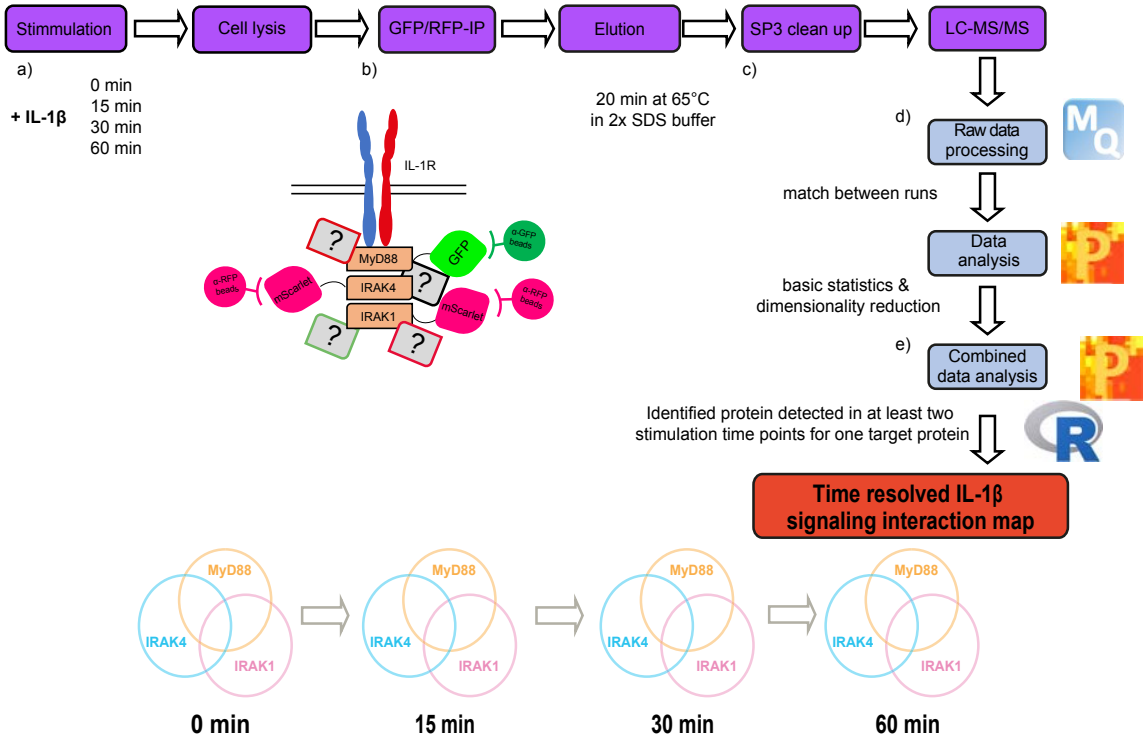

Fig. 6: IP-MS workflow for identifying the temporal dynamics of myddosome interacting proteins following IL-1β stimulation. a) EL4 cells endogenously tagged with C-terminal fluorophore tags to MyD88, IRAK4 and IRAK1 respectively were stimulated with IL-1β for 0-, 15-, 30- and 60-min and lysed for b) subsequent myddosome-IP using GFP- and RFP-trap magnetic beads. Interacting proteins were eluted by boiling. c) Eluates were further processed by SP3 cleanup for mass spec analysis. d) After raw data processing data was analyzed by performing basic statistics and reducing dimensionalities. e) Significantly enriched proteins of each IP-data sets were used to obtain a temporally resolved myddosome interaction map. Identified proteins detected in at least two stimulation time points of one IP-protein were included in the IL-1β-myddosome interaction map.

2.1.2 IP-MS of myddosome proteins identifies both new and known players in the IL-1β signal transduction

The goal of the IP-MS analysis was to identify interactors of MyD88, IRAK4 and IRAK1 across different IL-1β stimulation time points, and how these interactions differ from those in unstimulated cells. Quantitative data were normalized to allow sensitive detection of proteins interacting with the respective bait proteins (i.e. MyD88, IRAK4 and IRAK1) upon IL-1β stimulation. Specifically, protein abundances within each set (i.e., all samples corresponding to the same bait) were corrected by applying a scaling factor that normalizes the abundances of the bait proteins to their corresponding global mean. As a consequence, bait protein abundances are identical across conditions, enabling calculation of enrichment factors for interacting proteins in stimulated versus unstimulated control samples.

To obtain an IL-1β dependent-myddosome interactome, I was exclusively interested in identified proteins enriched in the stimulated conditions (Fig. 7, right side of all scatter plots). I classified proteins as significantly enriched if they met the following criteria: a) at least two-fold higher abundance after IL-1β stimulation (> 1 on the log2 scale, Fig. 6, x-axis), b) a $-\log_{10}$ p-value larger than 2 (Fig. 7, y-axis), and c) a false-discovery rate (FDR) of ≤ 0.05.

Using these criteria, I identified 72 proteins in the 15-min-MyD88-, 379 proteins in the 30-min-MyD88- and 288 proteins in the 60-min-MyD88-data sets (Fig. 7 a). For the IRAK4-data sets, 193, 240 and 68 proteins were found significant after 15-, 30- and 60-min of IL-1β stimulation, respectively (Fig. 7 b). No significantly enriched proteins in the IRAK1-data set after 15-min of IL-1β stimulation were identified in contrast to 31 proteins after 30-min and 4 proteins after 60-min of IL-1β stimulation. Overall, the number of significantly enriched proteins in the IRAK1-data sets is lower compared to the MyD88- and IRAK4-data sets (Fig. 7 c).

Proteins detected as potentially novel MyD88, IRAK4 or IRAK1 interactors were cross-referenced against the string-db.org database[126]. Proteins that are significantly enriched in at least one time point after IL-1β stimulation and that have previously been identified as an interacting protein are marked as red data points in the scatter plots (Fig. 7). Proteins only identified in the stimulated sample are listed on the right side of scatter plots. This strategy identified 9 proteins for the MyD88-IP, 3 for the IRAK4-IP and one protein for the IRAK1-IP data sets. Interestingly, not all of the previously known interactors are significantly enriched in all IL-1β stimulation conditions. Conversely, they partly show negative enrichment values (Fig. 7, left side of scatter plots). Given our IP-MS data set was able to identify previously known interaction, I conclude that the established IP-MS workflow and data analysis pipeline can be used to characterize the IL-1β-myddosome network and identify novel interactors. Furthermore, we can use this experimental strategy to temporally resolve how this interaction network is remodeled over the time course of IL-1β stimulation.

Beyond the proteins for which I calculated enrichment factors upon IL-1β stimulation there are a number of proteins that were exclusively detected upon stimulation. Consequently, no enrichment over unstimulated condition could be calculated, and the proteins are therefore not displayed in the volcano plots (Fig. 7). However, these proteins are of particular interest because they presumably only interact with the bait protein upon stimulation. They are (most likely) no unspecific-interactors of either the bait protein or the beads used for the IP process. For each IL-1β condition the number of these exclusively detected proteins is depicted on the x-axis at '∞' (Fig. 7, Sup. Tab. 1-8). The number of proteins identified only in stimulated conditions are

highest for MyD88 and lowest for IRAK1. These proteins are included in any further data analysis steps and are also classified as significantly enriched.

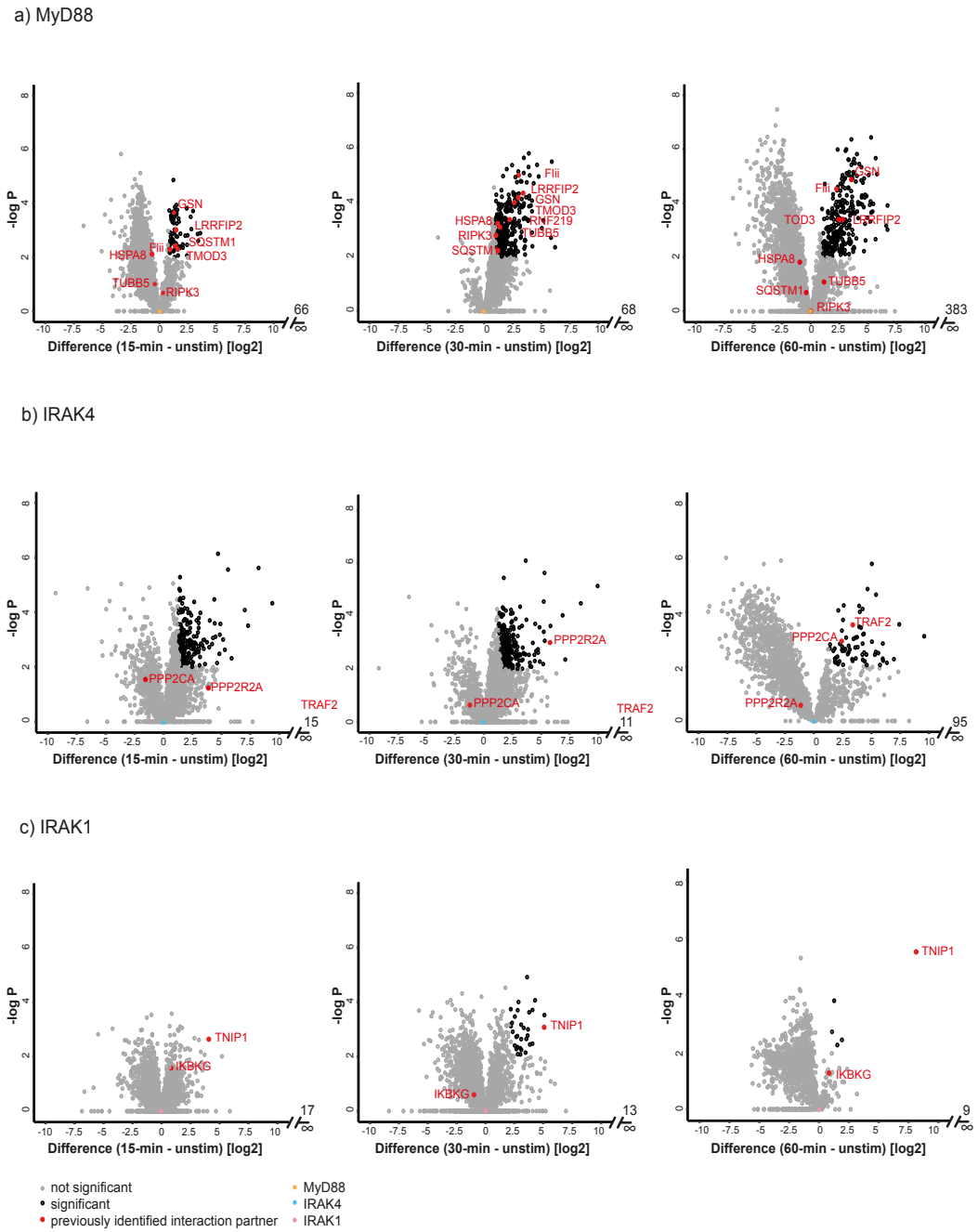

Fig. 7: Scatterplots of myddosome' proteins-IPs comparing identified proteins in unstimulated with 15-, 30- or 60-min of IL-1β stimulated conditions (from left to right). x-axis displays the enrichment [log_2], y-axis illustrates corresponding -log_{10} P-value. Significant proteins are marked in black, previously known interactors are emphasized in red. Corresponding IP-proteins are marked in individual colors: orange for MyD88, blue for IRAK4 and pink for IRAK1. The number over the '∞' on the x-axis indicates the number of proteins exclusively identified in the stimulated conditions.

a) Comparison of identified proteins in MyD88-IP after 15-, 30- and 60-min of IL-1β stimulation.
b) Comparison of identified proteins in IRAK4-IP after 15-, 30- and 60-min of IL-1β stimulation.
c) Comparison of identified proteins in IRAK1-IP after 15-, 30- and 60-min of IL-1β stimulation.

2.1.3 The IL-1β-myddosome interaction map identifies 54 proteins consistently across all IP-data sets

Appropriate interaction and dissociation of proteins to a signaling complex facilitates efficient signal initiation and termination, which in turn allows the cell to adapt to its consistently changing environment[117,127]. This dynamic turnover of proteins at signaling complexes means that important signaling proteins might only interact for a limited time. To characterize proteins interacting with and dissociating from the IL-1β-myddosome, I identified 52 proteins significantly enriched at least two stimulation time points for at least one myddosome protein (Fig. 8 a). The Venn diagram for each stimulation time point in Fig. 8 a reflects which of these 52 identified proteins are either shared or unique between the different MyD88, IRAK4 and IRAK1 interactomes and stimulation time points. Most of the identified proteins interact with all myddosome proteins independent of the stimulation time point (including the unstimulated, 0-min stimulation time point). This observation indicates that there is tonic interaction of many myddosome associated proteins in the absence of stimulation, which increases upon receptor stimulation.

Nevertheless, after 60-min of stimulation the number of proteins interacting with all myddosome proteins slightly decreases. This observation indicates that the myddosome interactome might dissociate or some components might be degraded[61]. Further, this observation emphasizes that the generated temporal IL-1β-myddosome interaction map is able to differentiate between the stimulation time-dependent interactomes.

In the unstimulated data sets I detected 46 proteins that interact with all of the myddosome proteins (Fig. 8 a, unstimulated). This observation emphasizes that Venn diagrams are restricted to similarities and differences between the different IP-data sets, but do not reflect the myddosome's dynamic reorganization process. For this purpose, I compared the proteins' abundance patterns between all IP-data sets. Specifically, I standardized the abundance patterns by performing a z-score analysis to allow an unbiased comparison (Fig. 8 b). The generation of the protein grouping (Fig. 8 b, clustering on the left) is based on similar abundance patterns (i.e., Euclidean distance). While half of the proteins' abundance patterns differ (group 1, indicated in dark green) the other 26 proteins (e.g. including LRRFIP2 to ACTR3) show a rather similar abundance pattern across all IP-proteins and time points (group 2, indicated in light green). These proteins increase in abundance with longer stimulation time in the MyD88 IP-data sets. Unexpectedly, basal abundance levels in the unstimulated IRAK4 IP-data sets were higher as compared to the IRAK1 and MyD88 IP experiments and only increased incrementally from 15-

to 30-min IL-1β stimulation time. Interestingly, after 60-min stimulation with IL-1β a strong decrease in those protein abundances is observed in the IRAK4 IP-data set, suggesting that these proteins dissociate from IRAK4 or get degraded. In the IRAK1 IP-data set these proteins show rather low abundances prior stimulation, an increase in abundance after 15- and 30-min of IL-1β stimulation followed by reduced abundance levels at 60-min of stimulation. While these proteins interact with IRAK4 independent of IL-1β stimulation, they are getting recruited to MyD88 and IRAK1 upon stimulation.

Only four proteins (IRAK1, TNIP1, VBP1 and FISP2 highlighted by '*') have not been detected in unstimulated data sets (indicated in grey), but only in their corresponding stimulated data sets. This indicates that these proteins need myddosome complex formation in order to interact. Another explanation why these proteins only interact with MyD88, IRAK1 and IRAK4 respectively after IL-1β stimulation may be that they require posttranslational modifications. These modifications may be required to activate the protein leading to the interaction with the myddosome and its corresponding function upon IL-1β stimulation[108,128]. In summary, the obtained dataset represents a rich resource to analyze the IL-1β-induced myddosome interactome at temporal resolution, emphasizing the dynamic recruitment and dissociation of various proteins to the different myddosome core components.

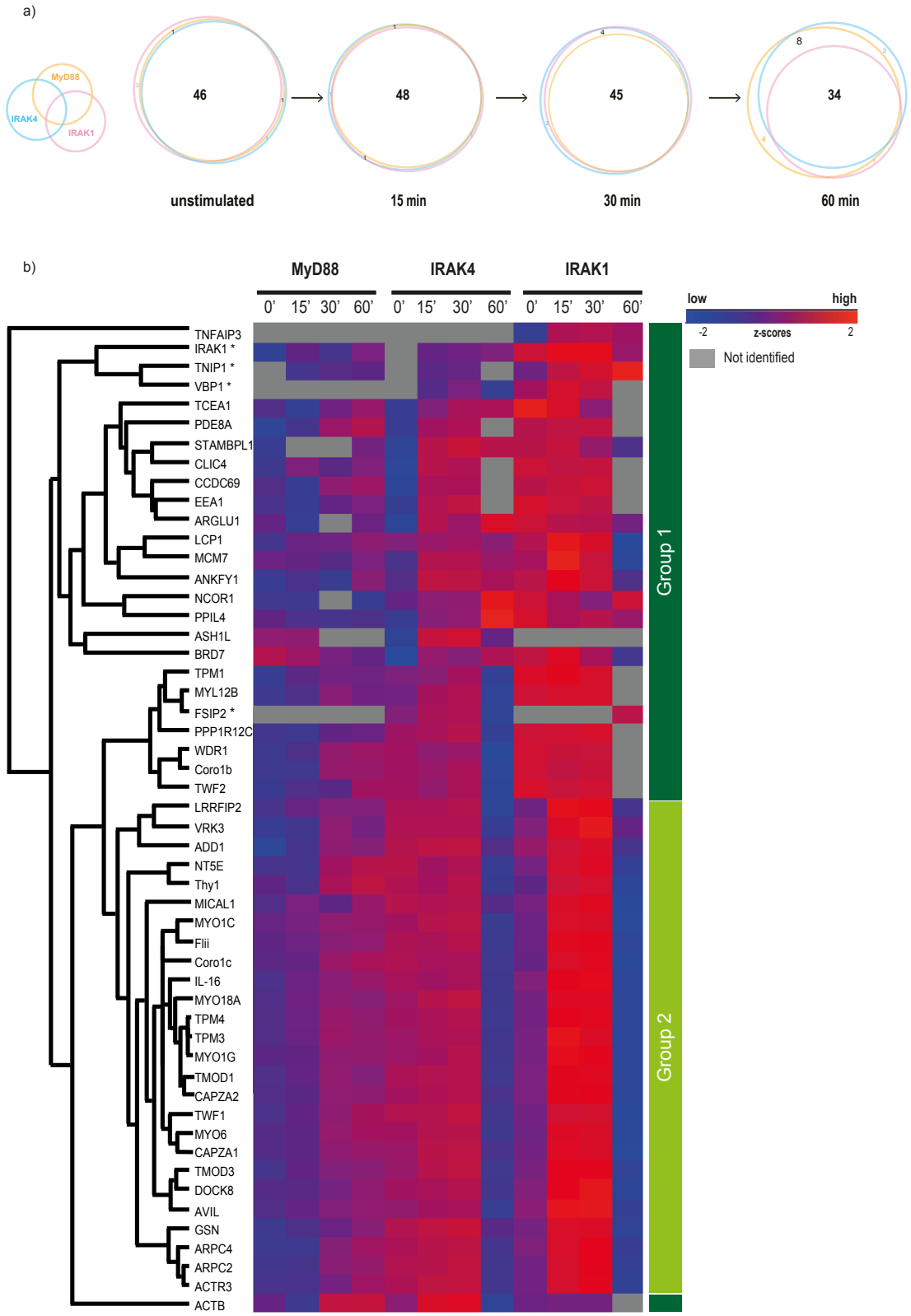

Fig. 8: Temporally resolved IL-1β-myddosome interaction map.

a) Venn diagrams of MyD88-, IRAK4- and IRAK1-IP data of different stimulation time points. The amount of overlap reflects the numbers of proteins that are identified in at least two myddosome-IP data sets.

b) Heatmap of hierarchical clustering based on Euclidean distance of Z-score abundances of IL-1β-myddosome interacting proteins identified in MyD88-, IRAK4- and IRAK1-IP data sets. * highlights proteins that have not been identified in unstimulated conditions. Green bars on the right highlight protein groups with differing (dark green, Group 1) and similar (light green, Group 2) abundance patterns.

2.1.4 Understanding the downregulation of the IL-1β-myddosome interactome

To prioritize potential candidates, putatively involved in downregulating IL-1β signal transduction, I examined the publicly available annotation databases (i.e. Gene Ontology and KEGG) for information about the protein molecular function, involvement in biological processes and localization. Next, I specifically searched for proteins that have been associated to 1.) downregulate signaling pathways, referring to the inhibition or termination further signal transduction or 2.) ubiquitination given its high importance in regulating the IL-1β signal cascade (section 1.2.3.2). That way I identified Tnfaip3 (also known as and further referred as 'A20'), TNIP1, STAMBPL1, NCOR1, VRK3 and Thy1 as the most relevant proteins potentially downregulating the IL-1β-signaling cascade (Fig. 9 a).

Investigation of the abundance patterns shows that A20 was only detected in the IRAK1-IP data sets (Fig. 9 a), emphasizing that A20 is an IRAK1 specific interaction partner and is being recruited after complete myddosome formation. TNIP1 was not detected in the unstimulated MyD88-IP, unstimulated IRAK4-IP and 60-min IRAK4-IP data set and shows highest abundance patterns in the IRAK1-IP data sets. These observations suggest that TNIP1 most likely requires activation in order to interact with MyD88 and IRAK4. Given that the highest abundance of TNIP1 was observed in the IRAK1-IP data sets it is most likely that it is being recruited after complete myddosome formation and later during the IL-1β mediated signal transduction. Stambpl1 was not detected after 15- and 30-min of stimulation in the MyD88-IP data sets but in all remaining IP data sets with highest abundances in the stimulated IRAK4-IP samples. Therefore, STAMBPL1 is most likely an IRAK4 specific interacting protein upon IL-1β stimulation. Ncor1 shows low abundances in the MyD88-IP data sets and was not detected after 30-min of stimulation. With longer stimulation time NCOR1's abundance increases in the IRAK4-IP data, reaching its peak abundance in the IRAK4-IP data set after 60-min stimulation. The observation that NCOR1's abundances are more or less stable at relatively high levels in the IRAK1-IP data set suggests that NCOR1 requires IRAK4 activation and recruitment to the myddosome for Ncor1 interaction. VRK3 and Thy1 were identified in all IP-samples with low abundances in the MyD88-IP data sets, increasing abundances with longer simulation duration in the IRAK4-IP data sets and highest abundances after 15- and 30-min of stimulation in the IRAK1-IP data sets, but low abundances after 60-min of stimulation in both IRAK4 and IRAK1-IP data sets. This abundance profile suggests that VRK3 and Thy1 are being recruited to both IRAK4 and IRAK1, most likely require myddosome formation. After executing their function, they dissociate or are getting degraded from the complex.

The Z-score analysis provides an intuitively accessible way to compare the different abundance patterns of proteins across the different IP-MS data sets, but does not show to which exact extent the abundances differ between unstimulated and stimulated conditions. Thus, I calculated the difference in abundances of all stimulation time points and their corresponding unstimulated abundance for all protein candidates (Fig. 9 b-g; order based on interactome z-Score analysis from Fig. 9 b). A20 shows an increase in abundance difference over time, indicating an enrichment due to stimulation, in the IRAK1-data sets only (Fig. 9 b). TNIP1 is (highly) enriched in all IP-MS data sets (Fig. 9 a & c). Besides, the difference in TNIP1 abundance increases over time and reaches its maximum after 60-min of stimulation in the IRAK1 IP-MS data set. Interestingly, the difference in abundance patterns in the IRAK1-data sets of TNIP1 and A20 correlate, reflecting the previously described link between these proteins in TNF and TLR signaling, further indicating a potential functional link of TNIP1 and A20 when associating to the IL-1β-myddosome (section 1.2.3.3). For STAMBPL1 (Fig. 9 d) and NCOR1 (Fig. 9 e) a positive difference in abundance with an increase over stimulation time is only observable for the IRAK4-data sets. The difference in abundances for Vrk3 decreases with proceeding IL-1β-stimulation time in the MyD88-IP data sets, is negative in the IRAK4-IP data sets and fluctuating in the IRAK1-IP data set (Fig. 9 f). Thy1 is increasingly enriched in the MyD88 data sets over time, but shows exclusively a negative difference in abundance for the IRAK4 data sets (Fig. 9 g).

To summarize, the identified candidates involved in downregulation mechanisms of IL-1β signal transduction are mostly enriched in the data sets of exclusively one myddosome protein and even partly show negative enrichments for other myddosome protein(s) (Fig. 9 b-g). TNIP1 is the exception, since it is enriched in all IP-data sets, indicating that TNIP1 exerts its function by interacting with several components of the myddosome. Further, TNIP1 shows the highest difference in abundance compared to all other identified candidates. Given the correlation of A20 and TNIP1 abundances in the IRAK1-IP data sets which resonates with the importance of ubiquitination degradation in downregulating other innate immune signaling pathways, I hypothesize that the TNIP1-A20 complex plays a pivotal role in counter balancing the IL-1β mediated signaling response.

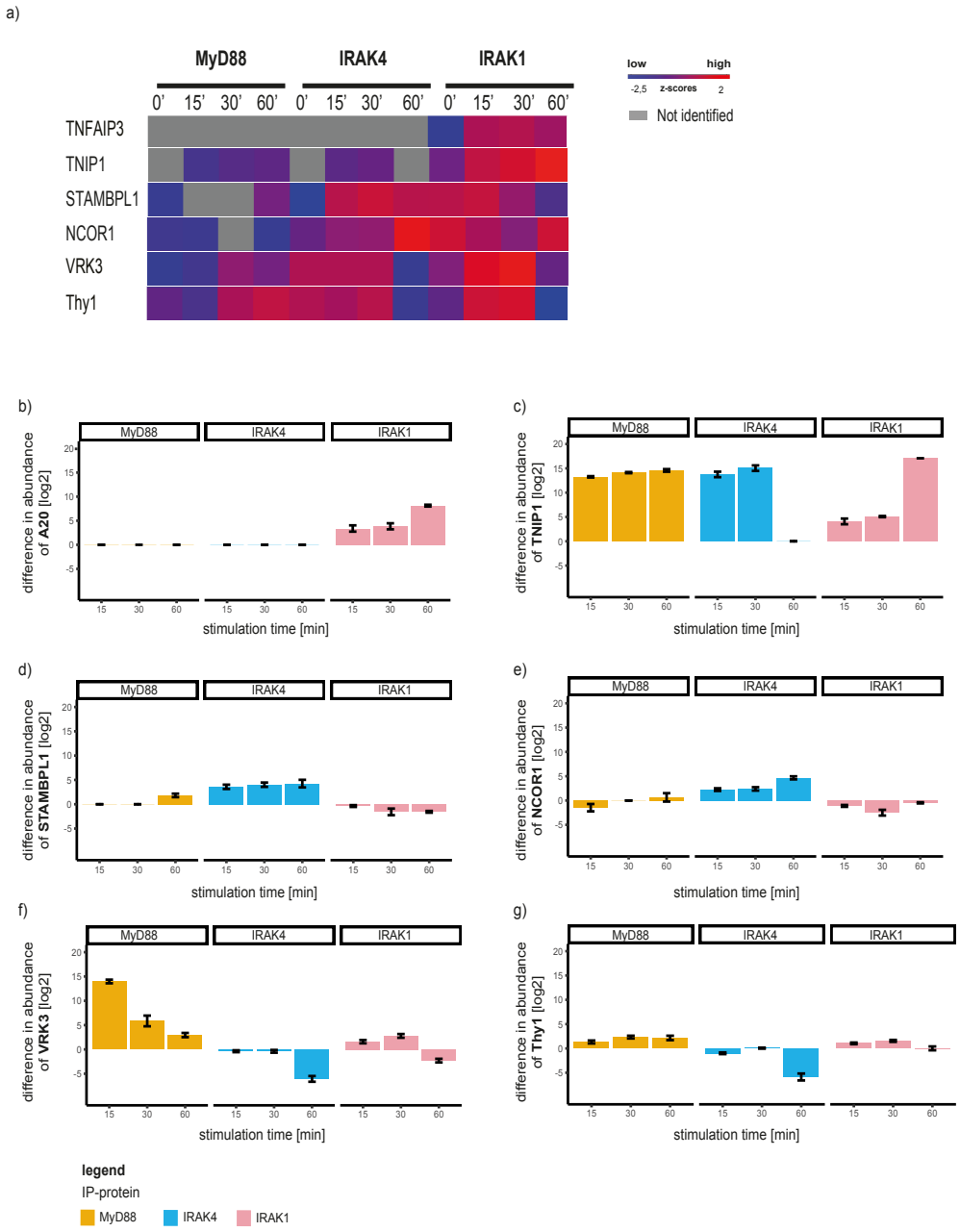

Fig. 9: Potential downregulators of IL-1β signal transduction identified in the IL-1β-myddosome interaction map.

a) Subset of Z-score based heatmap of potential IL-1β signal transduction downregulating proteins identified in myddosome-IPs. Potential downregulating proteins were identified through GOBP, GOCC, GOMF and KEGG pathway annotation followed by manual review for (i) proteins previously involved in downregulating any kind of signaling pathway and for (ii) proteins linked to ubiquitin.

b-g) Differences in abundance of all potential downregulators comparing unstimulated and stimulated conditions for each stimulation time point and myddosome-IP. Yellow = Difference of abundances identified in MyD88-IP; light blue = Difference of abundances identified in IRAK4-IP; pink = Difference of abundances identified in IRAK1-IP.

2.1.5 A20 is the most enriched TNIP1 interaction partner

TNIP1 is described as a physiological NF-κB inhibitor, not through executing enzymatic activities itself, but through linking proteins with enzymatic activity to the proteins involved in signal transduction[87]. In order to uncover how TNIP1 might downregulate IL-1β signal transduction, I mined my IP-MS data sets for previously identified TNIP1 interacting proteins (Fig. 10 a). Figure 10 a illustrates 10 known TNIP1 interactors based on experimental evidence curated in the string.db database[126]. My IP-MS data sets cover 6 out of 10 known TNIP1 interactors (Fig. 10 b). However, only NFKB2, RPS27a and A20 are significantly enriched in at least one of all IP-MS data sets. The remaining identified interactors IKBKG, NFKB1 and UBA52 do not show enrichment upon stimulation or do not reach statistical significance. A20 is highly enriched in the IRAK1-IP data sets, reaching its maximum after 60-min of IL-1β stimulation. As mentioned in 2.1.4, the difference in abundances of TNIP1 and A20 correlate in an IL-1β stimulation time-dependent manner (Fig. 9 a-c). Therefore, this analysis emphasizes that TNIP1 and A20 cooperate in IL-1β signal transduction, which is in line with their previously reported roles in TNFα signal transduction[84,87].

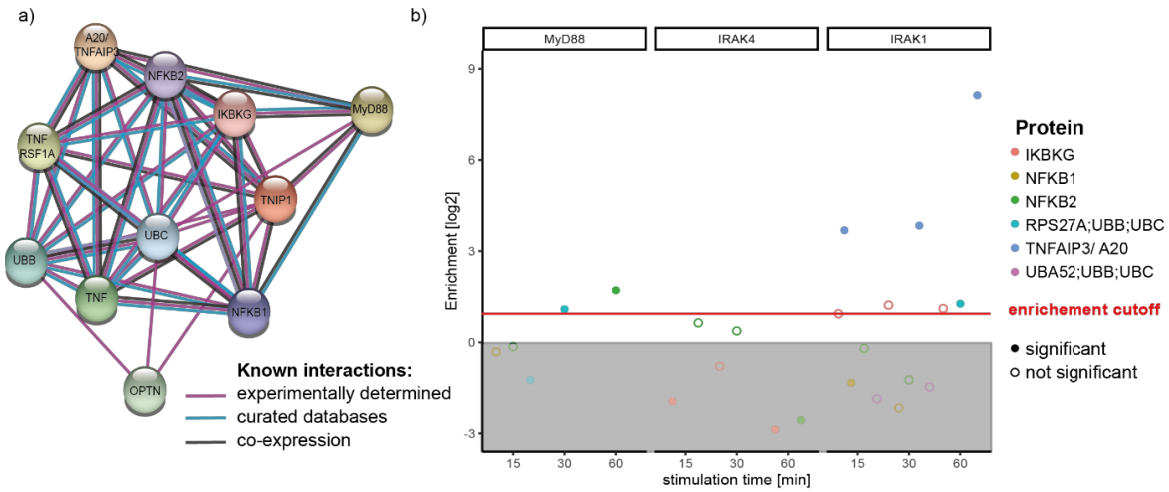

Fig. 10: Previously known interacting proteins of TNIP1 are identified in IP-MS data sets with A20 being the most enriched.

a) TNIP1's interaction map based on the string database arranges eleven interacting proteins.

b) Enrichment and significance of previously known TNIP1 interactors in MyD88-, IRAK4- and IRAK1-IP data sets after 15-, 30- and 60-min IL-1β stimulation. Identified proteins with significant enrichment patterns are fully colored, for not significant data points only protein color specific boundaries are shown. The enrichment cutoff was set at 1, enrichment is displayed in -log2 scale.

2.1.6 IP-MS and subsequent data analysis of MyD88-GFP in a WT, IRAK4 KO or IRAK1 KO background identifies protein networks at intermediate IL-1β signal transduction stages

Immune signaling events are believed to occur in a specific order to govern their signaling outputs[129]. Complete myddosome formation is indispensable to transduce the IL-1β signal[130]. However, the molecular mechanisms of myddosome assembly are not completely understood. Therefore, I performed MyD88-GFP IPs followed by LC-MS/MS (Fig. 6) in IRAK4 or IRAK1 KO cells. The 'WT' MyD88-IP data sets (cell line without protein perturbation) comprise interacting proteins of fully formed myddosomes. The MyD88-IP data sets in the IRAK4 KO background identifies proteins that associate with MyD88, when only MyD88 is recruited to the activated IL-1R. The MyD88-IP data sets in the IRAK1 KO background identifies proteins that associate with MyD88, when IRAK4 is also recruited. Conclusively, comparisons of the MyD88-IP data sets in the KO background with the 'WT' background allows to identify interactors at intermediate stages of myddosome assembly, because myddosome assembly is blocked at a intermediate assembly stages given the IRAK KO background.

To assess feasibility of this approach I first checked for IRAK1 abundances being the last protein getting recruited in the myddosome formation process (Fig. 11 a)[29]. Figure 11 a confirms the expectation that IRAK1 does not bind to MyD88 in an IRAK 4 KO and is not present in an IRAK 1 KO cell line.

To characterize the MyD88 interactome of these discrete stages I applied the same cutoffs as for the complete IL-1β-myddosome interaction network (Fig. 6), including identified proteins that were significantly enriched in at least two stimulation time points per cell line ('WT', 'KO IRAK 4', 'KO IRAK 1'). Based on these cutoffs, I identify 67 proteins (Fig. 11 b). Again, the majority of proteins were identified in MyD88-IPs independent of the stimulation time point (Fig. 11 b & c), emphasizing that most MyD88 interacting proteins are in tonic interaction in the absence of stimulation, but increase upon IL-1β stimulation.

To reflect the protein dynamics within the organization process of the myddosome and to characterize discrete stages, I compared the proteins' standardized abundance patterns (Fig. 11 d). The majority of proteins show highest abundances after 30- and 60-min of stimulation in the MyD88-WT cell line. For the MyD88-GFP/IRAK4-KO cell line the abundance is slightly higher for the 30-min stimulation time point, while for the MyD88- GFP/IRAK1-KO cell line-the abundance is highest for the 15-min stimulation time point (roughly EFR3A to ACTN4). This observation suggests that most proteins are MyD88 interactors but this interaction depends

on partly or fully assembled myddosome. Further, this analysis suggests that TNIP1 interacts with the assembled myddosome, as it is not identified in both IRAK KO backgrounds. TPM1, TRIM6, MICAL1 and IL-16 are not present in the MyD88-GFP/IRAK4 KO dataset, indicating that these proteins are recruited after MyD88 and IRAK4 association to the IL-1R. In summary, performing IP-MS of MyD88-GFP in different KO backgrounds allows to dissect discrete stages of IL-1β signal transduction, highlighting the dynamic recruitment and dissociation of various proteins to MyD88 mostly dependent on partly or fully assembled myddosome.

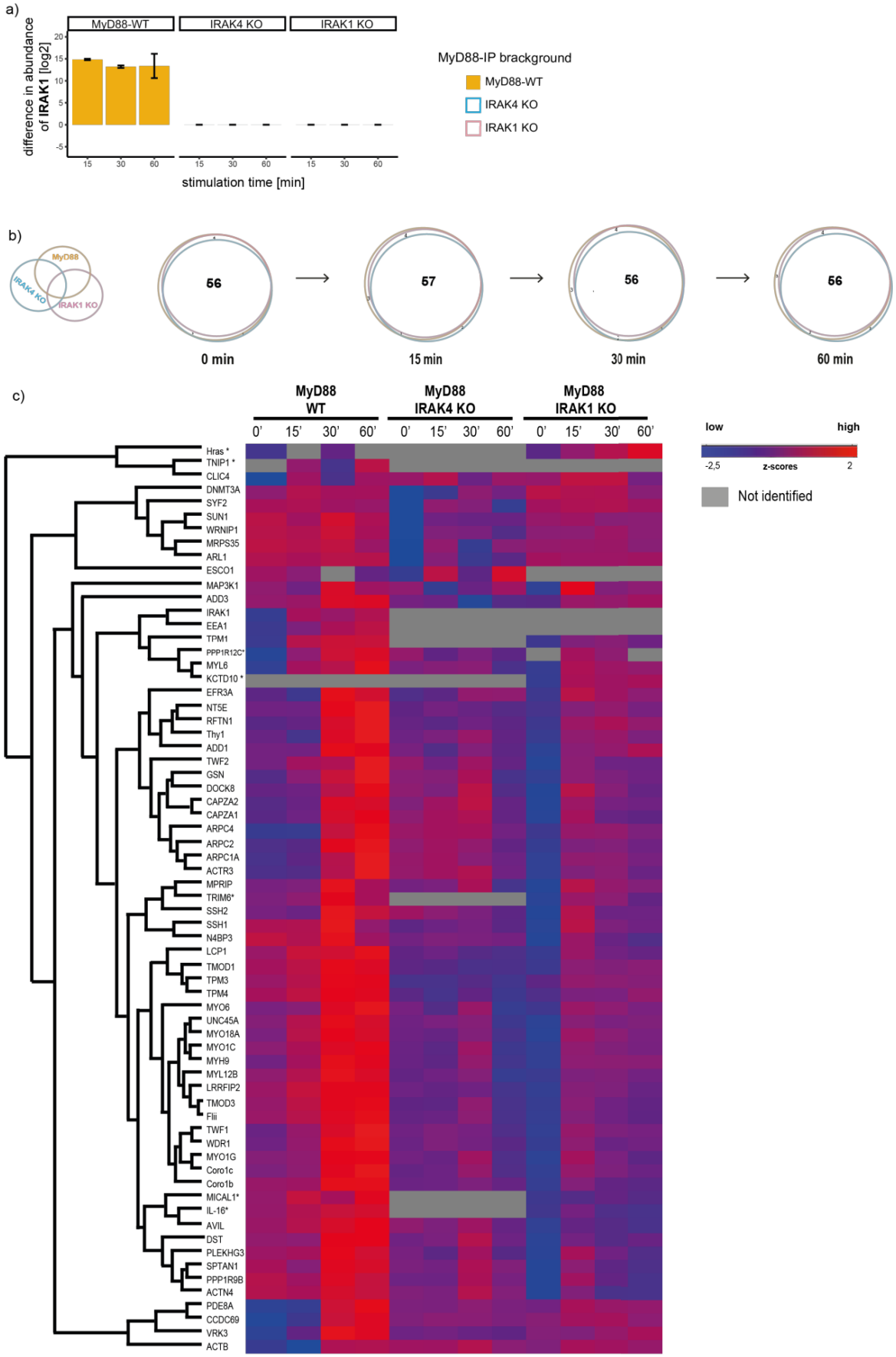

Fig. 11: Characterization of the IL-1β-myddosome's interaction network at its discrete stages.

a) Difference in abundance of IRAK1 identified by MyD88-IP and MS comparing unstimulated abundance and 15-, 30- and 60-min of IL-1β stimulation in WT- (yellow), IRAK4 KO (light blue) and IRAK1 KO background (pink).
b) Venn diagrams of MyD88-IP data of different stimulation time points in 'WT'-, IRAK4 KO and IRAK1 KO background. The amount of overlap reflects the numbers of proteins that are identified in two or all myddosome-IP data sets.
c) Heatmap of hierarchical clustering based on Euclidean distance of Z-score abundances of MyD88 interacting proteins identified at discrete myddosome stages. Discrete stages were identified using MyD88-GFP, MyD88-GFP/IRAK4-KO and MyD88- GFP/IRAK1-KO EL4 cell line and IL-1β stimulation for 0-, 15-, 30- and 60-min. * highlights proteins that have not been identified in unstimulated conditions.

2.1.7 TNIP1 is a myddosome associated protein only after complete myddosome formation

Next, I investigated proteins that potentially downregulate the IL-1β signaling cascade. To identify potential downregulating candidates based on the KO approach, all identified proteins were annotated with the GOPB, GOMF, GOCC and KEGG pathway databases. I applied the same analysis strategy (section 2.1.4), specifically searching for proteins that have been associated to (1) downregulate signaling pathways or (2) ubiquitination. Using these criteria, I identified TNIP1, MAP3K1, KCTD10, Thy1 and TRIM6 (Fig. 12 a).

Performing MyD88-IPs in the different IRAK KO cell lines allows for the identification of discrete interaction stages of the myddosome. IP-MS of all myddosome proteins individually allows to identify myddosome-dependent or myddosome protein-specific interactors. Therefore, I combined both approaches by comparing the difference in abundance for all proteins identified as potential downregulators by the different approaches (Fig. 9 a; Fig. 12 a).

TNIP1 is detected in all myddosome-IPs, but not in an IRAK KO background (Fig. 12 b), differentiating it from all other identified potential downregulators. This result indicates that TNIP1 is only binding to all myddosome proteins after complete myddosome formation consisting of MyD88, the IRAK proteins and possibly other proteins that require IRAK to bind to and form a signaling platform. The fully assembled myddosome therefore seems to be a prerequisite for TNIP1 to interact with components that assemble a functional molecular complex leading to signal transduction events.

All other potentially downregulating proteins that were identified based on the KO approach (Fig. 12 a) only showed a small difference in abundance for a stimulation time point in the MyD88 data set and slightly higher differences for the MyD88-IP data set in the IRAK1 KO background (Fig. 12 c-e), with the exception of KCTD10 (Fig. 12 d). KCTD10 is exclusively detected in the IRAK1 KO data set. Therefore, these proteins might only associate to MyD88 after MyD88 and IRAK4 interaction.

While A20 and STAMBPL1 are not detected in the IRAK KO backgrounds (Fig. 12 g-h), NCOR1 and VRK3 show a low increase in the IRAK1 KO data sets (Fig. 12 i-j), reemphasizing that these two proteins potentially interact with a subcomplex consisting of MyD88 and IRAK4.

Taken together, the given analysis using genetic KO cell lines and IP-MS to characterize discrete stages of myddosome maturation. For efficient IL-1β signal transduction, the myddosome requires complete formation. Therefore, it is likely specific downregulating processes are only triggered after complete myddosome formation. TNIP1 is the only protein that is i) present in all Myddosome-IP data sets, ii) not present in the IRAK KO background and iii) shows highest difference in abundance compared to any other identified protein potentially downregulating IL-1β signal transduction.

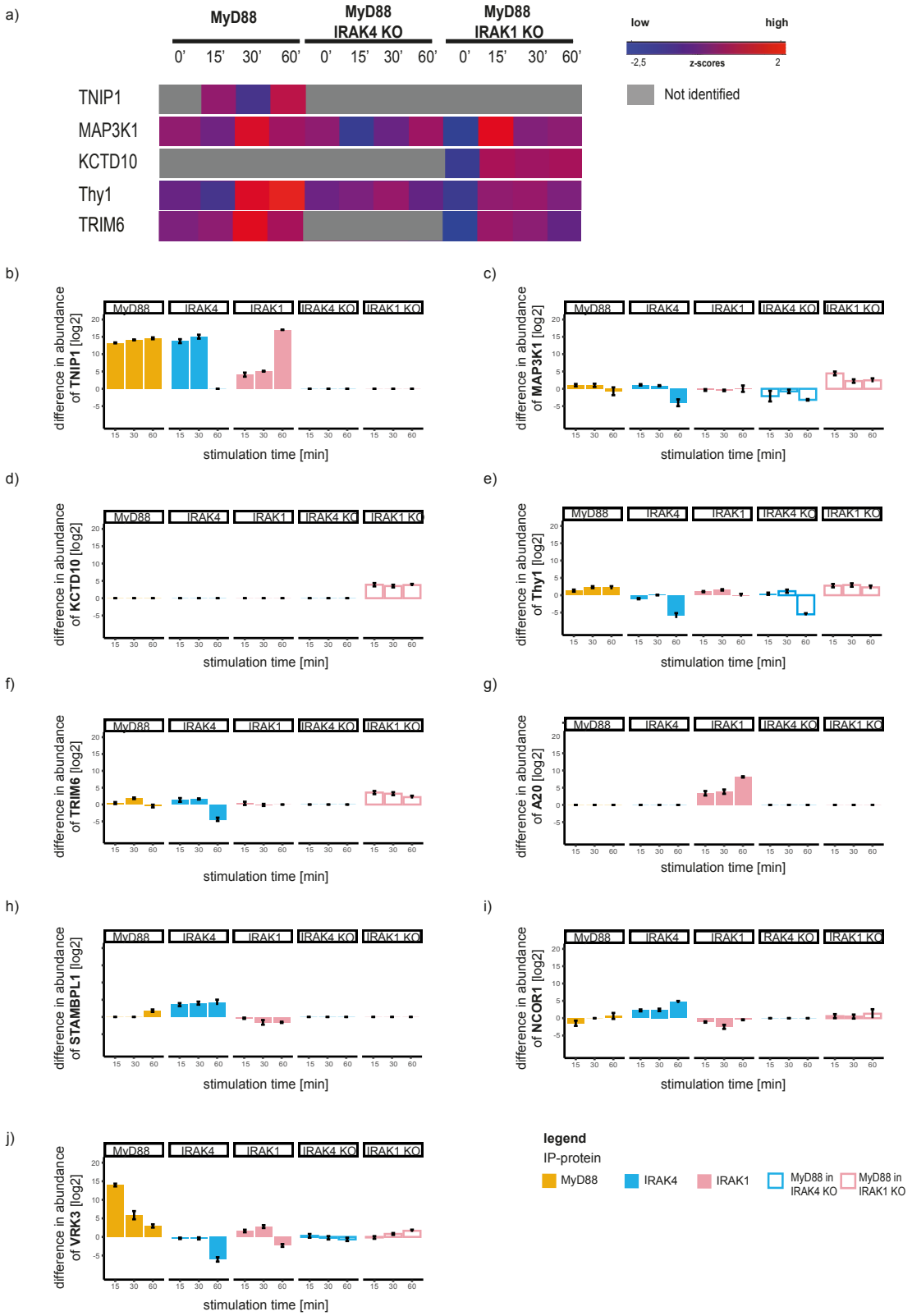

Fig. 12: Discrete stages of potential IL-1β signal transduction downregulating proteins.

a) Extract of Z-score based heatmap of potential IL-1β signal transduction downregulating proteins identified in MyD88-IPs in WT-, IRAK4 KO or IRAK1 KO background. Potential downregulating proteins were identified through GOBP, GOCC, GOMF and KEGG pathway annotation followed by a specific search for (i) proteins previously involved in downregulating any kind of signaling pathway and for (ii) proteins linked to ubiquitin.

b-i) Difference of abundances of all potential downregulators comparing unstimulated and stimulated conditions for each stimulation time point, myddosome-IP in WT and IRAK4/1 KO background. Yellow = Difference of abundances identified in MyD88-IP; light blue = Difference of abundances identified in IRAK4-IP; pink =

Difference of abundances identified in IRAK1-IP; light blue ring = Difference of abundances identified in MyD88-IP in IRAK4 KO background; pink = Difference of abundances identified in MyD88-IP in IRAK1 KO background.

2.2 TNIP1 undergoes post-transcriptional regulation upon IL-1β stimulation

Cell signal transduction is regulated at different stages such as the dynamic adjustment of protein synthesis and degradation[131]. A better characterization of protein level changes due to IL-1β stimulation will provide insights on the underlying biological processes and cellular response. As such, a temporally resolved protein level characterization can reveal how signaling might be regulated at the protein level. Therefore, in the next section I investigate IL-1β-dependent protein synthesis and degradation.

2.2.1 pSILAC and AHA combined with click chemistry and MS identifies IL-1β stimulation time dependent *de novo* synthesized proteins

To investigate IL-1β dependent protein synthesis in EL4 cells, I utilized metabolic labeling of proteins by pulse SILAC (pSILAC) and L-Azidohomoalanine (AHA) combined with click chemistry enrichment and MS analysis (Fig. 13 a). Metabolic pulse labeling of cells with stable isotope-labeled amino acids in cell culture (pSILAC) facilitates differential quantification of newly synthesized proteins by MS. Simultaneous metabolic labeling with noncanonical Methionine-analog AHA further enables efficient enrichment of *de novo* synthesized proteins by click chemistry[132,133]. Relative quantification comparing unstimulated (heavy labeling) to stimulated (intermediate) condition for each stimulation time point (30-, 60-, 120-, 240-min) allows to identify IL-1β-dependent *de novo* synthesized proteins. I defined proteins as IL-1β dependent *de novo* synthesized proteins if the $-\log_2$[p-Value] is ≥ 2 and the ratio of stimulated/ unstimulated is ≥ 1 for *de novo* synthesized proteins at any stimulation time point. Using these cutoff criteria, I identified 9 *de novo* synthesized proteins (Fig. 13 b). Time-resolved analysis reveals that 6 proteins (RELB, TNIP1, NFKB2, NFKBID, NKFBIZ and Bhlhe40) are increasingly *de novo* synthesized with increasing IL-1β stimulation time. On the other hand, IL-1β-dependent synthesis of NFKBIA, Jun peaks at 60-min, while maximum Junb synthesis is observed at 120-min post stimulation. Notably, all significant proteins except for Bhlhe40 are known players in NF-κB signaling. Since NF-κB signaling is activated upon IL-1β stimulation[134], detection of *de novo* synthesized NF-κB associated proteins proves feasibility of my experimental approach. Gene ontology annotation analysis reveals that NFBKID, NFKBIA and TNIP1 have previously been linked to signal downregulation. Interestingly, considering the IP-MS approach to identify potential proteins downregulating IL-1β signal transduction (sections 2.1.4; 2.1.6), TNIP1 is the only protein identified in both approaches, IP-MS and pSILAC-AHA. Therefore, TNIP1's

characteristics functions regarding the IL-1β mediated signaling pathway are investigated from this point further.

First, I assessed the extent of *de novo* synthesized TNIP1 over the time course of IL-1β stimulation relative to unstimulated cells (Fig. 13 c). At early time points after IL-1β stimulation (30- and 60-min) *de novo* synthesis of TNIP1 is similar to unstimulated cells. However, TNIP1 synthesis is more than two-fold higher after 120-min upon stimulation (log2 difference stimulated/unstimulated = 1.18) and remains at this high level until 240-min post IL-1β stimulation (Fig. 13 c).

These data provide evidence that *de novo* synthesis of TNIP1 is elevated in direct response to IL-1β stimulation.

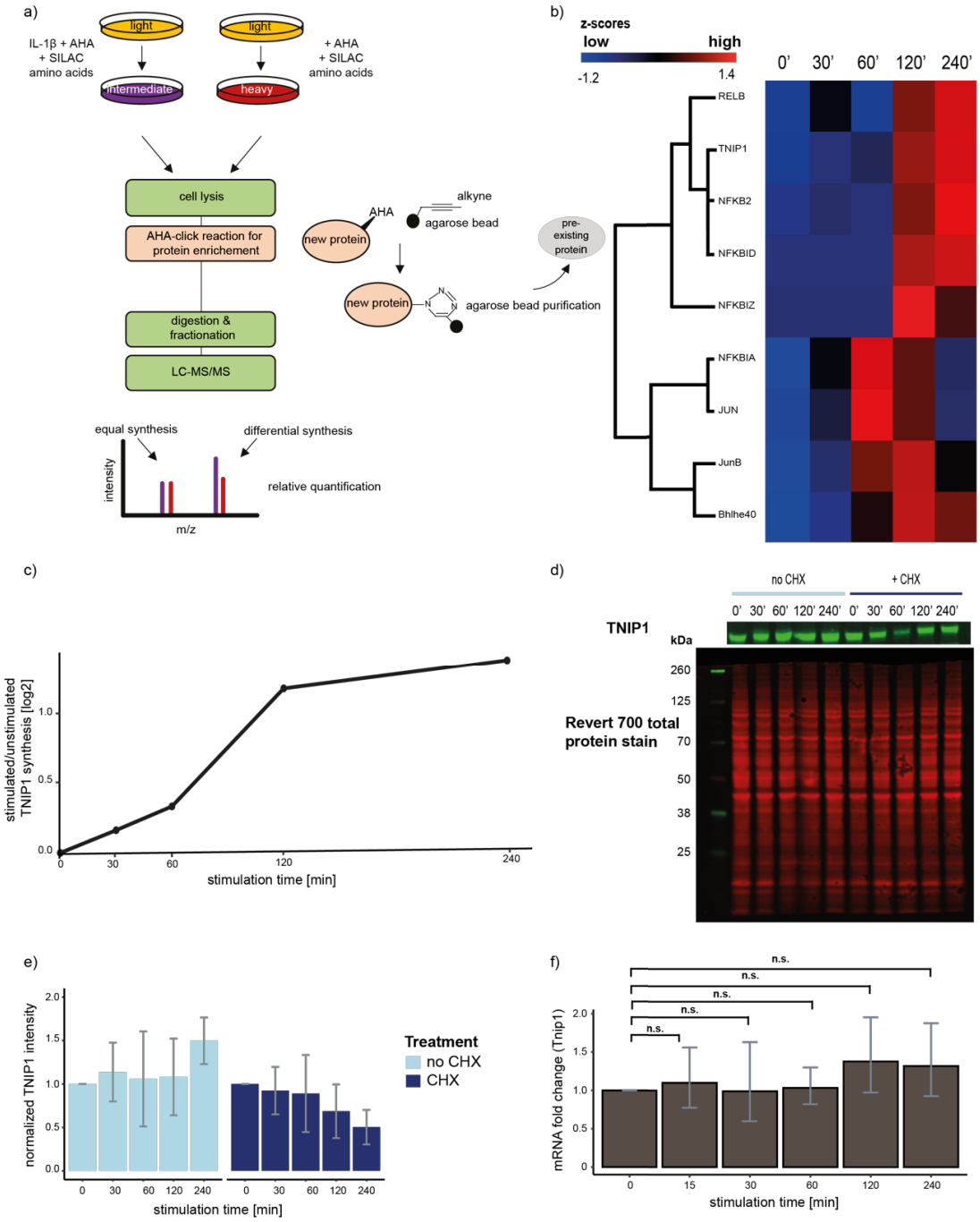

Fig. 13: TNIP1 is *de novo* synthesized as a translational feedback response to IL-1β stimulation.

a) Experimental overview of pSILAC and AHA combined with AHA-click chemistry to exclusively identify *de novo* synthesized proteins upon IL-1β stimulation.

b) Heat map based on Euclidean distance of Z-scored abundances of de novo synthesized proteins upon IL-1β stimulation of EL4 WT cells visualizing hierarchical clustering.

c) Log_2 ratio (stimulated/ unstimulated) of *de novo* synthesized TNIP1 after IL-1β (10 ng/ml) stimulation for 30-, 60-, 120- and 240-min.

d) Fluorescence based WB for TNIP1 (upper part, green) and total protein blotted identified by Revert™ total protein stain (lower part, red) after EL4 WT stimulation comparing unstimulated TNIP1 total protein level to 30-, 60-,120- and 240-min IL-1β (10 ng/ml) stimulation. Before stimulation half of the setups were treated with CHX (10 µg/ml) for 1 h. Western Blots were acquired with the Odyssey CLx Infrared Imaging System.

e) Quantification of TNIP1 signal after EL4 WT stimulation comparing unstimulated TNIP1 total protein level to 30-, 60-,120- and 240-min IL-1β (10 ng/ml) stimulation. Before stimulation half of the setups were treated with CHX (10 µg/ml) for 1h. Western Blots were acquired with the Odyssey CLx Infrared Imaging System.

TNIP1 signal was normalized to total protein. Images were analyzed using EmpiriaStudio. Shown are means from 6 independent experiments, error bars represent SEM.

f) Tnip1 expression comparing unstimulated (0-min) EL4 WT cells with stimulated IL-1β (10 ng/ml) EL4 WT cells for 30-, 60-, 120- and 240-min was analyzed by qPCR. Data were analyzed using the ΔΔCt method. Gapdh was used for normalization. qPCR for 6 replicates from 6 independent stimulation experiment. Error bars represent SEM. Data was analyzed by Shapiro-Wilk-Test, $\alpha = 0{,}05$, followed by one-way ANOVA test ($p<0.05$), n.s. = not significant.

2.2.2 Total TNIP1 protein level increases over the time course of IL-1β stimulation

pSILAC/AHA combined with click chemistry and MS quantifies abundances of *de novo* synthesized TNIP1 (Fig. 13 b & c), but not total TNIP1 protein levels which are governed by the interplay of synthesis and proteasomal degradation. To measure the change in total TNIP1 protein levels, I examined total TNIP1 protein level upon different IL-1β stimulation time points using a quantitative fluorescence-based WB system (Fig. 13 d). Specifically, I hypothesized that if TNIP1 *de novo* synthesis is elevated due to IL-1β stimulation then blocking protein biosynthesized prior to IL-1β stimulation should lead to identical, in case no TNIP1 degradation is occurring, or lower TNIP1 total protein amounts in case of TNIP1 degradation. To test this hypothesis, I stimulated EL4 WT cells for 0-, 30-, 60-, 120- and 240-min. At the same time, I arranged a second set up treating EL4 WT cells with cycloheximide (CHX) for 60-min pre-stimulation. After cell lysis and WB sample preparation and WB, I stained and acquired total protein amounts for later normalization purposes, followed by TNIP1 detection. Figure 13 d shows an exemplary WB for TNIP1 (upper part) and total blotted protein amounts identified by Revert^{TM} 700 total protein stain (lower part). This blot shows that total TNIP1 protein increases with increasing IL-1β stimulation time, but decreases if cells were treated with CHX pre-stimulation. To verify reproducibility, I repeated this experiment on three independent days and quantified total TNIP1. I normalized the ratio of TNIP1 per total protein amount blotted to the corresponding unstimulated sample (mean for control and CHX treatment, means ± SEM, Fig. 13 e). While IL-1β stimulation leads to an overall increase of total TNIP1 protein amount (Fig. 13 e, left), CHX treatment results in a decrease of total TNIP1 protein amount (Fig. 13 e, right).

To summarize, these results show that not only *de novo* synthesized TNIP1 amount increase over the time course of IL-1β stimulation, but also the total TNIP1 amount especially at the latest 240-min IL-1β stimulation time point.

2.2.3 *De novo* synthesis of TNIP1 is a translational but not transcriptional feedback response to IL-1β

Traditionally, protein synthesis has been assayed based on mRNA change. However, mRNA level and its corresponding protein amount do not always correlate[135]. To test if the observed increasing *de novo* TNIP1 synthesis correlates with a potential change in Tnip1 mRNA level, I investigated relative Tnip1 mRNA abundance again after 30-, 60-, 120- and 240-min IL-1β stimulation by qPCR (Fig. 13 g). These measurements revealed that Tnip1 mRNA levels are not significantly increased after any IL-1β stimulation time point. Conclusively, TNIP1 expression levels are regulated post-transcriptionally as no changes in mRNA levels could be detected at any time point prior and after IL-1β stimulation.

2.3 Characterization of TNIP1 in IL-1β signal transduction in EL4 cells

In the previous sections, I identified TNIP1 being a myddosome associated protein after complete myddosome formation and being *de novo* synthesized as a translational feedback response to IL-1β stimulation. TNIP1 has been characterized as an inhibitor of NF-κB activation in TNFα signaling[87]. However, the role of TNIP1 in IL-1β signal transduction is unknown. Therefore, in the next section I will characterize TNIP1 in IL-1β mediated signaling, starting from signal initiation at the myddosome level down to long-term IL-1β-dependent IL-2 secretion.

2.3.1 TNIP1 colocalizes with all myddosome proteins after IL-1β stimulation

IP-MS of myddosome proteins identified TNIP1 being interactor after 15-, 30- and mostly 60-min of IL-1β stimulation (section 2.1.4), but only after complete myddosome formation (section 2.1.6). TNIP1 association to MyD88, IRAK4 and IRAK1 was confirmed after 30-min of IL-1β stimulation using the same endogenously tagged EL4 cell lines (MyD88-GFP/IRAK4-mScarlet, MyD88-GFP/IRAK1-mScarlet) as used for IP-MS experiments and TNIP1-specific immunofluorescence staining (Fig. 14). Specifically, cells were stimulated using supported lipid bilayers (SLBs) functionalized with IL-1β, a system previously developed in the lab[122], fixed, stained for TNIP1 and visualized at the cell membrane using Total Internal Reflection (TIRF-) microscopy. TNIP1 co-localizes to MyD88 (Fig. 14 a & b), IRAK4 (Fig. 14 a) and IRAK1 (Fig. 14 b) respectively.

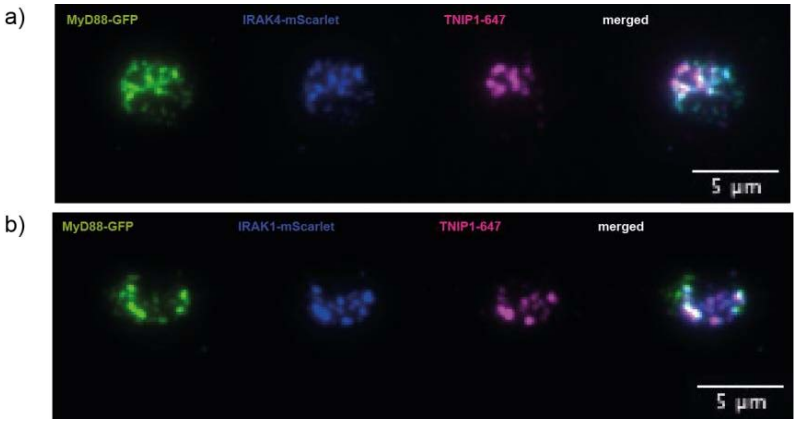

Fig. 14: TNIP1 is a myddosome-associate protein.
a) TIRF images of MyD88-GFP/IRAK4-mScarelt expressing cells fixed and stained for TNIP1-AF647 after 30-min of stimulation on IL-1β-functionalized SLBs. Scale bar = 5 µm.
b) TIRF images of MyD88-GFP/IRAK1-mScarelt expressing cells fixed and stained for TNIP1-AF647 after 30-min of stimulation on IL-1β-functionalized SLBs. Scale bar = 5 µm
(Data acquired and kindly provided by Fakun Cao).

2.3.2 TNIP1 and A20 co-localize after IL-1β stimulation

My IP-MS data revealed a link between TNIP1 and A20 (sections 2.1.4.; 2.1.7), which is further supported by evidence in other studies[84,86]. Next, I aimed to verify the interaction between TNIP1 and A20 by investigating their co-localization after IL-1β stimulation. For this purpose, an endogenously tagged MyD88-GFP/A20-mScarlet EL4 cell line was generated (by Fakun Cao & Elke Ziska). To verify that endogenously tagging A20 does not perturb IL-1β mediated signaling, I investigated IL-2 release after 24 h of IL-1β stimulation, since EL4 cells release IL-2 after 24 h of IL-1β stimulation[136] (App. Fig. 1). To assay the co-localization on A20 and TNIP1, MyD88-GFP-A20-mScarlet cells were stained for TNIP1 after 30-min stimulation on IL-1β functionalized SLBs and visualized using TIRF-microscopy (Fig. 15). Using an endogenous fluorophore N-terminal tag to A20 instead of an A20-specific antibody avoids the difficulty of general unspecific antibody binding that can result in high background fluorescence signals and thus potential misinterpretation of a putative A20 TNIP1 co-localization. Visualization of MyD88 with an endogenous GFP tag also overcomes the problem of general unspecific antibody binding and at the same time indicates myddosome formation. Figure 15 shows that TNIP1 co-localizes with both A20 and MyD88. Strikingly, TNIP1 co-localization with MyD88 depends on A20 and vice versa, emphasizing a functional link of TNIP1 and A20 in IL-1β signal transduction.

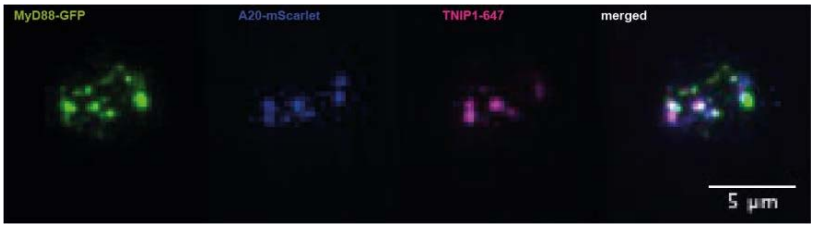

Fig. 15: Previously known interacting proteins of TNIP1 are identified in IP-MS data sets with A20 being the most enriched. TIRF images of MyD88-GFP/A20-mScarlet EL4 cells on IL-1β functionalized SLBs, fixed after 30-min of stimulation and stained for TNIP1 with AF647. Scale bar = 5 µm (data acquired and kindly provided by Fakun Cao).

2.3.3 KO of TNIP1 leads to increased phosphorylation of p65 but decreased phosphorylation of JNK

To characterize TNIP1 function in IL-1β signal transduction, I generated a TNIP1 KO cell line using CRISPR/Cas9 (Fig. 16 a). Given the correlation in abundances of TNIP1 and A20 in the IRAK4-IP MS results (section 2.1.4), the co-localization (section 2.3.1) of TNIP1 and A20, and the known functional link of TNIP1 and A20 in IL-1β-related TLR signaling I generated a TNIP1 KO in the MyD88-GFP/A20-mScarlet cell line[86]. This TNIP1 KO cell line further allows to investigate the effect of TNIP1 loss on A20 recruitment to the myddosome using life cell imaging in future experiments (currently on-going experiments). To confirm TNIP1 specificity, TNIP1 expressed in the TNIP1 KO cell line was rescued with TNIP1-Halo expressed from a lentiviral vector (Fig. 16 a; cell line produced by Mauriz Lichtenstein). Reconstitution of the KO cell line with a tagged TNIP1 allows to visualize recruitment of A20 and TNIP1 to MyD88 in live cells in future experiments (currently on-going experiments shown). The WB in Figure 16 a proves complete KO of TNIP1 (2nd lane) and successful rescue with TNIP1-Halo resulting in a 33 kDa bigger TNIP1 (3rd lane) compared to WT TNIP1 (1st lane).

IL-1β stimulation leads to IKK complex dependent phosphorylation of RelA/p65, and MAPK-dependent phosphorylation of p38, ERK and JNK[27]. I investigated phosphorylation levels of p65, ERK, p38 and JNK upon 0-, 15-, 30- and 60-min IL-1β stimulation in EL4 cells using WB specific for phosphorylated and corresponding non phosphorylated proteins. Since IL-1β stimulation does not affect phosphorylation levels of p38 and ERK in EL4 cells (Sup. Fig. 2), I characterized the effect of TNIP1 loss on p65 and JNK phosphorylation levels (Fig. 16 b & c). While IL-1β stimulated KO TNIP1 cells show higher p65 phosphorylation (pp65) levels especially after 15-, but also after 30- and 60-min of stimulation (Fig. 16 b), levels of phosphorylated JNK (pJNK) are lower compared to the parental cell line (Fig. 16 c). The IL-1β stimulated rescue TNIP1-Halo cell line shows similar pJNK levels as the parental cell line, thereby confirming these TNIP1-specific phenotype. However, pp65 levels in the rescue TNIP1-Halo cell line differ compared to the parental cell line. I stimulated the different cell lines and blotted for

corresponding phosphorylated and non-phosphorylated proteins on at least three independent days with similar results.

To summarize, these results show that loss of TNIP1 leads to increased phosphorylation of p65, emphasizing a down regulative function for TNIP1 in the IKK-complex mediated IL-1β signal response. At the same time knocking out TNIP1 results in decreased phosphorylation levels of pJNK, indicating a positive regulative role of TNIP1 in the MAPK mediated IL-1β signal transduction. Rescue experiments ensure the observed TNIP1 phenotype specificity.

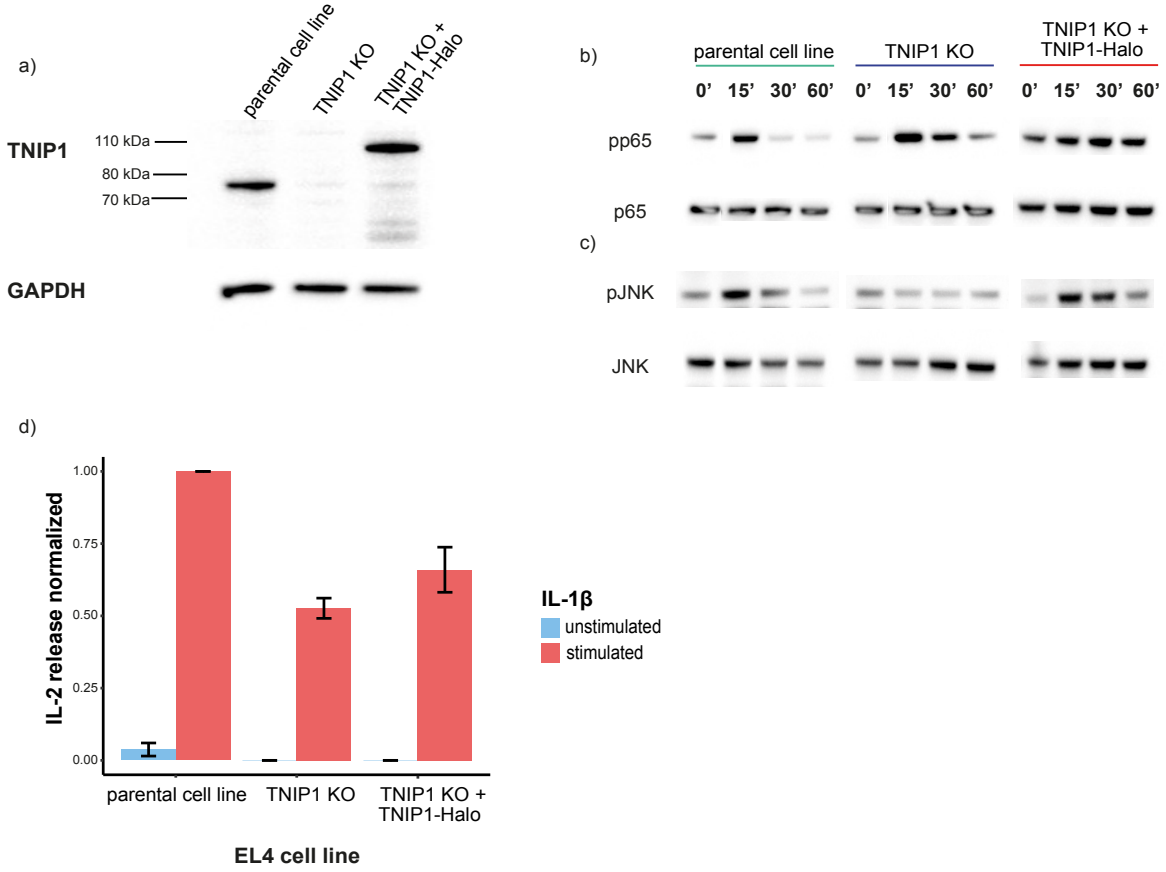

Fig. 16: KO of TNIP1 affects IL-1β mediated downstream signaling events.

a) Western blot analysis for TNIP1 of parental MyD88-GFP/A20-mScarlet EL4 cell line (1st lane: parental cell line) used to generate TNIP1 KO cell line (2nd lane). TNIP1 KO cell line was then rescued with TNIP1-Halo (3rd lane: TNIP1 KO + TNIP1-Halo). GAPDH detection (lower panel) was used as loading control.

b) Western blot analysis for phosphorylated p65 (pp65, upper panel) and p65 (lower panel) after 0-, 15-, 30- and 60-min of IL-1β stimulation of MyD88-GFP/A20-mScarlet (parental cell line), MyD88-GFP/A20-mScarlet/TNIP1-KO (TNIP1 KO) and MyD88-GFP/A20-mScarlet-TNIP1-Halo (TNIP1 KO + TNIP1-Halo) EL4 cells.

c) Western blot analysis of phosphorylated JNK (pJNK, upper panel) and JNK (lower panel) after 0-, 15-, 30- and 60-min of IL-1β stimulation of MyD88-GFP/A20-mScarlet (parental cell line), MyD88-GFP/A20-mScarlet/TNIP1-KO (TNIP1 KO) and MyD88-GFP/A20-mScarlet/TNIP1-Halo (TNIP1 KO + TNIP1-Halo) EL4 cells.

d) IL-2 release of MyD88-GFP/A20-mScarlet (parental cell line), MyD88-GFP/A20-mScarlet/TNIP1-KO (TNIP1 KO) and MyD88-GFP/A20-mScarlet/TNIP1-Halo (TNIP1 KO + TNIP1-Halo) EL4 cells. IL-2 release was measured by ELISA after 24 h of IL-1β stimulation. Values are shown relative to the parental MyD88-GFP/A20-mScarlet cell line. Average values were calculated from three independent experiments. Bars represent ± SEM.

2.3.4 IL-1β stimulation leads to lower IL-2 release in TNIP1 KO cells

Finally, I investigated how perturbation of TNIP1 effects the long-term IL-1β signaling response. Because EL4 cells release IL-2 after 24 h of IL-1β stimulation[136], I assessed IL-2 release of the parental MyD88-GFP/A20-mScarlet cell line, the corresponding TNIP1 KO and reconstituted TNIP1-Halo cell line using ELISA (Fig. 16 d). Unexpectedly, 24 h IL-1β stimulation of TNIP1 KO cells results in decreased IL-2 release by approximately a factor of 2. If TNIP1 is exclusively a down regulator in IL-1β mediated signaling, IL-1β stimulation of TNIP1 KO cells should result in higher IL-2 release compared to the parental cell line. Reconstitution of the TNIP1 KO cell line with TNIP1-Halo only partly rescues IL-2 release, showing a 1,5-fold lower IL-2 release compared to the parental cell line. To summarize, perturbation of TNIP1 leads to a lower long-term IL-1β signaling response as measured by IL-2 release as a read out. However, this phenotype cannot be confirmed by the rescue TNIP1-Halo cell line.

3 Discussion

IL-1β signal transduction is crucial for acute inflammation. Upon IL-1β stimulation MyD88, IRAK4 and IRAK1 are recruited to the activated receptor together forming the myddosome[27]. The myddosome triggers a series of biochemical reactions that culminates in the activation of the NF-κB and MAPK signaling pathways. Therefore, the activation of downstream signaling is encoded by the spatial and temporal dynamics of myddosome associated protein signaling networks[27,137]. The spatial and temporal dynamics of the intracellular IL-1β signaling network are indispensable for a specific cellular response[137], but to this day remain the magnitude and definitive list of myddosome associated signalling proteins remains uncharacterized.

In this thesis, I took a system approach to study the intracellular IL-1β protein signaling network, and using MS-IP I temporally characterized the myddosome associated interactome. This interactome identified known and unknown protein interactors with MyD88, IRAK4 and IRAK1 (Fig. 7). My analysis of this time-resolve proteomic data set found that the Myddosome associated interactome contains proteins associated with multiple cellular processes such as membrane trafficking, cytoskeleton and metabolism. The first conclusion I draw from this data set is that IL-1β signaling and myddosome are biochemically link to multiple cellular processes than was previously known or predicted.

In a follow up analysis, pathway annotation identified proteins potentially involved in the down-regulation of IL-1β mediated signaling (Fig. 9; Fig. 12). This analysis revealed the ubiquitin binding protein TNIP1 as a protein that binds to all myddosome proteins (MyD88, IRAK4, IRAK1), and this interaction was induced by IL-1β stimulation. Interestingly, an unbiased investigation of IL-1β dependent protein synthesis identified the increased *de novo* synthesis TNIP1 (Fig. 13). Colocalization experiments of TNIP1 revealed that TNIP1 colocalizes with MyD88, IRAK4, IRAK1 and A20, TNIP1's previously published interaction partner for NF-κB inhibition (Fig. 14; Fig. 15). Characterization of TNIP1 in IL-1β mediated signaling reveals that TNIP1 downregulates and attenuates IL-1β signal transduction (Fig. 16). While TNIP1 KO cells show an increase in phosphorylation levels of p65, phosphorylated JNK levels and IL-2 release are decreased. These result in TNIP1 KO cells were unexpected, and suggest that a TNIP1-A20 axis regulates both the MAPK and NF-kB signaling response. These results will be discussed below.

3.1 Interactome analysis of all myddosome proteins in endogenously tagged EL4 cells provides high temporal resolution of IL-1β mediated signaling dynamics

This work provides a highly temporally resolved interaction map of all myddosome components (MyD88, IRAK4, IRAK1) involved in IL-1β mediated signaling (Fig. 8). This interaction map is highly valuable for the field, because (1) it provides an IL-1β specific interactome analysis; (2) it infers the interaction kinetics; (3) it quantifies the interactome of all myddosome proteins individually at their endogenous expression levels, thus avoiding overexpression artifacts; (4) because the SP3 technology used in the preparation of the MS samples ensures highest sensitivity in the proteomic analysis; (5) it compares the full MyD88-interactome with those formed on IRAK4 an IRAK1 KO backgrounds, providing crucial insights into the specific roles of each myddosome component; and (6) it identifies proteins potentially involved in downregulation of IL-1β signal transmission.

The myddosome interactome analysis is specific for IL-1β signal transduction

So far, interactome analysis of the IL-1β dependent myddosome has been limited. These interaction analyses are limited in temporal resolution, being restricted to a single stimulation timepoint compared to unstimulated conditions. Further, only specific proteins are identified by immunoprecipitation followed by western blot analysis (e.g.[138–141]), therefore introducing a bias in analysis which is avoided in this work. Further, the myddosome's interactome upon TLR activation is often equated with the IL-1β-dependent myddosome's interactome. However, given the differences in TLR and IL-1R1 signaling outputs, the interactomes of the respective myddosomes, unsurprisingly, partially differ[142]. For example, TIR-containing adapter protein (TIRAP) binds to MyD88 upon TLR2 and TLR4 activation and is necessary for signal transduction, but is not required for IL-1β mediated signaling[143,144]. Besides, myddosome interactome studies in TLR-dependent contexts only examine the interactome of one myddosome protein, usually MyD88 (e.g.[145]). This data is valuable, but does not reflect the interactome similarities and differences of all myddosome components, specifically ignoring IRAK4 and IRAK1's interactome which are essential to understand their regulatory functions[31]. This is especially important since IRAK4 and IRAK1 are pharmaceutical drug targets in different diseases (e.g. hematologic malignancies including acute myeloid leukemia, or inflammatory diseases including rheumatoid arthritis)[146,147].Therefore, this work specifically examines the IL-1β-dependent myddosome interactome and extends the existing knowledge in the field by including protein interaction data of all myddosome components MyD88, IRAK4 and IRAK1, respectively.

The IL-1β-dependent myddosome interaction map allows to infer the interaction kinetics

Similar to this study, Wu and colleagues provide an interactome map of MyD88, TRAF6 and NEMO, though in a TLR4 dependent context. Yet, they were able to temporally resolve the interaction maps with only 5-min of stimulation differences [148]. Within my experimental setup, GFP-IP-MS analysis of 5-min IL-1β stimulated EL4 cells did not detect significant differences between unstimulated and 5-min stimulated samples (data not shown). These two results might reflect the kinetic differences between IL-1β signal transduction and other MyD88-dependent signaling pathways such as TLR4. Myddosome formation is not only essential for signal transmission after IL-1β, but also after IL-18, IL-33 stimulation or stimulating different TLRs[32,149]. These signals are transmitted through the myddosome, but generate a stimulus specific response. As such, IL-33 stimulation leads to B and T cell proliferation, stimulating TLR4 activates the proinflammatory response, and IL-1β stimulation activates both innate and adaptive immune cells[26,27,32,150]. Therefore, the myddosome is the core of these pathways, but triggers different downstream protein signaling networks with different kinetics dependent on the stimulus[32,137]. Accordingly, the IL-1β and TLR4 stimulation induced myddosome might activate a (1) a different downstream signaling network (2) with differing interaction kinetics post stimulation.

Application of EL4 cells to investigate the interactome of the myddosome

To construct and resolve the myddosome interaction map, I used gene edited derivatives of the mouse lymphoma T cell lines EL4.NOB1. This cell line is highly sensitive to IL-1β and can easily be genetically manipulated, therefore making a good cellular model to study molecular mechanism of IL-1 signaling[121,122]. The EL4 cell line is derived from a type of T cell cancer in mice[151,152]. Applying a cancer cell line to study an immune signaling pathway is accompanied by several disadvantages[153]. For example, cancer cell lines' signaling pathways might differ from non-cancer cell lines. These signaling differences are mostly due to oncogenic mutations, which are also observed in lymphoblastic lymphoma[152,153]. However, potential mutations in EL4 cells are not characterized. Besides, a variety of IL-1β signal transducing proteins have been shown to be cell type independent and have also been identified in EL4 cells[27,78,122,151,154]. Therefore, it is rather unlikely that IL-1β mediated signaling in EL4 cells differ from other non-cancer cell lines. Besides, ubiquitination events, also regarding the MAPK-JNK/ERK axis, can be perturbed in cancer cells[155–157]. Whether this is the case in EL4 cells is unknown. Currently ongoing IFS experiments for M1- and K63-ubiquitin in EL4 cells do not show any abnormalities (unpublished data, Fakun Cao). Last but not least, IL-1β stimulation of EL4 cells leads only

to IL-2 secretion, characterized after 24 h of IL-1β stimulation. In contrast, other cytokine responses to IL-1β stimulation have been observed in other cell lines. As such, fibroblasts release cytokines such as vascular endothelial growth factor (VEGF), matrix metalloproteinase-1 (MMP1) and prostaglandin E2 (PGE_2) also after 24 h of IL-1β stimulation[158]. Other studies in e.g. macrophages, the readout of IL-1β stimulation has focused more on gene expression e.g. by qPCR. Therefore, current investigations in the lab aim to identify other IL-1β dependent activated genes, also at timepoints earlier than 24 h post stimulation. To conclude, using EL4 cells to study IL-1β mediated signaling is accompanied by some uncertainties, but they are a well-established model system to study IL-1 signal transduction. Nevertheless, any finding should be validated using primary cells.

As a consequence, using myddosome-tagged EL4 cell lines, I was able to establish an IP-MS workflow for identifying the temporal dynamics of myddosome interacting proteins following IL-1β stimulation (Fig. 6). The feasibility of this approach is further underpinned by the identification of previously known interacting proteins of either MyD88, IRAK4 and IRAK1 (Fig. 7). However, not all previously known interacting proteins were identified. Most strikingly given the fact that myddosome formation is essential for IL-1β signal transduction[159], MyD88 was not detected in the IRAK4- and IRAK1-IPs after 15- and 30-min of IL-1β stimulation. Similarly, IRAK1 and IRAK4 were not detected in the MyD88-IPs after 15-min of IL-1β stimulation and only IRAK1 but not IRAK4 was detected in the 30-min MyD88-IP datasets. Only after 60-min of IL-1β stimulation were MyD88, IRAK4 and IRAK1 detected in all IP-samples (App. Tab. 3; App. Tab. 6; App. Tab. 9). Therefore, the myddosome proteins' interactions are stable after 60-min of IL-1β stimulation (as detected by IP-MS).

Utilization of fluorophore protein tags serves dual purposes, considering that they can be used for both imaging and interaction analysis (Fig 9; Fig. 14)[160]. Therefore, we can use identical cell lines for both interactome analysis and colocalization confirmations, at the same time avoiding noise from non-specific antibody binding signal in IFS. However, given the fluorescent protein's large size (28 kDa for GFP, 26.4 kDa for mScarlet) it may also interfere with the function of the protein it is fused to[161]. In part, this is also the case for this work: endogenous tagging of myddosome proteins with GFP and/ or mScarlet in EL4 cells leads to a decrease in IL-2 secretion upon 24 h of IL-1β stimulation (App. Fig. 3). Yet, translocation of p65 after 30-min of IL-1β stimulation was not statistically different between WT with MyD88, IRAK4 and IRAK1 tagged EL4 cell lines (App. Fig. 4)[122]. Therefore, we concluded that tagging MyD88, IRAK4 and IRAK1 does not interfere with the IL-1β mediated signaling response at the timepoints investigated by IP-MS.

As with any immunoprecipitation study, the resultant interaction map has its limitations. As such, some transient or weak interactions may have not been detected[162]. This limitation could be overcome by applying proximity-dependent proteomic analysis. Proximity labeling relies on genetically encoded enzymes to produce a short-lived free radical that is coupled to a detectable chemical group, usually biotin. The reactive biotin intermediate reacts with electron-rich amino acid side chains, thereby covalently biotinylating proteins in direct proximity to the enzyme. Biotinylated proteins are then purified using streptavidin and further prepared for MS analysis. A key feature of proximity labeling is that the genetically encoded enzyme is fused to the protein of interest, allowing labeling reactions in living cells. Therefore, coordination of IL-1β stimulation and enzyme activation time would allow temporally resolution of the IL-1β protein network[163,164]. However, proximity labeling technologies have their limitations[164]. The main limitation for this project is that proximity labeling has only been applied in standardized cell lines such as HEK cells, which naturally do not express IL-1R1. Therefore, applying this technique for IL-1β signaling network resolution would not be under physiological conditions, which was one major consideration in this work.

SP3 technology for MS sample preparation ensures highest sensitivity in proteomic analysis

Another unique feature and big advantage of this myddosome interaction map is the application of SP3 technology for proteomic sample preparation (Fig. 6 c). SP3 is based on paramagnetic beads, which are coated with carboxylate functional groups. Adding ACN to the proteomic sample induces protein binding to the beads. In a next step protein-bead mixture is washed to exclude any contaminants. Purified proteins are then eluted by enzymatic digestion for subsequent proteomic analysis. SP3 allows the processing of low input amounts and is further compatible with chemicals such as detergents such as SDS, which was present in the IP-sample buffer[165]. Proteomic analysis of SP3 processed samples identified more proteins and peptides compared to samples processed by other preparation methods, e.g. in-solution integrated StageTip (iST)[165,166]. Therefore, applying SP3 to process the myddosome-IP samples allowed enhanced protein and peptide recovery resulting in higher sensitivity in the proteomic analysis compared to other proteomic analysis of the myddosome interactome analysis (e.g.[145,167]).

Characterization of the MyD88's interactome at intermediate stages of myddosome formation

Complete myddosome formation is essential for IL-1β signal transduction, but the molecular mechanisms of myddosome assembly is not completely understood[130]. Therefore, I identified MyD88-interactors at the different stages of myddosome formation. Specifically, I compared IL-1β-dependent MyD88-interactomes in a 'WT' background to those in IRAK4 KO or IRAK1 KO backgrounds (section 2.1.6; Fig. 11). Since IRAK KO cells are unresponsive to IL-1β

(App. Fig. 3), because they cannot form full myddosomes, this approach identifies MyD88 interactors that dependent on (1) only MyD88, (2) MyD88 and IRAK4 or (3) full myddosome formation. Characterization of the interactome at its intermediate steps of assembly reveals unknown proteins involved in the assembly process, which could be helpful in developing allosteric regulators of the myddosome[168]. Ideally, to provide a complete characterization of the entire myddosome interactome, IL-1β-dependent IRAK4 and IRAK1 interactomes should also have been compared in a MyD88 KO and IRAK4/1 KO, respectively.

Interestingly, MyD88 forms big oligomers in IRAK4 KO but not IRAK1 KO cells after IL-1β stimulation[169]. A potential reason for this observed phenomenon might be a conformational change of MyD88, allowing more and more MyD88 to bind. Specifically, n-acetylation may lead to differences in protein conformation and interaction capacities[170]. Investigation of the different MyD88 interactomes shows that cohesin 1 homologue (ESCO1) binds to MyD88 in the WT and IRAK4 KO but not IRAK1 KO background (Fig. 11 c). Comparison of the differences in abundance (stimulated – unstimulated) of ESCO1 in the WT and IRAK4 KO background shows that the differences in abundances in the IRAK4 KO background are higher than in the WT background. Therefore, the higher differences in abundance of ESCO1 in the IRAK4 KO than in the WT background suggests that ESCO1 is involved in this observed phenomenon of big MyD88 oligomer formation. ESCO1 is a lysine-acteyltransferase with characterized function in the cell cycle, specifically chromatid cohesion. N-acetylation is a post-translational modification not restricted to histone-proteins. N-acetylation of non-histone proteins is engaged in further cellular processes amongst others signal transduction[169]. Given the restricted knowledge of substrate specificity for lysine transferases Esco1 might also exhibit its acetyltransferase function on MyD88, thereby inducing a conformational change leading to the observed big MyD88 oligomers[169]. Live cell imaging of MyD88-GFP/IRAK1-mScarlet cells on IL-1β functionalized SLB treated with a lysine-acteyltransferase inhibitor, would prove if acetylation effects MyD88 oligomerization. Performing this experiment in ESCO1 KO cells without prior lysine-acteyltransferase inhibitor treatment could also confirm if formation of big MyD88 oligomers is dependent on ESCO1.

The interactome analysis of MyD88-GFP in the different IRAK KO backgrounds, identified proteins that bind to MyD88 in the IRAK1 but not IRAK4 KO background, namely Hras, TPM1, TRIM6, MICAL1 and IL-16 (Fig. 11). Since IRAK4 binds to MyD88, initiating IRAK1 interaction, these proteins require IRAK4 for MyD88 binding[27]. However, comparison of the differences in abundances (stimulated – unstimulated) of those proteins identified in the IRAK1 but not IRAK4 KO background between the ‘WT’-MyD88 IP and the IRAK1-KO-MyD88-IP

indicates that Hras and TRIM6 show a higher the differences in abundances in the IRAK1 KO background than in the WT background. Since, IRAK1 is essential to initiate further downstream signaling events (Sub. Fig. 3)[171], proteins binding to MyD88 (including IRAK4) in IRAK1 KO cells might be degraded to enable Il-1R1 activation at another IL-1β stimulation time point. Trim6 is a E3-ubiqutin ligase generating K48-linked ubiquitin chains, targeting proteins for degradation[172]. Therefore, TRIM6 might ubiquitinate MyD88 and its interacting proteins for subsequent degradation. However, if IL-1β stimulation leads to degradation of MyD88 binding proteins in IRAK1 KO cells remains unknown and needs to be verified first. MyD88-IPs after stimulating MyD88-GFP/IRAK1-KO and MyD88-GFP cells, followed by K48-linked ubiquitin specific WB analysis could reveal that perturbation of IRAK1 leads to more K48-linked ubiquitination of MyD88. Repeating this experiment in IRAK1-TRIM6 double KO cells might show similar extents of K48-linked ubiquitination of MyD88 compared to MyD88-GFP cells. Hras is a Ras-GTPase, distributing to the disordered plasma membrane once activated, facilitating endocytosis[173,174]. Thus, Hras might initiate endocytosis of the activated IL-1R1 with bound MyD88, IRAK4 and other proteins to allow potential IL-1R1 re-activation at a later stimulation time point. MyD88-IPs after stimulating IRAK1 KO cells and WB analysis specific for early endosomes (e.g. Rab5[175]) could reveal if the MyD88 complex in IRAK1 KO cells gets endocytosed. Repeating this experiment using an IRAK1-Hras double KO cells might reveal if MyD88 complex endocytosis is Hras -dependent.

To summarize, the approach of linking immunoprecipitation with proteomic analysis in different KO backgrounds is unique and has so far not been performed even for other signal transmitting complexes e.g. TLR-dependent myddosomes. Therefore, the provided MyD88-interactome analysis in the 'WT', IRAK4 KO and IRAK1 KO cells reveals numerous proteins that may be involved in myddosome formation and the phenomenon of huge MyD88 oligomer formation in the absence of IRAK4, but further experiments are required to specifically identify their functions[122].

Pathway annotation analysis identifies proteins with potential downregulating properties in IL-1β signaling

To pursue the aim of identifying proteins potentially involved in downregulating IL-1β and myddosome signal transduction, I performed pathway annotations of all identified proteins in the temporally resolved interaction map. From this analysis, I identified TNIP1 as a prime candidate as a downregulation of IL-1β mediated signaling (Fig. 9 a & c). Pathway annotation strategies are valuable for understanding the underlying biology but are accompanied by several

limitations[176]. One limitation is that functional annotations are only available for limited numbers of proteins, simply because not every protein's function has been characterized[177]. Therefore, other proteins of the myddosome interaction map might exhibit downregulatory properties that have previously not been described, thus not identified by the here conducted pathway annotation strategy. Thus, the myddosome interaction map might include other important potential downregulating proteins other than TNIP1, MAP3K1, KCTD10, Thy1, TRIM6, A20, STAMBPL1, NCOR1 and VRK3 (Fig. 12).

Conclusion: The IL-1β-dependent myddosome is linked to multiple cellular processes

Taken together, the IL-1β-dependent myddosome interaction map is a novel approach for the field due to its specificity to IL-1β signal transduction, high temporal resolution and sensitivity, thereby temporally resolving previously known-, but especially previously novel myddosome interaction partners. Follow up investigations of those proteins may unravel new insights into IL-1β mediated signaling and its link to further cellular processes. Specifically, using KO cell lines of those proteins followed by the investigation of early, intermediate, and signaling events will characterize their function regarding IL-1β signal transduction.

3.1.2 TNIP1 is a myddosome associated protein upon IL-1β stimulation

TNIP1 is a known inhibitor of NF-κB activation in TCR/CD28, TLR, CD40, TNF-, IL-17 and partly in IL-1α mediated signaling and is known to interact with a variety of proteins (Fig. 10 a)[86,87,90–92,178,179]. In the context of the myddosome interactome, TNIP1 has been identified as a MyD88- and IRAK1 interacting protein upon TLR stimulation[93,180]. Here, I have shown that TNIP1 also interacts with MyD88 and IRAK1 upon IL-1β stimulation (Fig. 7; Fig 8). Further, analysis of the IL-1β-dependent myddosome interactome analysis reveals that TNIP1 also associates with IRAK4, extending the list of TNIP1-interacting proteins (Fig. 7). Other than previous studies, this work also temporally resolves the presence of TNIP1 over the course of IL-1β signaling, showing an increase in its abundance with increasing IL-1β stimulation time in all IP-datasets. Accompanied by the fact that TNIP1 does not bind to MyD88 in an IRAK4 and IRAK1 KO background (Fig. 11; Fig. 12) the results emphasize that TNIP1 only interacts with fully formed myddosomes. Combining its interaction with the IL-1β myddosome with previous reports that TNIP1 interacts with MyD88 and IRAK1 upon TLR, this work suggests that TNIP1 is a regulator of myddosome dependent signaling events[93,180].

Strikingly, TNIP1 is not identified in the IRAK4-IP after 60-min, but only after 15- and 30-min of IL-1β stimulation. This observation might explain why TNIP1 has previously not been identified as an IRAK4 interacting protein: TNIP1 interacts with IRAK4 at rather earlier stimulation

time points, which previously have not been investigated. As more time elapses after stimulation, IRAK4 is *trans*-autophosphorylated on three residues, which reduces protein-protein binding affinities[149,181,182]. As such, IRAK4's phosphorylation status is hypothesized to negatively affect myddosome stability[149,181]. Possibly, phosphorylation of IRAK4 might change the TNIP1 binding interface, thereby preventing TNIP1 binding after 60-min of stimulation. Colocalization experiments of TNIP1 and IRAK4 in cells treated with a specific IRAK4 phosphorylation inhibitor compared to untreated cells after 60-min of IL-1β stimulation could prove this hypothesis.

3.2 TNIP1 is *de novo* synthesized upon IL-1β stimulation

Cell signaling pathways influence different cellular systems including the secretory, transcriptional and translational networks[34,111]. Up to now, the effects of IL-1β stimulation have been defined in terms of cytokine release and the transcriptional changes[27,136]. However, mRNA increase due to transcriptional upregulation does not necessarily correlate with an increase at the translational level[111]. Therefore, I investigated IL-1β stimulation-dependent *de novo* protein synthesis in a time course of 0-, 30-, 60-, 120- and 240-min post stimulation (Fig. 13 a & b). Combining pSILAC with AHA-click chemistry and quantitative proteomics provides more indepths characterization of the regulation of protein synthesis[132,183]. However, pSILAC/AHA quantitative approaches are subjected to the following caveats: For one, the detected protein must have a turnover rate compatible with the experimental duration, even in the untreated condition. Otherwise, SILAC amino acids and AHA cannot be incorporated and detected accordingly[184]. Secondly, high levels of AHA in the labeling media and amino acid starvation prior pSILAC, AHA and according stimulation (here IL-1β) may change intracellular signaling as well as protein expression profiles[185,186]. Finally, some proteins might not get detected due to a low methionine content and/ or show generally a low incorporation of artificial amino acids. However, the effects of these technical concerns on my data are limited since stimulated samples are always normalized to corresponding unstimulated samples[186,187]. Consequently, the combined pSILAC/AHA quantitative approach revealed that IL-1β stimulation leads to *de novo* synthesis of nine proteins in WT EL4 cells (Fig. 13). Except for basic helix-loop-helix family member E4 Bhlhe40 (Bhlhe40) all significantly detected proteins are involved in NF-κB signaling. IL-1β mediated signaling activates the NF-κB pathway and NF-κB initiates the expression of its own signaling proteins[27,34,87,188,189]. Therefore, detection of these known NF-κB mediating proteins proves feasibility of the applied pSILAC-AHA approach using IL-1β stimulated EL4 cells.

The remaining identified protein, Bhlhe40, is a transcription factor, crucial for tissue resident memory T (T_{RM}) cell survival and activity amongst others in the context of infection. Influenza infection of T_{RM} cells leads to the upregulation of Bhlhe40, which in turn activates the expression of multiple mitochondrial genes important for cell survival[190,191]. Accordingly, expression of Bhlhe40 upon IL-1β stimulation in EL4 cells might therefore also contribute to EL4 cell survival by supplying energy through upregulation of mitochondrial genes. Investigation of IL-1β -dependent upregulated genes in EL4 cells could prove if mitochondrial genes are indeed upregulated. Additionally, comparison of IL-1β-dependent upregulated mitochondrial genes in EL4 WT with Bhlhe40 KO cells could confirm that Bhlhe40 upregulates these genes for cell survival.

One aim of this work was to identify proteins potentially involved in downregulating IL-1β mediated signaling. Pathway annotation analysis of IL-1β -dependent *de novo* synthesized proteins identified the two NF-κB inhibitors NFKBIA and NFKBID, whose inhibitory function has explicitly been characterized[192]. Further, this pathway annotation analysis identified TNIP1, as previously in the IP-MS myddosome interactome analysis (Fig. 7). First, I hypothesized that IL-1β-dependent *de novo* synthesis of TNIP1 compensates TNIP1 degradation, since TNIP1 associates to the formed myddosome, whose components -potentially including TNIP1 - eventually get degraded[131]. However, with increasing IL-1β stimulation time even total TNIP1 protein slightly increases (Fig. 13 d). Comparison of the amounts of *de novo* synthesized and total TNIP1 protein indicates that some TNIP1 degradation is happening, but IL-1β -dependent TNIP1 *de novo* synthesis prevails (Fig. 13 c & d). These observations are striking since TNIP1 is specifically degraded in the IL-1-related TLR4 and IL-17R signaling pathways[90,108]. Therefore, this work indicates a new characteristic of TNIP1 in the context of the IL-1β signaling pathway. In TLR4 and IL-17R signaling, TNIP1 exclusively inhibits NF-κB activation[90,108]. Therefore, TNIP1 degradation allows the cell to respond to a potential reoccurring stimulation. Indeed, re-activation of TLR4 initiates a NF-kB response. At the same time, re-exposure to IL-1β also initiates a NF-κB response[120]. Since TNIP1 does not exclusively attenuate but also activates IL-1β signal transduction (Fig. 16), *de novo* synthesis of TNIP1 enables the cell to respond to IL-1β in case of a re-exposure. A comparison the NF-κB response of IL-1β re-stimulated WT and TNIP1 KO cells could prove this hypothesis.

TNIP1 expression levels have been shown to vary by cell type and stimulus[87,88,90,92,108–110]. This work demonstrates an IL-1β-dependent increase in TNIP1 protein levels, driven by *de novo* synthesis, specifically in EL4 cells. TNIP1 expression differs dependent on the cell types and stimuli[87,88]. Therefore, it remains elusive if and to what extent IL-1β -dependent TNIP1 protein

level is changing in different cell lines. TNIP1 protein level investigations in other IL-1 responsive cells may confirm this hypothesis and reveal potential differences in TNIP1 amounts between different cell types.

3.2.1 IL-1β-dependent *de novo* synthesis of TNIP1 is a translational but not transcriptional feedback in EL4 cells

IL-1β stimulation of EL4 cells leads to *de novo* synthesis of TNIP1 (Fig. 13 b & c). Since protein translation is thought to be dependent on mRNA expression, I hypothesized that TNIP1 mRNA levels upon IL-1β stimulation are increased[193]. However, TNIP1 specific qPCR contradicts this expectation and shows that TNIP1 mRNA expression level is largely unchanged (Fig. 13 e). Therefore, IL-1β-dependent *de novo* synthesis of TNIP1 is a translational but not transcriptional feedback in EL4 cells. Many pathways, including the MAPK pathway, have been shown to regulate protein synthesis, e.g. through phosphorylation of translation factors or modulating the stability of specific mRNAs[194]. Since IL-1β signal transduction also activates the MAPK pathway, this signaling route might also induce *de novo* synthesis of TNIP1, by e.g. stabilizing TNIP1 mRNA for subsequent translation[27,32]. Investigation of TNIP1 *de novo* synthesis after IL-1β stimulation with MAPK inhibition would reveal if IL-1β-activated MAPK signaling is involved in IL-1β-dependent synthesis of TNIP1.

In contrast, mRNA analysis of other cell lines stimulated with IL-1β do show an increase in TNIP1 mRNA[92,195]. EL4 cells generally do not show high gene expression levels post-stimulation, even after treatment with strong stimuli such as phorbol myristate acetate (PMA) and calcium ionomycin (I)[196]. These results are coherent with a microarray analysis of EL4 cells, performed in-house, upon IL-1β stimulation (data not shown). Since other cell lines than EL4 cells do show an increase in TNIP1 mRNA level, investigation of IL-1β-dependent *de novo* synthesized TNIP1 in other cell lines might be reveal a greater increase *de novo* synthesized TNIP1 than detected here in EL4 cells. Nevertheless, *de novo* synthesis of TNIP1 emphasizes that IL-1β mediated signaling can potentiate protein translation.

3.3. TNIP1 in IL-1β mediated signaling: a protein with dual functionalities?

Most protein interactions of TNIP1 connect it to inhibition of NF-κB signalling[87]. To evaluate the possible function of TNIP1 in IL-1β signaling, I searched for TNIP1 interaction partners in the MyD88-, IRAK4- and IRAK1-IP data sets (Fig. 10). This analysis suggests a correlation in abundance of TNIP1 and A20 (Fig. 9 b & c; Fig. 10): smaller increase after 15- and 30-min stimulation but a larger increase after 60-min of stimulation. Because TNIP1 only binds to

MyD88 in 'WT' but not IRAK4/1 KO cells and A20 only associates with IRAK1 (Fig. 11 c; Fig. 12 a & b; Fig. 9 b & c), I infer that TNIP1 and A20 both require full myddosome formation for interaction. Colocalization of MyD88 and TNIP1 with A20 after 30-min of IL-1β stimulation further highlights this correlation (Fig. 15). Performing TNIP1-IPs post IL-1β stimulation with the detection of A20 could prove a stable, IL-1β-dependent and stable TNIP1-A20 interaction.

To characterize TNIP1's functionality in the context of IL-1β mediated signaling in general but also specifically regarding its interaction with A20, I generated a TNIP1 KO cell line in an MyD88-GFP/A20-mScarlet background (Fig. 16 a). However, I was able to generate only one TNIP1 KO monoclonal cell line. As a consequence, characterizations of TNIP1 perturbation in IL-1β mediated signaling are based on only one TNIP1 KO monoclonal cell line (Fig. 16 b-d). This caveat can be problematic and lead to misinterpretation of TNIP1's function in IL-1β mediated signaling, because different KO clones show different signaling effects (e.g.[197–199])[200]. Therefore, all conclusions derived from the TNIP1 KO EL4 cells should be verified using another newly generated TNIP1 KO monoclonal cell line.

Deletion of TNIP1 on an MyD88-GFP/A20-mScarlet background enables the characterization of the TNIP1-A20 relationship when getting recruited to the activated myddosome in live cells. As expected, first results show that in the absence of TNIP1, less A20 is recruited to the myddosome (data not shown; ongoing work). Previous studies characterized the TNIP1-A20 relationship after TCR and TLR4 stimulation and in TNFα and IL-17 mediated signaling[90,91,93,103]. This work confirms the TNIP1-A20 relationship in an IL-1β stimulation setting.

TNIP1 binds to A20 and M1-linked ubiquitinated substrates, thereby linking A20 to its substrate and facilitating A20's deubiquitinating activity. Subsequently, IKK-complex activity is prevented and p65 is phosphorylation is inhibited [85,88]. Therefore, since A20 is not recruited to the myddosome in TNIP1 KO cells upon IL-1β stimulation, phosphorylation levels of p65 in the TNIP1 KO are increased compared to the parental cell line, while the reconstituted TNIP1-Halo cell line shows similar levels of phosphorylated p65 as the parental cell line (Fig. 16 b). Taken together, we conclude that TNIP1 facilitates A20 binding to ubiquitin to downregulate phosphorylation of p65, also in an IL-1β stimulation setting. As evidence that the observed increased phosphorylation of p65 is due to the association of A20 with TNIP1, A20 KO cells should show similarly increased levels of phosphorylated p65. Nevertheless, the level of phosphorylated p65 in the TNIP1 KO also decreases from 15- to 60-min of IL-1β stimulation time,

suggesting that other downregulatory mechanisms apply to prevent continuous phosphorylation of p65 (Fig. 16).

Next to the IKK-IκB pathway, IL-1β signaling is also transduced by the M1-linked ubiquitin independent MAPK-JNK/ERK pathway[27,32]. To clarify the effect of TNIP1 perturbation on this IL-1β signaling route, I evaluated the phosphorylation level of JNK in TNIP1 KO, parental and reconstituted TNIP1-Halo cell lines after 0-, 15-, 30- and 60-min of IL-1β stimulation (Fig. 16 c). Unexpectedly, TNIP1 KO cells do not show any phosphorylation of JNK at any stimulation time point while the parental and the reconstituted TNIP1-Halo cell line show phosphorylation of JNK after 15- and 30-min of stimulation.

The MAPK-JNK/ERK pathway is initiated by K63-linked ubiquitin chain generation. K63-linked ubiquitin chains are also bound by TNIP1. However, binding of TNIP1 to K63-linked ubiquitin binding does not recruit A20. Instead, TNIP1's binding to K63-linked ubiquitin is thought to inhibit the IKK-IκB pathway by competing for K63-linked ubiquitin with NEMO[86]. However, NEMO binds M1-linked ubiquitin with 100x higher affinity than K63-linked ubiquitin[201]. Therefore, it is rather unlikely that TNIP1 and NEMO compete for K63-linked ubiquitin. The lack of JNK phosphorylation in TNIP1 KO cells also suggests that TNIP1 binding to K63-linked ubiquitin chains exerts a different function (Fig. 16 c). In the MAPK-JNK/ERK pathway, K63-linked ubiquitination of the TAB-TAK1-TRAF6 complex initiates a MAPK signaling cascade[27,32,33]. While K63-linked ubiquitination of TAK1 (a MAPKKK) has already been characterized, ubiquitination characteristics of the subsequently activated MAPKKs remain elusive[202]. Yet, MAPKK3 has been shown to contain conjugated K63-linked ubiquitin chains in the context of cell differentiation. MAPKK3 is also involved in the IL-1β signaling mediated MAPK-JNK/ERK pathway[203]. Therefore, TNIP1's binding to K63-linked ubiquitin chains may facilitate MAPKKs' binding to K63-linked ubiquitin chains. In turn, this is necessary for the activation of further downstream MAPK-JNK/ERK signaling events such as phosphorylation of JNK. Consequently, if TNIP1 is absent, phosphorylation of JNK cannot occur (Fig. 16 c). IP analysis of TNIP1 and MAPKKs in an IL-1β stimulation context with and without prior K63-linked ubiquitin chain inhibitor treatment in different cell lines could confirm (1) a TNIP1-MAPKK interaction, (2) a potential K63-linked ubiquitin chain dependency and (3) a cell type independence of the observed MAPKK interaction.

Lastly, I characterized how TNIP1 affects long-term IL-1β mediated signaling, in the form of IL-2 secretion after 24 h of IL-1β stimulation in EL4 cells. I compared IL-2 secretion of stimulated TNIP1 KO cells to the parental cell line (Fig. 16 d)[136]. If TNIP1 would exclusively be a

down-regulator of IL-1β mediated signaling, TNIP1 KO cells should secrete more IL-2 than the parental cell line. Unexpectedly, TNIP1 KO cells secrete roughly half as much IL-2 compared to their parental cell line (Fig. 16 d). Unlike phosphorylation of signaling proteins, the decrease of IL-2 production in TNIP1 KO cells in response to IL-1β stimulation was not completely rescued in the reconstituted TNIP1-Halo cell line, therefore suggesting that the observed decrease in IL-2 might not be specifically due to a loss of TNIP1. However, the reconstituted TNIP1 cells do not express native TNIP1 protein, but instead a Halo-tag fused to the C-terminus of TNIP1. Comparison of IL-2 secretion from EL4 cells expressing various endogenously-tagged proteins show that, with an increasing number of expressed tags, IL-2 secretion decreases (App. Fig. 3)[122]. Reconstitution of the TNIP1 KO cell line with a TNIP1 construct not bearing a tag would allow us to evaluate if the IL-2 decrease in TNIP1 KO cells is TNIP1-dependent.

Even though stimulated EL4 cells generally show low gene expression levels, microarray analysis of IL-1β stimulated EL4 WT cells show an increase in IL-2 mRNA already after 2 h of stimulation (Fig. 17)[196]. The kinetics of IL-2 transcription can serve as an intermediate readout of IL-1β stimulation between the rapid protein phosphorylation and longer-term cytokine production. To evaluate the effect of TNIP1 perturbation on IL-2 mRNA levels we repeated the microarray analysis, but this time with the MyD88-GFP/A20-mScarlet/TNIP1-KO cell line (Fig. 17). IL-1β stimulation of TNIP1 KO cells for 2 and 4 h resulted in a decreased IL-2 mRNA fold change by a factor of approximately 2 compared to WT cells. This result correlates with halved IL-2 release detected for TNIP1 KO cells (Fig. 17, Fig. 16 d). IL-2 mRNA levels after 8 h and 24 h of IL-1β stimulation in TNIP1 KO cells are only slightly enriched (Fig. 17). The microarray assessed IL-1β-dependent mRNA changes in EL4 WT cells, not expressing any fluorophore tag. In contrast, the TNIP1 KO cells do also endogenously express MyD88-GFP and A20-mScarlet. Since, these fluorophore tags reduce IL-2 secretion (App. Fig. 2; App. Fig. 3), the induction of IL-2 transcription in the TNIP1 KO cells is most likely affected and predicted to be lower than EL4 WT cells. Even though, I cannot specifically quantify in how far IL-2 mRNA expression is decreased due to TNIP1 perturbation, the microarray data shows that IL-2 mRNA expression is negatively affected in TNIP1 KO cells. Therefore, I conclude that the reduced IL-2 secretion observed in TNIP1 KO cells results from decreases IL-2 gene activation and not exclusively from perturbed IL-2 protein translation or secretion. To specifically quantify and evaluate the effect of TNIP1 perturbation on IL-2 expression IL-2 mRNA levels of the TNIP1 KO and its parental cell line need to be investigated side by side.

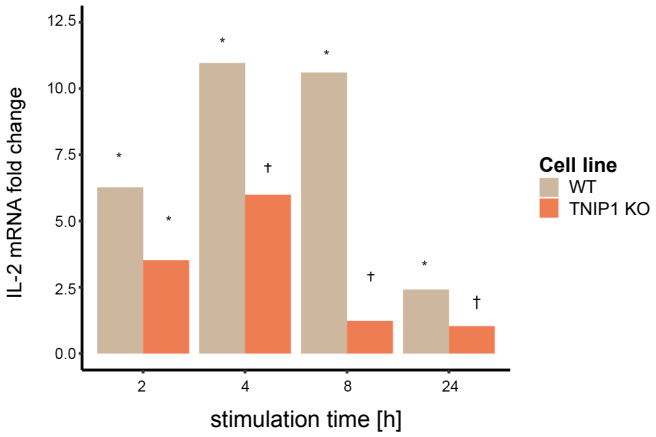

Fig. 17: IL-2 mRNA fold change comparing unstimulated and stimulated EL4 WT and MyD88-GFP/A20-mScarlet/TNIP1-KO (TNIP1 KO) cells identified by microarray analysis. Cell lines were stimulated with IL-1β for 0, 2, 4, 8 and 24 h, at two independent time points in triplicates. Cells were harvested and total RNA was isolated for subsequent microarray analysis. * indicates a fold change with a p-values < 0.01, † indicates a fold changes with p-values > 0.01 (RNA isolation and microarray measurements were executed by Ina Wagner, subsequent data analysis was done by Hans-Joachim Mollenkopf).

Both AP-1 and NF-κB signaling induce IL-2 expression[204]. However, it is not clear to what extent one or the other pathway drives IL-2 expression in EL4 cells. Accordingly, I cannot reason that the reduced IL-2 secretion in TNIP1 KO cells are exclusively a result of missing JNK phosphorylation. To evaluate if missing TNIP1 expression only affects AP-1-dependent IL-2 gene expression, drug induced activation of JNK, e.g. by SB202190, should rescue the IL-2 phenotype[205]. AP-1 and NF-κB partially cooperate to induce gene expression corresponding to specific stimuli by enhancing each other's activities, but can also exert inhibitory effects on one another[206]. Accordingly, TNIP1 might regulate NF-κB and AP-1 activity by attenuating NF-κB but enhancing AP-1 activation to balance their activity and temporally regulate the IL-1β stimulation output. AP-1 activation has a broad functional spectrum, including cell differentiation, proliferation, survival and apoptosis as well as activation of innate and adaptive immunity[207]. Therefore, TNIP1 enhanced AP-1 activation might contribute to a broad AP-1-dependent output.

Taken together, the characteristics of TNIP1 observed here are contradictory, in the sense that phosphorylation levels of p65 are increased, but phosphorylation levels of JNK and IL-2 secretion in TNIP1 KO cells are decreased. These observations suggest that TNIP1 exerts dual functionality: both downregulating and activating IL-1β mediated signaling. So far, TNIP1 has exclusively been described as a signal attenuator. Therefore, the signal-activating capacities of TNIP1 observed here contrast with our previous understanding of TNIP1. However, so far TNIP1 has not yet been characterized in an IL-1β stimulation-dependent context. Further, another protein of the Tnip protein family, Tnip2, has been shown to exhibit dual functionalities

by facilitation A20-dependent deubiquitination for signal attenuation and activation of the NF-κB signaling pathway[81–83]. As with TNIP1, Tnip2's characterized functions rely on its AHD1 for A20 binding and AHD2 for ubiquitin binding[87]. Interestingly, Papoutsopulou and colleagues showed that Tnip2 does not affect NF-κB signaling but is essential for sufficient MAPK-JNK/ERK pathway activation upon LPS or TNFα stimulation[208]. Accordingly, TNIP1 also exerts signal transduction activating functions by also activating the MAPK-JNK/ERK signaling pathway upon IL-1β stimulation in EL4 cells. Yet again, it remains to be seen if this observation also holds true in other IL-1β stimulated cells than EL4 cells.

3.4 Conclusion & Outlook: TNIP1 is a mediator in IL-1β signaling, restoring homeostasis post-stimulation by exerting both signal-downregulating and activating functions

Based on the findings presented here and previously published, I suggest the following functionalities of TNIP1 in IL-1β mediated signaling (Fig. 18). Upon IL-1β stimulation and myddosome formation TNIP1 associates with all myddosome components through binding to K63-linked ubiquitin chains, generated by TRAF6 and Pellino1/2. After LUBAC catalysis of M1-linked ubiquitin chains to myddosome proteins, more TNIP1 is recruited to the myddosome and binds to M1-linked ubiquitin chains. This interaction downregulates IL-1β mediated signaling through (1) facilitating A20's DUB activity and (2) repressing NEMO binding to M1-linked, K63-linked hybrid ubiquitin chains, therefore preventing further downstream NF-κB activation. Simultaneously, TNIP1 binding to K63-linked ubiquitin facilitates MAPKK activation, resulting in phosphorylation of JNK and AP-1 activation.

IL-1β mediated signaling cross talks with the translation machinery, thereby initiating *de novo* synthesis of TNIP1. Some TNIP1 is degraded upon IL-1β stimulation, potentially as a part of the endocytosed receptor complex. In the case of another exposure to IL-1β or other inflammatory mediators e.g. TNFα, *de novo* synthesized TNIP1 would allow the cell to respond and regulate the signaling response accordingly.

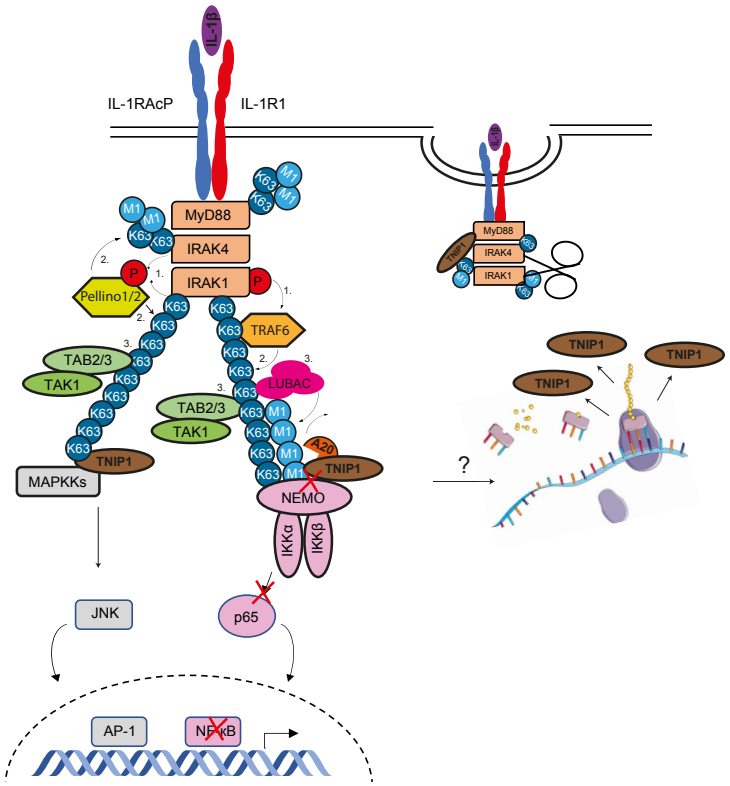

Fig. 18: TNIP1 in IL-1β signal transduction. TNIP1 binds to the fully formed myddosome, facilitating MAPK-JNK/ERK signalling, but inhibiting IKK-NF-κB activation. IL-1β mediated signalling induces *de novo* synthesis of TNIP1 to enable a sufficient signalling response upon re-stimulation.

Possible next steps in order to completely understand TNIP1's functionalities in IL-1β mediated signaling would be to further characterize TNIP1 in the MAPK-JNK/ERK signaling pathway by investigating if the depleted levels of phosphorylated JNK in TNIP1 KO cells can be restored by using a JNK activating drug. Next, a K63-linked ubiquitin -dependent interactor analysis of TNIP1 might reveal the association with specific MAPKKs. In order to understand, if the elevated levels of phosphorylated p65 in TNIP1 KO cells are exclusively the result of a missing A20 interaction and subsequent DUB activity, investigations of phosphorylated p65 in A20 KO cells should show similar p65 phosphorylation trends. Furthermore, the purpose of *de novo* synthesized TNIP1 remains to be characterized. Investigations of IL-1β-dependent signaling outputs after re-stimulating TNIP1 KO cells might elucidate the purpose of TNIP1's *de novo* synthesis upon IL-1β stimulation. Last but not least, characterization of TNIP1's functions in other IL-1β responding cells reveal if the here observed functions are IL-1β-dependent but cell type independent. Together, these findings will reveal previously unknown and underestimated signal-activating capacities of TNIP1 in IL-1β mediated signaling.

4 Material and Methods

4. 1 Material

4.1.1 Cell strains

Purchased cell lines

Name	Source	Supplier	Medium and culture conditions
EL4.NOB-1 (ECACC 87020408)	murine, derived from mouse C57BL/6N ascites lymphoma lymphoblasts, selected for high IL-1R	Sigma-Aldrich	RPMI complete medium, 37°C, 5 % CO2, split every 2-3 days at ratio 1:5 or 1:10
HEK293T	human, embryonic kidney cell line	American Type Culture Collection	DEMEM complete medium, 37°C, 5 % CO2, split every 2-3 days at ratio 1:10 or 1:20

Endogenously tagged EL4 cell lines

Name	Description	Producer
MyD88-GFP	MyD88 tagged with enhanced GFP at the C-terminus	E. Ziska, M. J. Taylor
MyD88-GFP/A20-mScarlet	A20 tagged with mScarlet-I at their N-terminus in MyD88-GFP cell line	E. Ziska, F. Cao, M. J. Taylor
MyD88-GFP/A20-mScarlet/TNIP1-KO	CRISPR/Cas9 knockout of TNIP1 in MyD88-GFP-A20-mScarlet cell line	F. H. U. Gerpott
MyD88-GFP/A20-mScarlet/TNIP1-Halo	Lentiviral reconstituted MyD88-GFP-A20-mScarlet cell line with TNIP1-Halo	M. A. Lichtenstein, M. J. Taylor
MyD88-GFP/IRAK1-mScarlet	IRAK1 tagged with mScarlet-I at their C-terminus in MyD88-GFP cell line	E. Ziska, N. Auevechanichkul, M. J. Taylor
MyD88-GFP/IRAK4-mScarlet	IRAK4 tagged with mScarlet-I at their C-terminus in MyD88-GFP cell line	E. Ziska, N. Auevechanichkul, M. J. Taylor
MyD88-GFP/IRAK1-KO	CRISPR/Cas9 knockout of IRAK1 in MyD88-GFP cell line	E. Ziska, N. Auevechanichkul, M. J. Taylor
MyD88-GFP/IRAK4-KO	CRISPR/Cas9 knockout of IRAK1 in MyD88-GFP cell line	E. Ziska, N. Auevechanichkul, M. J. Taylor

4.1.2 Media

Media name	Ingredients
Conditioned Media	15 % parental cell medium (0.2 µM filtered), 100 µg/ml Normocin, RPMI complete
DMEM complete	DMEM, 10 % (v/v) FCS, 2 mM L-glutamine, 1 mM Pyruvate, 100 U/ml Penicillin, 100 µg/ml streptomycin
Freezing medium	90 % FCS, 10 % DMSO

RMPI complete	RPMI, 10 % (v/v) FCS, 2 mM L-glutamine, 100 U/ml Penicillin, 100 µg/ml streptomycin
pSILAC depletion medium	SILAC RPMI 1640, 10 % dialyzed FCS, 1x Antibiotics, 1x L-Glutamine, 1x Proline, 1x Leucine
pSILAC heavy medium	SILAC RPMI 1640, 10 % dialyzed FCS, 1x Antibiotics, 1x L-Glutamine, 1x Proline, 1x L-Leucine, 1x L-Lysine $^{13}C_6$ $^{15}N_2$ HCl, 1x L-Arginine $^{13}C_6$ $^{15}N_4$ HCl, 0.1 mM AHA
pSILAC intermediate medium	SILAC RPMI 1640, 10 % dialyzed FCS, 1x Antibiotics, 1x L-Glutamine, 1x Proline, 1x Leucine, 1x L-Lysine [4,4,5,5-D_4] HCl, 1x L-Arginine $^{13}C_6$ HCl, 0.1 mM AHA

4.1.3 gRNA CRISPR

Target gene	guide number	gRNA sequence (no PAM) 5'→3'
mTnfaip3	1	TTCAGCCATGGTCCTCGACA
	2	AGGAAGAAGTTGTTCAGCCA
mTnip1	1	TACGGGATCTACGACCCAGG

For CRISPR/Cas9 TNIP1-specific knockout generation a single stranded donor sequence (ssODN) introducing a frameshift and a stop codon with the following sequence was used:
5'-AGCTGCGGACACCTCTCCCAGAGGCGTGCTGCGCCCTGGGTCCTAGATCCCGT AGGGTCCTCTCCCTTCCATGAGGGTGGCTCAA-3'

4.1.4 Oligonucleotides

Primer for A20 HDR template vector (pMK-puroR-2A-mScarlet-A20-N-HDR)

Amplification target	Orientation	Sequence 5'→ 3'
A20 3'-homolgy arm	fwd	GCTGAACAACTTCTTCCTCAAGCTTTG TATTTGAGCAATATGCGGAAAGC
	rev	GGAAACAGCTATGACCATGAATGACAGTG GCAAACAACTGTGATTCTGAT
A20 5'-homolgy arm	fwd	TTGTAAAACGACGGCCAGCTATTTGCTGCC TTGTAGCATCAAGAAGGG
	rev	CATGGTCCTCGACAAtGCtTGAAGAGGAAGG GGTAAAGCCCAT
mScarlet-I-2A-PuroR cassette	fwd	AAGCATTGTCGAGGACCATGACCGAGTAC AAGCCCACGGT
	rev	TTGAGGAAGAAGTT-GTTCAGCGCTTCCTCCACTGCCTCCTG
pMK vector backone	fwd	CATGGTCATAGCTGTTTCCTTGC
	rev	CTGGCCGTCGTTTTACAACG

Primer for TNIP1-Halo lentiviral vector pHR-TNIP1-Halo generation

Amplification target	**Orientation**	**Sequence 5'→ 3'**
3xGSS-Halo	fwd	CAGGGAGGAAGTGGAGGTTCTGGTGG
	rev	TCGACTCTAGAG-TCGCGGCCTCAGGCCAGCC CGGGGAGC
Tnip1-3xGSS	fwd	TCTCGAGAATTCTCACGCGGCCAC-CATGGAG GGAAGAGGCCCTTATAGG
	rev	ACCAGAACCTCCAC-TTCCTCCCTGTGGCCCAT CGCAATCGTTATCG

Primer for qPCR

Gene	**Orientation**	**Sequence 5'→3'**
mGapdh	fwd	AGGTCGGTGTGAAC-GGATTTG
	rev	GGGGTCGTTGATGG-CAACA
mTnip1	fwd	CAAAGAGGAGGA-GAAGGCCA
	rev	CCAGATCCGA-TACCCTCCAC

4.1.5 Plasmids

Designation	**Application**	**Source**
pHR-CMV-GFP	HIV-based lentiviral vector for pHR-TNIP1-Halo generation	Kindly provided by M. Taylor (Addgene #14858)
pMD.2G	Envelope plasmid for lentiviral production	Kindly provided by M. Taylor
pMK	pMK backbone was used for plasmid DNA repair template design for endogenous tagging of A20	Kindly provided by M. Taylor
psPAX2	Packaging plasmid for lentiviral production	Kindly provided by M. Taylor
pX330-U6-Chimeric_BB-CBh-hSpCasp	Chimeric guide RNA expression plasmid for endogenous tagging of A20	Kindly provided by M. Taylor (Addgene #42230)

4.1.6 Buffers

Buffer/ Solution	**Ingredients**
Acetonitrile (ACN) wash buffer	20 % ACN in LC grade water
Digestion buffer	100 mM Tris-HCl pH 8.0, 2 mM $CaCl_2$, 5 % (vol/vol) ACN
ELISA block buffer	PBS, 1 % BSA
ELISA dilution buffer	TBS, 0.1 % BSA, 0.05 % Tween20, pH 7.2-7.4
ELISA stop solution	2 N H_2SO_4 in dH_2O
ELISA wash buffer	PBS, 0.05 % Tween20, pH 7.2-7.4

FACS buffer	PBS, 2.5 % FCS (0.2 uM filtered)
Gibson assembly master mix	320 µL 5X ISO Buffer, 0.64 µL of 10U/ µL T5 exonuclease, 20 µL 2 U/µL Phusion polymerase, 160 µL 40 U/µL Taq ligase, 1.7 mL dH2O
Guanidine wash buffer	100 mM Tris-HCl pH 8.0, 6M Guanidine-HCl in dH_2O
HBS buffer	10 mM Glucose, 1X HBS
HEPES buffered saline (HBS) buffer (10X)	135 mM NaCl, 4 mM KCl, 0.5 mM $MgCl_2$
IP-elution buffer	dH_20, 4 % (w/v) SDS, 100 mM DTT, 50 mM Tris
MS loading buffer (10X)	dH_20, 20 % (vol/vol) ACN, 1 % (vol/vol) TFA
MS loading buffer (1X)	2 % (vol/vol) ACN, 0.1 % (vol/vol) TFA
NP-40 lysis buffer	dH_20, 50 mM NaCl, 1% (v/v) Ipegal (NP-40), 50 mM Tris-Base, pH 8.0
PBS (10X)	dH_20, 1,37 M NaCl, 81 mM Na_2HPO_4, 15 mM KH_2PO_4
pSILAC digestion buffer	1 M Tris HCl, 1 M $CaCl_2$, 1.5 % (v/v) ACN in dH_2O
SDS-wash buffer	1 M Tris HCl, 20 % SDS, 5M NaCl, 0.5 M EDTA in dH_2O
TBS (10X)	dH_20, 1.5 M NaCl, 0.5 M Tris-HCl, pH 7.6
TBS-T	1 % Tween20 in TBS
Urea lysis buffer	8M Urea, 200 mM Tris pH 8, 4 % (v/v) CHAPS, 1 M NaCl
Western blot buffer (10X)	dH_20, 0.25 M Tris-Base, 1.92 M Glycine
Western blot transfer buffer	20 % Methanol in western blot buffer

4.1.7 Kits

Kit	Company	Catalog#
Click-iT Protein Enrichment Kit	Thermo Scientific	C10416
Murine IL-2 DuoSet ELISA	R&D Systems	DY402
Monarch™ DNA Gel Extraction kit	New England Biolabs	T1020L
Monarch™ PCR & DNA Cleanup kit	New England Biolabs	T1030L
Monarch™ Plasmid Miniprep kit	New England Biolabs	T1010L
MycoAlert Mycoplasma Detection Kit	Lonza	LT07-418
NEB® PCR Cloning Kit	New England Biolabs	E1202S
Neon Transfectionsystem 10µL Kit	Invitrogen	MPK1025
NucleoSpin RNA® Plus	Macherey-Nagel	740984.50
NucleoBond Xtra Midi Plus	Macherey-Nagel	740422.50
Odyssey Western Blotting Starter Kit 2 (TBS/PVDF) Pack Insert	LI-COR Biosciences	925-35011
Pierce BCA Protein Assay Kit	Thermo Scientific	23227
Pierce 660 nm Protein-Assay-Kit	Thermo Scientific	22662
Revert 700 Total Protein Stain and Wash Solution Kit	LI-COR Biosciences	926-11015
SF Cell Line 4D-Nucleofector™ X Kit L	Lonza	V4SC-2012

4.1.8 Antibodies & Dyes

Primary antibodies

Antibody name & Source	Application	Company	Catalog#
Anti-Glyeraldehyde 3-phosphate dehydrogenase (GAPDH) murine mAB (6C5)	Western Blot	Thermo Scientific	AM4300
Anti-TNIP1 rabbit mAB	Western Blot, IFS	Sigma Life Science	HPA037893
GFP rabbit polyclonal AB	Western Blot	Chromotek	PABG1
NF-κB p65 (D14E12) XP rabbit mAB	Western Blot	Cell Signaling	8242
Phospho-NF-κB p65 (Ser536) rabbit mAB	Western Blot	Cell Signaling	3031
Phospho-SAPK/JNK (Thr183/Tyr185) (81E11) rabbit mAB	Western Blot	Cell Signaling	4668
p-p38 MAPK (T180/Y182) rabbit mAB	Western Blot	Cell Signaling	9211
p38 MAPK rabbit mAB	Western Blot	Cell Signaling	9212
RFP mouse mAB (6G6)	Western Blot	Chromotek	6G6
SAP/JNK rabbit mAB	Western Blot	Cell Signaling	9252

Secondary antibodies

Antibody name	Application	Company	Catalog#
Peroxidase AffiniPure Goat Anti-mouse IgG (H+L), HRP-linked Antibody	Western Blot	Jackson ImmunoResearch Laboratories	115-035-166
Peroxidase AffiniPure Goat Anti-rabbit IgG (H+L)	Western Blot	Jackson ImmunoResearch Laboratories	111-035-144
Nano-Secondary® alpaca anti-human IgG/ anti-rabbit IgG Alexa Fluor® 647	IFS	Chromotek	srbAF647-1-100
FluoTag®-X4 anti-GFP-Atto488	IFS	Nano Tag Biotechnology	N0304-At488-L

Dyes

Dye	Application	Company	Catalog#
Janelia Fluor® HaloTag® 635	FACS	Promega	CS315103
Janelia Fluor® HaloTag® 647	FACS	Promega	GA1120

4.1.9 Enzymes

Enzyme	Company	Catalog#
BbsI-HF	New England Biolabs	R3539L
Benzonase	Sigma Aldrich	E1014
Mlu1-HF	New England Biolabs	R3198L
Not1-HF	New England Biolabs	R3189L
Q5® High-Fidelity 2X Master Mix	New England Biolabs	M0492S
T4 Polynucleotide Kinase	New England Biolabs	M0201L

4.1.10 Markers

Name	Company	Catalog#
Chameleon Duo Pre-stained Protein Ladder	LI-COR Biosciences	928-60000
100 bp DNA Ladder	Promega	G210A
PageRuler Plus Prestained Protein Ladder	Thermo Scientific	26619

4.1.11 Reagents & Chemicals

Reagent or Chemical	Company	Catalog#
Acetonitril (ACN), HPLC grade	Merck	100030
Agarose	Biozym Biotech GmbH	840004
Ampicillin	Thermo Scientific	BP1760-25
4-Azido-L-homoalanine HCl (L-AHA)	Jena Bioscience	CLK-AA005
Bacto™ Agar	Becton Dickinson (BD)	214010
Bovine serum albumin (BSA)	Sigma-Aldrich	A9647-100G
CHAPS Detergent (3-((3-cholamidopropyl)dimethylammonio)-1-propanesulfonate)	Thermo Scientific	28299
Chloroacetamide (CAA)	Thermo Scientific	A15238.30
cOmpleteTM, EDTA-free protease inhibitor chocktail	Roche	11873580001
Cyclohexamide	Sigma Aldrich	C1988-1G
1,4-Dithiothreitol (DTT)	Roth	6908.1
Dimethylsulfoxide Hybri-Max™, sterile-filtered	Sigma-Aldrich	D265
1,2-dioleoyl-sn-glycero-3-[(N-(5-amino-1- carboxypentyl)iminodiacetic acid)succinyl] (DGS-NTA)	Avanti	790528C-5MG
1,2-dioleoyl-sn-glycero-3- phosphoethanolamine-N- [methoxy(polyethylene glycol)-5000] (PEG5000-PE)	Avanti	880230C-25MG
Ethanol absolute	VWR Chemicals	1.00983.2511
Ethanol, HPLC grade	Merck	111727
Ethylene diaminetetraacetic acid (EDTA), Tetrasodiume Tetrahydrate Salt	Santa Cruz Biotechnology Inc.	sc-204735
Fetal Bovine Serum (FBS)	Sigma Aldrich	F0804 (Lot# BCCC4773)
FBS, dialyzed	Athena	0427
Gel Loading Dye, Purple (6x)	New England Biolabs	B7024S

Gel red Nucleic Acid Stain	Merck	SCT1020
GFP-Trap Magnetic Particles	Chromotek	M-270 gtd-10
Gibco Trypan Blue (0.4 %)	Thermo Scientific	15250-061
Gibco DMEM, high glucose, NEAA, no glutamine	Thermo Scientific	10938-025
Gibco DPBS, no calcium, no magnesium	Thermo Scientific	14190169
Gibco L-Glutamine (200 mM)	Thermo Scientific	25030024
Gibco OPTI-MEM (1X)	Thermo Scientific	31985-062
Gibco Penicillin-Streptomycin (10,000 U/mL)	Thermo Scientific	15140122
Gibco Puromycin (10 mg/ mL)	Thermo Scientific	A11138-03
Gibco Sodium Pyruvate (100 mM)	Thermo Scientific	11360039
Gibco RPMI 1640 wo	Thermo Scientific	32404014
Gibco RPMI 1640	Thermo Scientific	31870074
Glycine ≥ 99 %	Roth	3790.2
Glycerin ROTIPURAN ≥ 99 %	Roth	3783.3
Halt Protease & Phosphatase Inhibitor	Thermo Scientific	1861282
HDR enhancer buffer	Integrated DNA Technologies	10007910
Hellmanex III	Sigma-Aldrich	Z805939-1EA
Hydrochloric acid 37 %	Fisher Scientific	H1150 PB15
Intercept Protein-Free Blocking Buffer	LI-COR	927-80001
IPEGAL CA-630	Sigma Aldrich	I8895-100ML
Isopropanol	Merck	1.09634.2551
iScript Reverse Transcription Supermix	Bio-Rad Laboratories Inc.	1708841
iTaq universal SYBR Green supermix	Bio-Rad Laboratories Inc.	172-5121
Kanamycin	Sigma-Aldrich	BP861
L-Arginine $^{13}C_6$ HCl	Sigma-Aldrich	88210
L-Arginine $^{13}C_6$ $^{15}N_4$ HCl	Sigma-Aldrich	608033
L-Lysin [4,4,5,5-D_4] HCl	Sigma-Aldrich	616192
L-Lysin $^{13}C_6$ $^{15}N_2$ HCl	Sigma-Aldrich	608041
L-Proline	Sigma-Aldrich	P0380
Lysyl Endopeptidase (Lys-C)	Wako	125-05061
Magnesium chloride - hexahydrate	AppliChem GmbH	A4425
MES SDS Running Buffer (20x)	Thermo Scientific	NP0002
Methanol	VWR Chemicals	1.06009.2511
Methanol hypergrade for LC-MS	Merck	106025
NEB® stable competent *E. coli* (High Efficiency)	New England Biolabs	C3040I
Nickel (II) chloride hexahydrate	Thermo Scientific	053131.18
Normocin	InvivoGen	ant-nr-1
Nuclease-free Water, not DEPC Treated	Thermo Scientific	AM9937
NuPAGE™ 4-12% Bis-Tris Protein Gels, 1.0 mm 10 wells	Thermo Scientific	NP00323Box
NuPAGE™ 4-12% Bis-Tris Protein Gels, 1.0 mm 15 wells	Thermo Scientific	NP00321Box
PageBlue Protein Staining Solution	Thermo Scientific	24620
1-palmitoyl-2-oleoyl-glycero-3-phosphocholine (POPC)	Avanti	850457C-200MG

Paraformaldehyde 32 % Solution EM Grade	Electron Microscopy Sciences	15714
PCR-grade water	Jena Bioscience	PCR-258-100
Phenylmethylsulfonyl fluorid (PMSF)	Roche	10837091001
PhosphoSTOP *EASYpack*	Roche	04906837001
Potassium chloride	Sigma-Aldrich	P9541
Protease inhibitor cocktail 100x	Sigma-Aldrich	P8849
QuickExtract DNA extraction solution	Lucigen	QE09050
Recombinant Murine IL-1β	PeproTech	211-11B
Restore Western Blot Stripping Buffer	Thermo Scientific	21059
RNase*Zap*	Invitrogen	AM9780
RFP-Trap Magnetic Particles	Chromotek	M-270 rtd-10
Laemmli SDS sample buffer reducing (6x)	Thermo Fisher	J61337.AC
Sodium dodecyl sulfate (SDS) Pellets ≥ 99 %	Roth	CN30.2
Sera-Mag beads hydrophilic	GE Healthcare	24152105050250
Sera-Mag beads hydrophobic	GE Healthcare	44152105050250
SILAC RPMI 1640	Athena	0422
Skim milk powder	Sigma-Aldrich	70166-500G
Sodium chloride	Roth	S7653
Sulfuric acid 2.5 mol/l (5N)	Sigma-Aldrich	4803641000
SuperSignalWest Femto Maximum Sensitivity Substrate	Thermo Scientific	34095
*Trans*IT-293 transfection reagent	Mirus Bio LLC	MIR 2700
TritonX-100 reduced	Sigma-Aldrich	282103-25G
Triethylammoniumbicarbonat (TEAB)	Sigma-Aldrich	11268-25G-F
Trifluoroacetic acid (TFA)	Thermo Scientific	28904
Trishydroxymethylaminomethane (Tris)-Base	Thermo Scientific	BP152-1
TrypLE Express, no phenol red	Thermo Scientific	12604013
Trypsin protease	SERVA	37286.03
Tween 20, research grade	MP Biomedicals	TWEEN201
Urea (Harnstoff) ≥ 99.6 % krist.	Roth	7638.2
Water, HPLC grade	Merck	115333

4.1.12 Consumables

Name	**Company**	**Catalog#**
Cell culture bottle T25, T75, T175	Sarstedt	83.3910.002, 83.3911.002, 83.3912.002
Cell scraper 25 cm	Sarstedt	83.1830
Countess cell counting chamber slides	Invitrogen	C10283
Falcon 15 mL, 50 mL	Corning	430791, 430829
MicroAmp Fast Optical 96-Well Reaction Plate	Applied Biosystems	4346906
Micro tube 1.5 mL, 2.0 mL	Sarstedt	72.690.001, 72.691
Multiply-µStrip Pro 8-strip	Sarstedt	72.991.002
Nunc Cryotubes 1.0 mL	Thermo Fisher	377224
Immobilon-P Transfer Membrane (PVDF, 0.45 µM)	Sigma Aldrich	IPHV00010
Immuno 96-well-plate, clear flat-bottom	Thermo Scientific	442404
Lid for 96-well plates, nonsterile	Thermo Scientific	263339

Optical Adhesive Covers	Applied Biosystems	4360954
Petri dish, 92 x 16 mm	Sarstedt	82.14731.001
Millex®-GP Filter Unit 0.2 µM, Millex®-HA Filter Unit 0.45 µM	Merck	SLGP033RS, SLHA033S
Polystrene Round-Bottom Tube with Cell-Strainer Cap, 5 mL	Croning	352235
Stericup Quick Release Express Plus, 0.22 µM	Sigma Aldrich	S2GPU05RE
Stripette 5 mL, 10 mL, 25 mL, 50 mL	Corning	4051, 4101, 4489, 4490
Stuffed tips 10 µL, 20 µL, 200 µL, 1000 µL	Starlab	1121-3810, 112-3810, 1120-8810, 1126-7810
Syringe Omnifix Luer 50 mL	Braun	4616502F
Tips 10/20 µL, 200 µL, 1000 µL	Starlab	1110-3700, 1111-0700-C, 1111-6701-C
Whatman Gel Blot Paper	GE Healthcare	10427826
6-well plate	Sarstedt	83.3920.005
48-well plate	Corning	3548
96-well plate	Sarstedt	83.3924.005
96-well glass bottom plates	MateriCal	MGB096-1-2-LG-L

4.1.13 Technical Equipment

Equipment	Company
Agarose gel + combs	Biorad
Bacterial Incubator	Memmert
Bravo Automated Liquid Handling Platform	Agilent
Bioruptor Pico Sonicator	Diagenode
Centrifuge 5415R	Eppendorf
Centrifuge 5804R	Eppendorf
ChemiDoc XRS + System	Biorad
CO_2-Incubator	Binder
Concentrator plus System	Eppendorf
Countess II automated cell counter	Thermo Scientific
4D-Nucleofector® System	Lonza
DynaMag-2	Invitrogen
FAIMS Pro Interface	Thermo Scientific
Innova 4000 incubator shaker	New Brunswick Scientific
Integra Vacusafe	Integra Biosciences
Micro Centrifuge	Roth
Microscope Inverse TS100PH	Olympus Lifescience
Minicentrifuge SU1550	Sunlab
Mr. Frosty Freezing Container	Fisher Scientific
NanoDrop® Spectrophotometer ND-1000	PeQLab
Neon Transfection System	Thermo Scientific
Odyssey CLx Infrared Imaging System	LI-COR
Orbitrap Fusion Lumos	Thermo Scientific
pH/mV Benchtop Meter	Hanna Instruments
Power Pac Basic	Biorad

StepOnePlus Real-Time PCR System	Applied Biosystems
Thermal cycler, C100 Touch	Biorad
ThermoMixer F1.5	Eppendorf
TIRF microscope Eclipse Ti2	Nikon
UltiMate 3000 RSLCnano System	Thermo Scientific
Vortex D-6012	neuLab
Wet tank system	Polymehr
XCell SureLock Mini-Cell Electrophoresis system	Thermo Scientific

4.1.14 Software

Name	Version	Supplier
Adobe Illustrator	26.1	Adobe
DeepVenn	-	Hulsen et al., 2008[209]
EmpiriaStudio	2.2.0.141	LI-COR GmbH
GraphPad Prism	9.3.1	GraphPad Software
ImageJ	2.0.0-rc-69/1.52	National Institute of Health, USA
MaxQuant	1.6.0.1	Cox & Mann, 2008[210]
MS office	16.59	Microsoft
Perseus	1.6.2.3	Tyanova et al., 2016[211]
R Studio	1.2.5033	RStudio, Inc.

4.2 Methods

4.2.1 Cell Culture

EL4 WT and endogenously tagged EL4 cells were cultivated in RPMI complete medium at 37°C, 5% CO_2 at a density of 0.1 – 0.5 x 10^6 cells/ml. All cells were negative for mycoplasma as characterized by the MycoAlert detection kit.

4.2.2 Characterization of the IL-1β-myddosome interactome

IL-1β stimulation and subsequent IP of GFP- and mScarlet-tagged proteins

For the IPs the different endogenously tagged EL4 cell lines MyD88-GFP, MyD88-GFP/IRAK4-mScarlet or MyD88-GFP/IRAK1-mScarlet were transferred from cell culture flasks into a 50 ml falcon and counted. GFP-IPs allowed the interactome analysis of MyD88 and RFP-IPs the interactome analysis of IRAK1 and IRAK4 respectively. 1 x 10^7 for GFP-IPs and 2 x 10^7 for RFP-IPs were transferred into a 15 ml falcon in a total of 6 ml RPMI complete.

Each stimulation time point (0-, 15-, 30- and 60-min) was performed in quadruplicates: Cells were stimulated in a reverse chronological order with a final IL-1β concentration of 100 ng/ml or PBS for the unstimulated samples (or 0-min). During stimulation periods falcons were care-

fully mixed every 5 min and incubated (37°C, 5% CO_2) with loose lids to enable oxygen exchange. To stop stimulation 3 ml of ice-cold PBS containing phosphatase inhibitor were added to the tube, inverted and immediately pelleted for 5 min at 400 × g at 4°C. Supernatant was aspirated. Cells were washed with 3 ml of ice-cold PBS containing phosphatase inhibitors and again pelleted for 5 min at 400 × g at 4°C. After aspiration of supernatant tubes were kept on ice for further cell lysis. For this purpose, cells were resuspended in ice-cold NP-40 lysis buffer containing 1X PMSF and 1X protease inhibitor in the following volumes: 200 µl for MyD88-GFP cells, 266 µl for MyD88-GFP/IRAK1-mScarlet cells and 400 µl for MyD88-GFP/IRAK4-mScarlet cells. After incubating for 15 min on ice, cell lysates were transferred into 1.5 mL tubes and sonicated in the Bioruptor® (duty cycle: 30/30 sec on/off) to enable complete lysis, thus leading to higher protein concentrations. Next, tubes were spined at 16.000 rpm for 10 min at 4°C. Supernatants of the same stimulation time points were transferred to the same tube to guarantee more homogenic samples and compensate inaccuracy of stopping the stimulation reaction. Protein concentrations were measured using the Pierce™ 660-nm Protein Assay. 25 µl of bead slurry (GFP-/ RFP-trap magnetic particles) were distributed into 1.5 mL tubes. Again, for each stimulation time point and cell line samples were prepared in quadruplicates. For bead equilibration, beads were washed x 3 with NP-40 lysis buffer: after resuspending beads in 500 µl of ice-cold buffer, tubes were incubated on a magnetic rack until beads completely accumulated to the rack and buffer could be withdrawn without touching the beads. Off the rack, beads were resuspended in ice-cold buffer again and washing steps were repeated. After the final washing step, equal amounts of protein were added to beads and filled up with NP-40 lysis buffer to a final volume of 500 µl to enable complete rotation. Lysates and beads were then incubated rolling at 4°C overnight.

On the next day, tubes were incubated on the rack again and supernatant withdrawn. To reduce background, beads were resuspended in 500 µl ice-cold NP-40 lysis buffer and transferred to a new tube. Then, beads were washed x 3 as described for bead equilibration. Between each washing step, tubes rotated for approximately 5 min upside down to decrease unspecific binding proteins. Beads were never dry at any timepoint of equilibration and washing. After the final wash step, NP-40 lysis buffer was completely withdrawn using a P200 pipet after a quick spin down on a mini table top centrifuge. Then 50 µl of IP-elution buffer was added to the beads, tubes were vortexed and boiled for 20 min at 65°C. The elution temperature of 65°C was chosen, because this temperature is critical for myddosome islation[212]. Tubes cooled down at RT, were briefly spined down and placed on the magnetic rack for the final elution step by carefully

transferring the eluate to a new tube without touching any beads. Eluates were stored at -20°C until further SP3 clean-up and subsequent proteomic analysis.

On a general notice, the number of used cells and subsequent lysate volume per IP was optimized, ensuring bead saturation (but not oversaturation). For this purpose, different amounts of total proteins were used for IPs and the subsequent eluates as well as their supernatants were analyzed for GFP-signal for MyD88-GFP-IPs or RFP-signal for IRAK4/1-mScarlet-IPs using WB. The protein concentration per 25 µl bead slurry that did not result in any GFP or RFP signal respectively was chosen for the interactome MS experiment.

Single-pot, soldi-phase-enhanced sample preparation (SP3) of IP-eluates for proteomic analysis

To enable highest sensitivity in the proteomic analysis of the Co-IP eluates, the single-pot, solid-phase-enhanced sample-preparation (SP3) technology was performed[165]. Briefly, thawed samples were alkylated with CAA with a final concentration of 160 mM at 95°C for 5 min. Next, 2 µl of paramagnetic Sera-Mag speed beads (1:1 mixture of Sera-Mag beads hydrophilic and Sera-Mag beads hydrophobic) were added to the samples. Samples were supplemented with 100 % ACN to a final amount of 50 %, mixed and incubated at RT for 10 min to induce binding. The protein-bead mixture was captured using an in-house build magnetic rack and washed x 2 with 180 µl 80 % EtOH (v/v) to exclude any contaminants. Next, samples were air-dried and reconstituted in 30 µl of 50 mM TEAB containing 1 µg trypsin and 1 µg Lys-C. After a 30 min RT incubation, samples were incubated for 14 h (overnight) at 37°C in a PCR cycler for enzymatic digestion. On the next day, samples were spined down for 1 min and placed on the magnet to carefully recover the supernatant (without touching the beads) into a clean tube and mixed with 10X MS loading buffer to final concentration of 2 % (vol/vol) ACN, 0.1 % (vol/vol) TFA. Samples were stored at -20°C prior MS analysis. The described SP3 procedure was either performed manually or semi-automatic using the Bravo Automated Liquid Handling Platform specifically programmed by Florian Kondrot.

MS analysis of IP-samples

Samples were analysed on Orbitrap Fusion Lumos, which was both equipped with a FAIMS Pro device and coupled to 3000 RSLC nano UPLC. Samples were loaded on a pepmap trap cartridge (300 µm i.d. × 5 mm, C18, Thermo) with 2% acetonitrile and 0.1% TFA at a flow rate of 20 µl/min. Peptides were separated over a 50 cm analytical column (Picofrit, 360 µm o.d., 75 µm i.d., 10 µm tip opening, non-coated, New Objective) that was packed in-house with Poroshell 120 EC-C18, 2.7 µm (Agilent). Solvent A consists of 0.1 % formic acid in water. Elution was carried out at a constant flow rate of 250 nL/min within 180 min: 6 to 30% (vol/vol) solvent

B (0.1 % (vol/vol) formic acid in 80 % (vol/vol) acetonitrile) within 120 min, 30 to 45 % (vol/vol) solvent B within 25 min, 45 to 98 % (vol/vol) solvent B within 1 min, followed by column washing and equilibration.

The spray voltage was set to 2.2 kV. The ion transfer tube temperature was set to 275 °C. A survey MS1 scan was acquired from m/z 375–1500 at a resolution of 240,000. The normalized AGC target was set to standard mode and the maximum injection time was set to 50 ms. Monoisotopic precursor selection was activated. Precursor ions with charge states 2–5 were isolated within a 1.6 Da window and subjected to CID fragmentation (normalized collision energy 35%) with an CID activation time of 10 ms. All MS/MS scans were recorded in the linear ion trap. The normalized AGC target was set to standard mode, and the maximum injection time was set to dynamic. Ion trap scan rate was set to rapid. The cycle time was set to 1 s for each of the three FAIMS voltages of −40, -60 and −80 V.

Raw MS data processing of IP-samples

All files were processed using the Andromeda search engine integrated into the MaxQuant. The MS/MS spectra were searched against *Mus musculus* proteins from the UniProt sequence database (downloaded March 19th 2021) containing 55,315 protein sequences. All MS/MS spectra were searched with default MaxQuant parameters, and the following modifications were used: cysteine carbamidomethylation was set as a fixed modification; methionine oxidation, acetylation of protein N-terminus, and asparagine deamidation were allowed as variable modifications. False discovery rate (FDR) of the peptide spectral matches (PSMs), protein, and site were set to 1% based on Andromeda score. Match between runs (MBR) algorithm was activated to allow matching MS features between the different sample fractions and improve quantification. For the following analysis steps iBAQ-values (intensity-based absolute quantification of proteins) were chosen. This value is calculated by dividing the sum of peptide intensities of a given protein by the number of theoretically observable peptides.

IP-data analysis

The myddosome interactome analysis focuses on proteins that bind to MyD88, IRAK4 and IRAK1, respectively, dependent on IL-1β stimulation. Therefore, the IP-proteins represent the center of the analysis, which is achieved by normalizing the protein abundances within the IP-data sets towards the IP-protein mean abundance over all samples. I applied the following normalization procedure separately for each set of experiment: First, within each sample the abundance of the corresponding bait protein was subtracted from all proteins. Second, the global mean abundance of the bait protein across all replicates and samples was added to all proteins.

Consequently, this normalizes the data such that the bait protein's abundance is identical among replicates while it preserves the relative abundance differences between proteins within each sample. This allows the enrichment analysis comparing unstimulated to stimulated conditions, since now the IP-protein has an enrichment factor of 0 (meaning its abundance does not change due to stimulation).

The normalized data was further analyzed in Perseus by performing basic statistics and reducing dimensionalities. To obtain an IL-1β-dependent-myddosome interactome, I was exclusively interested in identified proteins enriched in the stimulated conditions. I defined proteins as significantly enriched if they were enriched at least twofold (corresponding to a $\log_2$ difference stimulated – unstimulated >1), a $-\log_{10}$ p-value > 2 and an FDR ≤ 0.05.

To obtain a temporally resolved IL-1β-myddosome interaction map, I included identified proteins that were significantly enriched after at least two stimulation time points for at least one myddosome protein (analysis done in R). To visualize abundances of IL-1β-myddosome interaction map proteins Z-score transformation was performed in Perseus. Venn diagrams were generated using the DeepVenn webtool[209]. The extent of overlap of the different circles reflects the number of overlapping proteins identified in one, two or all myddosome-IPs.

4.2.3 Investigation of IL-1β-dependent degradation and *de novo* protein synthesis

Pulsed-labelling with SILAC and AHA of IL-1β stimulated or unstimulated EL4 WT cells

EL4 WT cells were seeded at 2,6 x 10^5 cells/ ml in T175 flasks two days prior pulsed-labeling with stable-isotope labeling with amnio acids in cell culture (pSILAC) and AHA. On the day of the experiment cells reached a ~70 % confluency. Media was removed, cells were washed with pre-warmed PBS and pre-warmed pSILAC depletion medium was added. After 30-min of incubation, depletion media was removed and corresponding SILAC media (pSILAC intermediate or pSILAC heavy media) with or without IL-1β was added: for the unstimulated set ups, 25 ml of "intermediate" pSILAC media and for the IL-1β stimulated set ups, 25 ml of "heavy" pSILAC media with 10 ng/ml IL-1β was added to the flasks. After incubation (37°C, 5 % CO_2) for the indicated times (30-, 60-, 120- and 240 min) cells were washed with pre-warmed PBS, harvested by force (with cell scrapers) in ice-cold PBS, transferred into separated tubes and cells were counted. Equal amounts of cells (unstimulated vs. stimulated) were combined, spun down at 400 × g and 4°C. Cell pellets were washed with ice-cold PBS, spun down again, flash frozen in liquid nitrogen and stored at -20°C until cell lysis. This experiment was repeated six times on independent days.

Preparation of cell lysates for peptide enrichment of newly synthesized proteins

Cells were lysed on ice in 200 µl of Urea lysis buffer. Lysates were supplemented with Benzonase (1U per $1x10^5$ cells), transferred into 1.5 ml micro tubes and incubated for 30 min at 37°C while shaking at 750 rpm. To ensure complete lysis samples were sonicated for 15 min using the Bioruptor® (duty cycle: 30/30 sec on/off). Next, lysates were clarified by centrifugation for 30 min at 15.000 × g at 4°C. Supernatants were transferred to a new tube and protein concentration was determined using the Pierce™ Micro BCA assay following the manufacturer's instructions. 2 mg of total protein were transferred into a new tube and volume was filled up to 450 µl with Urea lysis buffer supplemented with protease inhibitors. Samples were stored on ice till click chemistry reaction.

Click chemistry reaction and peptide enrichment

Before the click chemistry reaction samples were alkylated by adding CAA to a final concentration of 20 mM and incubating for 30 min while centrifugation at 15,000 × g at 20°C. Next, click chemistry reaction mixture was prepared in a 15 ml falcon using the Click-iT™ Protein Enrichment Kit based on manufacturer's instructions. Further, alkyine agarose beads were prepared by pipetting 100 µl of bead slurry using a cut tip into a 2 ml micro tube, adding 1.9 ml of milliQ water and centrifugating the mixture for 5 min at 1.000 × g at RT. 1.9 mL of supernatant was removed. 500 µl of alkylated sample were then transferred into the tubes containing washed alkyne agarose beads. 500 µl of the prepared click chemistry reaction mixture was added to each sample. Samples incubated overnight (14 h) at RT while rotating in the dark.

On the next day, resins were pelleted for 5 min at 1,000 × g at RT (further referred to as pelleting). 50 µl of supernatant was transferred into a new tube and saved as input (stored at -20°C). 850 µl of remaining supernatant was discarded, beads were washed in milliQ water, briefly vortexed and pelleted. Again, 1.9 ml of supernatant was removed, 1.9 ml of SDS wash buffer and DTT to a final concentration of 5 mM was added. Mixture was briefly vortexed and incubated for 30 min at 55°C to ensure complete protein reduction. For the following alkylation step, CAA was added to a final concentration of 40 mM, vortexed and incubated for 1h at RT in the dark. Resins were pelleted, the supernatant was removed. Next, the resins were extensively washed in spin columns provided in the kit and an extensive washing protocol: 10 x 1 ml SDS wash buffer, 2 x 1 ml MilliQ water, 10 x 1 ml Guanidine wash buffer, 10 x 1 mL ACN wash buffer.

Overnight digestion of enriched proteins

Following the last wash step, the resin was resuspended in the spin column using a cut P200 tip in 500 µl digestion buffer and transferred into a 1.5 ml Eppendorf tube. Another 500 µl of digestion buffer was used to recover remaining beads in the spin column and was also transferred the same tube. After pelleting the resin, the supernatant was removed, leaving approximately 200 µl with the resin. For the overnight digestion (14 h at 37°C in the thermo cycler) 1 µg Trypsin and 0.5 µg Lys-C was added to each sample.

Peptide purification

On the next day the resin was pelleted. 100 µl of the supernatant was transferred to a new tube without touching the resin. 700 µl of MilliQ water was added to the resin and mixed by a brief vortex. Resin was pelleted. The supernatant carefully transferred to a new tube without any resin. Samples were acidified with formic acid to a final concentration of 0.1 % and desalted using OASIS HLB 96-well cartridges based on manufacturers' instructions. Samples were dried down in a Concentrator plus System and resuspended in 30 µl 1X Mass Spec loading buffer. Samples were stored at -20°C till MS analysis.

MS analysis of enriched proteins

Samples were analysed as described in 4.2.2.3.

Raw MS data processing of identified enriched proteins

Raw MS data was performed using MaxQuant. MS/MS spectra were searched using the Andromeda search engine against *Mus musculus* proteins from the UniProt sequence database (downloaded March 19th 2021) containing 55,315 protein sequences. Again, the following modifications were used: cysteine carbamidomethylation was set as a fixed modification; methionine oxidation, acetylation of protein N-terminus, and asparagine deamidation, 18O deamidation and replacement of methionine by AHA were allowed as variable modifications. SILAC labels were specified for quantification. FDR of the PSMs, protein, and site were set to 1% based on Andromeda score. MBR algorithm was activated to allow matching MS features between the different sample fractions and improve quantification. Protein groups were filtered out if the fraction of PSM that were triggered on the "intermediate" or "heavy" SILAC labelling states were < 20%.

Data analysis of enriched proteins dependent on IL-1β stimulation

The processed data was further analyzed in Perseus. SILAC heavy/intermediate ratios were log2 transformed. One one-sample T-Test was employed to determine significantly changing proteins. I defined *de novo* synthesized proteins as IL-1β-dependent if the -$\log_{10}$[p-Value] is

≥ 2 and the T-Test difference is ≥ 1 at any stimulation time point. Z-score transformation of the ratios was performed prior to hierarchical clustering. T-Test difference values for TNIP1 (ratio of stimulated to unstimulated) were plotted using R.

4.2.4 Investigation of IL-1β-dependent TNIP1 mRNA levels

IL-1β stimulation of EL4 WT for qPCR analysis

EL4 WT cells were counted and plated at 5 x 10^6 cells per T25 flasks in 4.5 ml RPMI complete media. After letting the cells settle and attach to the flask bottom 0.5 ml RPMI complete media containing IL-1β to final concentration of 10 ng/ml was added. For the unstimulated control only RPMI complete was added. After the different stimulation timepoints (0-, 15-, 30-, 60-, 120- and 240-min) supernatant was transferred into a 15 ml falcon. 5 ml ice-cold PBS was added to the flask, cells were removed by force using a cell scraper and also transferred to the same falcon. After centrifugation at 400 × g at 4°C and supernatant removal, cells were washed in 10 ml ice-cold PBS. Pellets were then flash frozen in liquid nitrogen and stored at -80°C until RNA isolation. The experiment was repeated on six independent days.

RNA isolation & reverse transcription (RT)

After thawing samples on ice RNA was isolated using the NucleoSpin RNA® Plus kit based on manufacturer's instructions and eluted in 60 µl RNAse-free H_2O (provided by kit). RNA concentration was measured using the NanoDrop® Spectrophotometer ND-1000.

1 µg of RNA was reversed transcribed into cDNA using the iScript™ Reverse Transcription Supermix for RT-qPCR according to manufacturer's instructions.

Reaction Mix

iScript RT Mix	4 µl
RNA	1 µg
dH_2O	Ad 20 µl

RT-PCR Program

Priming	5 min	25°C
RT	20 min	46°C
Reverse Transcriptase inactivation	1 min	95°C
Long term hold	∞	12°C

cDNA was diluted at 1:4 with dH2O and stored at -20°C till subsequent qPCR.

qPCR

To quantify the reversed transcribed amounts of Tnip1 cDNA qPCR for Tnip1 and glyceraldehyde-3-phosphate dehydrogenase (Gapdh) for normalization purposes was performed. Tnip1 primers were designed using the open source Primer3 program (http://frodo.wi.mit.ed/) using

the default settings. The chosen primers cover an intron-exon span to precisely distinguish between Tnip1 cDNA and gDNA. Gapdh primers were kindly provided by Olivia Majer. Initially, forward and reverse primers were mixed at a final concentration of 3 µM each. A mastermix was setup consisting of the following (here just shown per reaction):

Primer Mix	2 µl
2x Sybr Green Supermix	10 µl

12 µl of reaction mix was added per well of a 96-well plate. Diluted cDNA was thawed on ice and diluted again 1:4 corresponding to 2.5 ng/µl or 20 ng total mRNA. 8 µl per well was added. Each experimental sample was measured in triplicate. After sealing qPCR plate with foil and centrifugation, cycle of threshold (C_t) values were analyzed using StepOnePlus Real-Time PCR System with 40 amplification cycles. Primer annealing temperature was validated by melt curve analysis of the qPCR products.

Data were analyzed using the $\Delta\Delta C_t$ method. To normalize for equal amounts of cDNA the Tnip1 C_t value was subtracted by the Gapdh C_t value for each sample. The obtained ΔC_t value was subtracted from the unstimulated ΔC_t value. The resulting $\Delta\Delta C_t$ value was used to obtain the logarithmic ($\log_2$) fold change with $FC = 2^{-\Delta\Delta Ct}$.

For statistical analysis, the Shapiro-Wilk-Test ($\alpha = 0.05$) identified that a parametric test had to be used. Using the one-way ANOVA test ($p<0.05$) was used to identify statistical significance. Statistical analysis was done using GraphPad PRISM. Results were plotted using R.

4.2.5 Cell line generation

CRISPR/Cas9 endogenously tagging of A20 with mScarlet-I in MyD88-GFP cells

A20 (TNFAIP3) was endogenously tagged in MyD88-GFP cells using CRISPR/Cas9 as previously published[122]. A pMK vector backbone was used for generating the plasmid DNA repair template. Specifically, 5' and 3' homology arms were designed from the mouse Tnfaip3 gene (ENSMUSG00000019850) covering a distance of 500 bp and 800 bp on either side of the ATG start codon. A mScarlet-I-2A-PuroR cassette was inserted between these homology arms and fused to the A20 N terminus via a 3×(Gly-Gly-Ser) linker. pMK-puroR-2A-mScarlet-A20-N-HDR vector was generated using Gibson Assembly and sequence-verified.

Complementary oligonucleotides for A20 specific gRNAs were designed to be ligated into the Bbs1-digested pX330-U6-Chimeric_BB-CBh-hSPCas9 plasmid. The resulting sgRNA plasmid was sequence-verified.

Cell lines were generated as previously described[122] with the following modification: after electroporation cells were incubated at 32°C (instead of 37°C) and puromycin concentration was reduced to 1 µg/ml.

A20-mScarlet expression was verified using RFP specific Western Blot analysis. IL-1β dependent signaling efficiency was validated using ELISA (comp. section 4.2.8). Resulting MyD88-GFP-A20-mScarlet cell line was generated by Fakun Cao, Elke Ziska and Marcus Taylor and kindly provided for this work.

Generation of TNIP1 specific CRISPR/Cas9 knockouts in MyD88-GFP/A20-mScarlet cells
TNIP1 specific CRISPR/Cas9 knockout in MyD88-GFP-A20-mScarlet cells were generated using the Alt-R™ CRISPR-Cas9 system (Integrated DNA Technologies (IDT)). The Tnip1 specific CRISPR (cr) RNA was designed using the IDT webtool (https://eu.idtdna.com/site/order/designtool/index/CRISPR_CUSTOM) and targets exon 3 of the murine TNIP1 gene (ENSMUSG00000020400). Given low efficiency in a first experiment, a crRNA specific ssODN was designed inserting a frameshift and a stop codon after 30 bp after the crRNA binding site. An optimized protocol based on the manufacturer's protocol was kindly provided by Jackson Emanuel: 1.8 x 10^6 cells were used for final nucleofection using the 4D-Nucleofector® System. Nucleofected cells were incubated overnight in 4 ml RPMI complete with 3 µM (instead of 1 µM as recommended by manufacturer) HDR-enhancer V2 at 37°C, 5 % CO_2.
On the next day, nucleofected cells were distributed on a 96-well plate at a concentration of 0.5 cells/well for single cell cloning. After approximately 10 days, grown cells were expanded into a T25 flask.

Potential positive TNIP1 KO cells were initially screened using TNIP1 specific Western Blot analysis (4.2.7).

The potential TNIP1 KO cell line was then gnomically verified. For this purpose, gDNA was extracted using 0.5 ml of a confluent flask, washed in PBS, resuspended in 50 µl QuickExtract DNA extraction solution and heated at 65°C for 6 min and 98°C for 2 min. After centrifugation, supernatant was transferred into a new tube. To identified introduced TNIP1 perturbation the CRISPR target region was amplified using 5'-ACAGAGCAGTCATGACCTGCGA-3' as the forward primer and 5'-TGGTCCCTCAAGGACACCCTTT-3' as the reverse primer. The amplified region was subcloned using the NEB® PCR Cloning Kit and subsequently sequence-verified. Target region amplification, subcloning and sequence-verification was done by Kathrin Lättig.

Reconstitution of TNIP1 KO with TNIP1-Halo

The generated MyD88-GFP/A20-mScarlet/TNIP1-KO cell line was reconstituted with TNIP1-Halo expressed from a lentiviral vector. For lentiviral vector generation, Tnip1 and the Halo-tag were amplified with a 3×(Gly-Gly-Ser) linker at the 3'-end of Tnip1 and at the 5'end of the Halo-tag. Mlu1 and Not1 digested pHR vector backbone and the amplified Tnip1 and Halo fragments were used for Gibbson Assembly. Generated pHR-Tnip1-Halo plasmid was sequence-verified.

For subsequent lentiviral production, HEK293T cells were transfected in a T25 flask using TransIT-293T based on the manufacturer's instructions. 2.1 µg of pHR-Tnip1-Halo, the packaging vector psPAX and the envelope vector pMD2G mixed with 630 µl OPTI-MEM were used. Lentivirus was harvested after 3 days, filtered through a 45 µM PES filter after centrifuging at 2,000 rpm for 2 min. For lentiviral transduction, 1 ml of virus was added to 1.5 ml RPMI complete containing 0.5 x 10^6 MyD88-GFP-A20-mScarlet-KOTNIP1 cells and together transferred to a T25 flask. On the next morning, 2.5 ml fresh RPMI complete was added. After 2 days, transduced MyD88-GFP/A20-mScarlet/TNIP1-KO cells were labelled with 200 nM Janelia Fluor® HaloTag® 635 (JF635) and sorted. JF635 positive cells were cultured for 5 more days. After cell labelling with 200 nM Janelia Fluor® HaloTag® 647 (JF647) for 30 min at 37°C, 5 % CO_2 cells were re-sorted for JF647 positives. The resulting MyD88-GFP/A20-mScarlet/TNIP1-Halo cell line was generated and kindly provided by Mauriz Lichtenstein and Marcus Taylor.

TNIP1-Halo expression was verified using TNIP1-specific Western Blot analysis.

4.2.6 Immunofluorescence staining of TNIP1

To visualize the localization of TNIP1 on plasma membrane in IL-1β-stimulated EL4 cells, we introduced IL-1β-functionalized supported lipid bilayers (SLBs). Detailed preparation of SLBs was described previously[122]. EL4 cells endogenously expressing MyD88-GFP and IRAK4-mScarlet, IRAK1-mScarlet or A20-mScarlet were starved for 3 h before seeding on IL-1β-SLBs. Cells were incubated at 37°C for 30 min before fixation (3.5 % PFA, 0.1 % triton) for 20 min at RT. Cells were washed with PBS then blocked in 10 % BSA overnight (or 1 h at RT). The next day, fixed cells were stained with a mixture of TNIP1-antibody (1:400) and Nano-Secondary® alpaca anti-human IgG/ anti-rabbit IgG Alexa Fluor® 647 (1:1000) diluted in 10 % BSA containing 0.1 % TritonX-100 for 1 h at room temperature, followed by staining with

FluoTag®-X4 anti-GFP-Atto488 (1:500) to boost MyD88-GFP signal for 1 h at room temperature. Finally, cells were washed with PBS and imaging with TIRF microscopy. Fakun Cao did this experiment and kindly provided experimental details and the data.

4.2.7 Western Blot analysis

Lysate generation

For phosphor-protein quantification of p38, p65, ERK and JNK in different gene-edited backgrounds, 2 x 10^6 cells were stimulated in 0.5 ml RPMI complete with 10 ng IL-1β for 0-, 15-, 30- and 60-min in a reverse chronological order. Stimulation was stopped as described in 4.2.2. If not previously stimulated e.g. for TNIP1 blots, 2 x 10^6 cells were washed once in 5 mL ice-cold PBS. All samples were resuspended in 100 µl NP40-buffer freshly supplemented with PMSF, protease inhibitor and phosphatase inhibitor, incubated on ice for 15-30 min and sonicated in the Bioruptor® with a 30 second duty cycle. After centrifugation for 10 min at 16.000 × g at 4°C supernatant was transferred into a new 1.5 ml micro tube. 10 – 20 µl of lysate were mixed with 6x SDS loading buffer in a new tube, boiled for 10 min at 95°C on a heating block and either directly applied on an SDS-PAGE or stored at -20°C for later usage.

SDS-PAGE

For protein separation, either freshly prepared or samples stored at -20°C were used. Initially, samples were brought to RT and quickly spined down. 10 µl of samples, 5 µl of PageRuler Plus Prestained Protein Ladder for the chemiluminescence blot or 2 µl of Chameleon Duo Prestained Protein Ladder for the fluorescence-based blot were loaded onto a NuPAGE 4-12% Bis-Tris Gel. Gels were run in 1x MES SDS running buffer at 50 V for 15 min and then at 150 V for 65 min.

Protein transfer

Following protein separation proteins were transferred onto a methanol activated 0.45 µm PVDF membrane. For protein transfer, whatmann blotting paper was soaked in cooled 1x transfer buffer, gel and membrane were ‘sandwiched’ in between. Proteins were transferred at 350 mA for 1 h in the wet tank system at 4°C (cold room).

Chemiluminescence based signal detection

All phospho-blots and TNIP1-blots for cell line characterization were developed chemiluminescence based. First, membranes for phosphor-protein detection were blocked for 1 h at RT by rolling in 2,5 % BSA/ 2,5 % skim milk in TBST. The blots for the corresponding non-phosphorylated proteins were blocked in 5 % skim milk in TBST. For primary antibody incubation for the phospho-blots, membranes were incubated in 5 % BSA in TBST containing 1:1000 of

phospho-antibodies. For the corresponding non-phosphorylated protein and TNIP1 blots, primary antibodies were added directly to the blocking solution at 1:1000. Membranes were incubated rolling overnight at 4 °C. The next day, the membrane was washed 4 x 10 min in TBST. Next, membranes for phospho-blots were incubated rolling for 2 h at RT in secondary HRP-conjugated goat anti-rabbit antibody solution (1:10.000 in 5 % BSA TBST). For corresponding non-phosphorylated protein and TNIP1 blots, membranes were incubated for 1 h at RT in secondary HRP-conjugated goat anti-rabbit antibody solution (1:20.000 in 5 % skim milk TBST). After repeating the previous washing step, protein signal was amplified by incubating the membrane for 40 – 90 sec at 1:1of SuperSignalWest Femto Maximum Sensitivity Substrate solution and detected on the ChemiDoc XRS + System using the single accumulation setting with 1 sec between each acquisition as well as the automated acquisition settings.

Fluorescence based signal detection

After protein transfer, membranes were stained for whole blotted protein for later normalization. For this purpose, membranes were first rinsed in ddH_2O and immediately stained with Revert^{TM} 700 Total Protein Stain Solution according to the manufacturer's protocol. Total protein stain signal was detected on the Odyssey CLx Infrared Imaging System using the auto-acquisition settings. To increase primary antibody binding, membrane was dried (between two whatmann paper in 37 °C for approx. 5-min) and re-activated in methanol, rinsed in ddH_2O, incubated for 5 min in TBS followed by an 1 h blocking step using Intercept Protein-Free Blocking Buffer. Anti-TNIP1 antibody was added to the blocking solution as well as 0.2 % Tween and 0.01 % SDS and incubated gently shaking overnight at 4 °C overnight. On the next day, membrane was washed 4 x 10 min in TBST. Next, membrane was incubated in blocking solution containing 1:20,000 IRDye® 680 Goat anti-Rabbit Secondary antibody (LI-COR, 926-68171), 0.2 % Tween and 0.01 % SDS for 1 h at RT gently shaking. After washing the membrane 3 x with TBST and 1x with TBS TNIP1 for 10 min each signal was detected using the Odyssey CLx Infrared Imaging System in auto-acquisition settings. Data analysis was performed in EmpiriaStudio. Specifically, TNIP1 signal per total protein input as detected by Rever^{TM} 700 Total Protein Solution was calculated for each sample. Next, the TNIP1 signal was normalized to the unstimulated control with or without prior CHX treatment. Corresponding means and SEMs of all replicates were plotted using R.

4.2.8 IL-2 ELISA

EL4.NOB-1WT cells release IL-2 after 24 h of IL-1β[136]. To characterize the long-term IL-1β signaling output in EL4 cells, IL-2 amounts were detected using enzyme-linked immunosorbent assay (ELISA). For this purpose, $1x10^6$ cells in 150 µl per well were distributed in a 48-well plate. After 30 min of settling time, cells were stimulated with IL-1β with a final concentration of 10 ng/ml in 50 µl medium per well. For the unstimulated control 50 µl medium was added. After 24 h plates were centrifuged (300 × g for 5 minutes). Supernatants were transferred in to a new plate and stored at -80°C until subsequent IL-2-ELISA analysis. To measure released IL-2, the Mouse IL-2 DuoSet ELISA was performed based on the manufacturers protocol. Stimulation experiments were performed on three independent days in triplicates. The obtained results were normalized to the corresponding parental cell line's IL-2 release.

References

1. Murphy KM, Weaver C. *Janeway's Immunology*. 9th Edition. Taylor & Francis Group; 2011.
2. Bennett JM, Reeves G, Billman GE, Sturmberg JP. Inflammation-nature's way to efficiently respond to all types of challenges: Implications for understanding and managing "the epidemic" of chronic diseases. *Front Med*. 2018;5. doi:10.3389/fmed.2018.00316
3. Jusko WJ, Lon HK, Liu D. Pharmacokinetic/pharmacodynamic modeling in inflammation. *Crit Rev Biomed Eng*. 2012;40(4):295-312. doi:10.1615/CritRevBiomedEng.v40.i4.50
4. Duque GA, Descoteaux A. Macrophage cytokines: Involvement in immunity and infectious diseases. *Front Immunol*. 2014;5(OCT). doi:10.3389/fimmu.2014.00491
5. Liu C, Chu D, Kalantar-Zadeh K, George J, Young HA, Liu G. Cytokines: From Clinical Significance to Quantification. *Advanced Science*. 2021;8(15). doi:10.1002/advs.202004433
6. Basil MC, Levy BD. Specialized pro-resolving mediators: Endogenous regulators of infection and inflammation. *Nat Rev Immunol*. 2016;16(1):51-67. doi:10.1038/nri.2015.4
7. Kotas ME, Medzhitov R. Homeostasis, Inflammation, and Disease Susceptibility. *Cell*. 2015;160(5):816-827. doi:10.1016/j.cell.2015.02.010
8. Chen L, Deng H, Cui H, et al. *Inflammatory Responses and Inflammation-Associated Diseases in Organs*. Vol 9.; 2018. www.impactjournals.com/oncotarget/
9. Matzinger P. Tolerance, danger, and the extended family. *Annu Rev Immunol*. 1994;12(1):991-1045. doi:10.1146/annurev.iy.12.040194.005015
10. Matzinger P. The danger model: A renewed sense of self. *Science (1979)*. 2002;296(5566):301-305. doi:10.1126/science.1071059
11. Medzhitov R. The spectrum of inflammatory responses. *Science*. 2021;374(6571):1070-1075. doi:10.1126/science.abi5200
12. Medzhitov R. Origin and physiological roles of inflammation. *Nature*. 2008;454(7203):428-435. doi:10.1038/nature07201
13. Zhang JM, An J. Cytokines, inflammation, and pain. *Int Anesthesiol Clin*. 2007;45(2):27-37. doi:10.1097/AIA.0b013e318034194e
14. Turner MD, Nedjai B, Hurst T, Pennington DJ. Cytokines and chemokines: At the crossroads of cell signalling and inflammatory disease. *Biochim Biophys Acta Mol Cell Res*. 2014;1843(11):2563-2582. doi:10.1016/j.bbamcr.2014.05.014
15. Sugimoto MA, Sousa LP, Pinho V, Perretti M, Teixeira MM. Resolution of inflammation: What controls its onset? *Front Immunol*. 2016;7. doi:10.3389/fimmu.2016.00160
16. Schwartz M, Baruch K. The resolution of neuroinflammation in neurodegeneration: Leukocyte recruitment via the choroid plexus. *EMBO Journal*. 2014;33(1):7-22. doi:10.1002/embj.201386609
17. Paludan SR, Pradeu T, Masters SL, Mogensen TH. Constitutive immune mechanisms: mediators of host defence and immune regulation. *Nat Rev Immunol*. 2021;21(3):137-150. doi:10.1038/s41577-020-0391-5
18. Schmitz ML, Weber A, Roxlau T, Gaestel M, Kracht M. Signal integration, crosstalk mechanisms and networks in the function of inflammatory cytokines. *Biochim Biophys Acta Mol Cell Res*. 2011;1813(12):2165-2175. doi:10.1016/j.bbamcr.2011.06.019
19. Fields JK, Günther S, Sundberg EJ. Structural basis of IL-1 family cytokine signaling. *Front Immunol*. 2019;10. doi:10.3389/fimmu.2019.01412
20. Boraschi D. What Is IL-1 for? The Functions of Interleukin-1 Across Evolution. *Front Immunol*. 2022;13. doi:10.3389/fimmu.2022.872155

21. Schroder K, Tschopp J. The Inflammasomes. *Cell*. 2010;140(6):821-832. doi:10.1016/j.cell.2010.01.040

22. Dinarello CA. A clinical perspective of IL-1β as the gatekeeper of inflammation. *Eur J Immunol*. 2011;41(5):1203-1217. doi:10.1002/eji.201141550

23. Garlanda C, Dinarello CA, Mantovani A. The Interleukin-1 Family: Back to the Future. *Immunity*. 2013;39(6):1003-1018. doi:10.1016/j.immuni.2013.11.010

24. Kaneko N, Kurata M, Yamamoto T, Morikawa S, Masumoto J. The role of interleukin-1 in general pathology. *Inflamm Regen*. 2019;39(1). doi:10.1186/s41232-019-0101-5

25. Dinarello CA. Interleukin-1 in the pathogenesis and treatment of inflammatory diseases. *Blood*. 2011;117(14):3720-3732. doi:10.1182/blood-2010-07-273417

26. Chan AH, Schroder K. Inflammasome signaling and regulation of interleukin-1 family cytokines. *Journal of Experimental Medicine*. 2020;217(1). doi:10.1084/jem.20190314

27. Weber A, Wasiliew P, Kracht M. Interleukin-1 (IL-1)Pathway. *Immunology*. 2010;3(105).

28. Gabay C, Lamacchia C, Palmer G. IL-1 pathways in inflammation and human diseases. *Nat Rev Rheumatol*. 2010;6(4):232-241. doi:10.1038/nrrheum.2010.4

29. Lin SC, Lo YC, Wu H. Helical assembly in the MyD88-IRAK4-IRAK2 complex in TLR/IL-1R signalling. *Nature*. 2010;465(7300):885-890. doi:10.1038/nature09121

30. Kawagoe T, Sato S, Matsushita K, et al. Sequential control of Toll-like receptor-dependent responses by IRAK1 and IRAK2. *Nat Immunol*. 2008;9(6):684-691. doi:10.1038/ni.1606

31. Vollmer S, Strickson S, Zhang T, et al. The mechanism of activation of IRAK1 and IRAK4 by interleukin-1 and Toll-like receptor agonists. *Biochemical Journal*. 2017;474(12):2027-2038. doi:10.1042/BCJ20170097

32. Cohen P. The TLR and IL-1 signalling network at a glance. *J Cell Sci*. 2014;127(11):2383-2390. doi:10.1242/jcs.149831

33. Sun L, Chen ZJ. The novel functions of ubiquitination in signaling. *Curr Opin Cell Biol*. 2004;16(2):119-126. doi:10.1016/j.ceb.2004.02.005

34. Courtois G, Fauvarque MO. The many roles of ubiquitin in NF-κB signaling. *Biomedicines*. 2018;6(2). doi:10.3390/biomedicines6020043

35. Chen ZJ, Parent L, Maniatis T. Site-Specific Phosphorylation of IκBα by a Novel Ubiquitination-Dependent Protein Kinase Activity. *Cell*. 1996;84(6):853-862. doi:10.1016/S0092-8674(00)81064-8

36. Schomer-Miller B, Higashimoto T, Lee YK, Zandi E. Regulation of IκB kinase (IKK) complex by IKKγ-dependent phosphorylation of the T-loop and C terminus of IKKβ. *Journal of Biological Chemistry*. 2006;281(22):15268-15276. doi:10.1074/jbc.M513793200

37. Carter RS, Pennington KN, Ungurait BJ, Ballard DW. In Vivo Identification of Inducible Phosphoacceptors in the IKKγ/NEMO Subunit of Human IκB Kinase. *Journal of Biological Chemistry*. 2003;278(22):19642-19648. doi:10.1074/jbc.M301705200

38. Dainichi T, Matsumoto R, Mostafa A, Kabashima K. Immune control by TRAF6-mediated pathways of epithelial cells in the EIME (epithelial immune microenvironment). *Front Immunol*. 2019;10. doi:10.3389/fimmu.2019.01107

39. Chang L, Karin M. Mammalian MAP kinase signalling cascades. *Nature*. 2001;410(6824):37-40. doi:10.1038/35065000

40. Dinarello CA. Immunological and inflammatory functions of the interleukin-1 family. *Annu Rev Immunol*. 2009;27:519-550. doi:10.1146/annurev.immunol.021908.132612

41. Huang Q, Yang J, Lin Y, et al. Differential regulation of interleukin 1 receptor and toll-like receptor signaling by MEKK3. *Nat Immunol*. 2004;5(1):98-103. doi:10.1038/ni1014

42. Hinz M, Scheidereit C. The IκB kinase complex in NF-κB regulation and beyond. *EMBO Rep*. 2014;15(1):46-61. doi:10.1002/embr.201337983

43. Gottschalk RA, Martins AJ, Angermann BR, et al. Distinct NF-κB and MAPK Activation Thresholds Uncouple Steady-State Microbe Sensing from Anti-pathogen Inflammatory Responses. *Cell Syst*. 2016;2(6):378-390. doi:10.1016/j.cels.2016.04.016

44. Dunne A, O'Neill LAJ. The interleukin-1 receptor/Toll-like receptor superfamily: signal transduction during inflammation and host defense. 2003;171. doi:10.1126/stke.2003.171.re3

45. Cohen P, Tcherpakov M. Will the ubiquitin system furnish as many drug targets as protein kinases? *Cell*. 2010;143(5):686-693. doi:10.1016/j.cell.2010.11.016

46. Emmerich CH, Schmukle AC, Walczak H. The Emerging Role of Linear Ubiquitination in Cell Signaling. *Cell Biology*. 2010;4(204).

47. Malcova H, Strizova Z, Milota T, et al. IL-1 Inhibitors in the Treatment of Monogenic Periodic Fever Syndromes: From the Past to the Future Perspectives. *Front Immunol*. 2021;11. doi:10.3389/fimmu.2020.619257

48. Ridker PM, Thuren T, Zalewski A, Libby P. Interleukin-1β inhibition and the prevention of recurrent cardiovascular events: Rationale and Design of the Canakinumab Anti-inflammatory Thrombosis Outcomes Study (CANTOS). *Am Heart J*. 2011;162(4):597-605. doi:10.1016/j.ahj.2011.06.012

49. Ridker PM, Everett BM, Thuren T, et al. Antiinflammatory Therapy with Canakinumab for Atherosclerotic Disease. *New England Journal of Medicine*. 2017;377(12):1119-1131. doi:10.1056/nejmoa1707914

50. Baldo BA. Side Effects of Cytokines Approved for Therapy. *Drug Saf*. 2014;37(11):921-943. doi:10.1007/s40264-014-0226-z

51. Lin X, Twelkmeyer T, Wang SY, et al. An immunopathogenic perspective of interleukin-1 signaling. *Cell Mol Immunol*. 2020;17(8):892-893. doi:10.1038/s41423-020-0475-y

52. Sims JE, Smith DE. The IL-1 family: Regulators of immunity. *Nat Rev Immunol*. 2010;10(2):89-102. doi:10.1038/nri2691

53. Tsuchiya K, Hosojima S, Hara H, et al. Gasdermin D mediates the maturation and release of IL-1α downstream of inflammasomes. *Cell Rep*. 2021;34(12). doi:10.1016/j.celrep.2021.108887

54. Malik A, Kanneganti TD. Function and regulation of IL-1α in inflammatory diseases and cancer. *Immunol Rev*. 2018;281(1):124-137. doi:10.1111/imr.12615

55. Marino A, Tirelli F, Giani T, Cimaz R. Periodic fever syndromes and the autoinflammatory diseases (AIDs). *J Transl Autoimmun*. 2020;3. doi:10.1016/j.jtauto.2019.100031

56. Man SM, Karki R, Briard B, et al. Differential roles of caspase-1 and caspase-11 in infection and inflammation. *Sci Rep*. 2017;7(1):45126. doi:10.1038/srep45126

57. Evavold CL, Ruan J, Tan Y, Xia S, Wu H, Kagan JC. The Pore-Forming Protein Gasdermin D Regulates Interleukin-1 Secretion from Living Macrophages. *Immunity*. 2018;48(1):35-44.e6. doi:10.1016/j.immuni.2017.11.013

58. Denes A, Lopez-Castejon G, Brough D. Caspase-1: Is IL-1 just the tip of the ICE berg? *Cell Death Dis*. 2012;3(7). doi:10.1038/cddis.2012.86

59. Boraschi D, Tagliabue A. The interleukin-1 receptor family. *Semin Immunol*. 2013;25(6):394-407. doi:10.1016/j.smim.2013.10.023

60. Arend WP, Palmer G, Gabay C. IL-1, IL-18, and IL-33 families of cytokines. *Immunol Rev*. 2008;223(1):20-38. doi:10.1111/j.1600-065X.2008.00624.x

61. Hermanns HM, Wohlfahrt J, Mais C, Hergovits S, Jahn D, Geier A. Endocytosis of pro-inflammatory cytokine receptors and its relevance for signal transduction. *Biol Chem*. 2016;397(8):695-708. doi:10.1515/hsz-2015-0277

62. Johannes L. Endocytosis: Remote Control from Deep Inside. *Current Biology*. 2017;27(13):R663-R666. doi:10.1016/j.cub.2017.05.018

63. Schmid SL, Sorkin A, Zerial M. Endocytosis: Past, Present, and Future. *Cold Spring Harb Perspect Biol*. 2014;6(12):a022509-a022509. doi:10.1101/cshperspect.a022509

64. di Fiore PP. Endocytosis, signaling and cancer, much more than meets the eye. *Mol Oncol*. 2009;3(4):273-279. doi:10.1016/j.molonc.2009.06.002

65. Sorkin A, von Zastrow M. Endocytosis and signalling: Intertwining molecular networks. *Nat Rev Mol Cell Biol*. 2009;10(9):609-622. doi:10.1038/nrm2748

66. Murphy JE, Padilla BE, Hasdemir B, Cottrell GS, Bunnett NW, Lefkowitz RJ. Endosomes: A Legitimate Platform for the Signaling Train. *Proc. Nat. Acad. Sci*. 2009;106(42):17615-17622. doi:https://doi.org/10.1073/pnas.0906541106

67. Zhang G, Ghosh S. Negative regulation of toll-like receptor-mediated signaling by Tollip. *Journal of Biological Chemistry*. 2002;277(9):7059-7065. doi:10.1074/jbc.M109537200

68. Kowalski EJA, Li L. Toll-interacting protein in resolving and non-resolving inflammation. *Front Immunol*. 2017;8. doi:10.3389/fimmu.2017.00511

69. Didierlaurent A, Brissoni B, Velin D, et al. Tollip Regulates Proinflammatory Responses to Interleukin-1 and Lipopolysaccharide. *Mol Cell Biol*. 2006;26(3):735-742. doi:10.1128/mcb.26.3.735-742.2006

70. Fuseya Y, Iwai K. Biochemistry, pathophysiology, and regulation of linear ubiquitination: Intricate regulation by coordinated functions of the associated ligase and deubiquitinase. *Cells*. 2021;10(10). doi:10.3390/cells10102706

71. Smith H, Peggie M, Campbell DG, Vandermoere F, Carrick E, Cohen P. Identification of the Phosphorylation Sites on the E3 Ubiquitin Ligase Pellino That Are Critical for Activation by IRAK1 and IRAK4. *Proceedings of the National Academy of Sciences.* 2009;106(12):4584-4590. doi:10.1073/pnas.0900774106

72. Cohen P, Strickson S. The role of hybrid ubiquitin chains in the MyD88 and other innate immune signalling pathways. *Cell Death Differ*. 2017;24(7):1153-1159. doi:10.1038/cdd.2017.17

73. Emmerich CH, Ordureau A, Strickson S, et al. Activation of the canonical IKK complex by K63/M1-linked hybrid ubiquitin chains. *Proc Natl Acad Sci U S A*. 2013;110(38):15247-15252. doi:10.1073/pnas.1314715110

74. Nguyen LK. Dynamics of ubiquitin-mediated signalling: Insights from mathematical modelling and experimental studies. *Brief Bioinform*. 2016;17(3):479-493. doi:10.1093/bib/bbv052

75. Lork M, Verhelst K, Beyaert R. CYLD, A20 and OTULIN deubiquitinases in NF-κB signaling and cell death: So similar, yet so different. *Cell Death Differ*. 2017;24(7):1172-1183. doi:10.1038/cdd.2017.46

76. Shembade N, Harhaj EW. Regulation of NF-κB signaling by the A20 deubiquitinase. *Cell Mol Immunol*. 2012;9(2):123-130. doi:10.1038/cmi.2011.59

77. Ma A, Malynn BA. A20: Linking a complex regulator of ubiquitylation to immunity and human disease. *Nat Rev Immunol*. 2012;12(11):774-785. doi:10.1038/nri3313

78. Shembade N, Harhaj NS, Liebl DJ, Harhaj EW. Essential role for TAX1BP1 in the termination of TNF-α-, IL-1- and LPS-mediated NF-κB and JNK signaling. *EMBO Journal*. 2007;26(17):3910-3922. doi:10.1038/sj.emboj.7601823

79. Shembade N, Pujari R, Harhaj NS, Abbott DW, Harhaj EW. The kinase IKKα inhibits activation of the transcription factor NF-κB by phosphorylating the regulatory molecule TAX1BP1. *Nat Immunol*. 2011;12(9):834-843. doi:10.1038/ni.2066

80. Momtazi G, Lambrecht BN, Naranjo JR, Schock BC. Regulators of A20 (TNFAIP3): new drug-able targets in inflammation. *Am J Physiol Lung Cell Mol Physiol*. 2019;316(3):456-469. doi:10.1152/ajplung.00335.2018

81. van Huffel S, Delaei F, Heyninck K, de Valck D, Beyaert R. Identification of a Novel A20-binding Inhibitor of Nuclear Factor-κB Activation Termed ABIN-2. *Journal of Biological Chemistry*. 2001;276(32):30216-30223. doi:10.1074/jbc.M100048200

82. Laplantine E, Fontan E, Chiaravalli J, et al. NEMO specifically recognizes K63-linked poly-ubiquitin chains through a new bipartite ubiquitin-binding domain. *EMBO Journal*. 2009;28(19):2885-2895. doi:10.1038/emboj.2009.241

83. Leotoing L, Chereau F, Baron S, et al. A20-binding inhibitor of nuclear factor-κB (NF-κB)-2 (ABIN-2) is an activator of inhibitor of NF-κB (IκB) kinase α (IKKα)-mediated NF-κB transcriptional activity. *Journal of Biological Chemistry*. 2011;286(37):32277-32288. doi:10.1074/jbc.M111.236448

84. Verstrepen L, Carpentier I, Verhelst K, Beyaert R. ABINs: A20 binding inhibitors of NF-κB and apoptosis signaling. *Biochem Pharmacol*. 2009;78(2):105-114. doi:10.1016/j.bcp.2009.02.009

85. Wagner S, Carpentier I, Rogov V, et al. Ubiquitin binding mediates the NF-κB inhibitory potential of ABIN proteins. *Oncogene*. 2008;27(26):3739-3745. doi:10.1038/sj.onc.1211042

86. Shamilov R, Aneskievich BJ. TNIP1 in autoimmune diseases: Regulation of toll-like receptor signaling. *J Immunol Res*. 2018;2018. doi:10.1155/2018/3491269

87. G'Sell RT, Gaffney PM, Powell DW. A20-binding inhibitor of NF-κB activation 1 is a physiologic inhibitor of NF-κB: A molecular switch for inflammation and autoimmunity. *Arthritis and Rheumatology*. 2015;67(9):2292-2302. doi:10.1002/art.39245

88. Verstrepen L, Carpentier I, Beyaert R. The Biology of A20-Binding Inhibitors of NF-κb activation *(ABINS)*. In: *Advances in Experimental Medicine and Biology*. Springer New York; 2014:13-31. doi:10.1007/978-1-4939-0398-6_2

89. Shiote Y, Ouchida M, Jitsumoir Y, et al. Multiple splicing variants of Naf1/ABIN-1 transcripts and their alterations in hematopoietic tumors. *International Journal of Molecular Medicine*. 2006. doi:10.3892/ijmm.18.5.917

90. Cruz JA, Childs EE, Amatya N, et al. IL-17 Signaling Triggers Degradation of the Constitutive NF-κB Inhibitor ABIN-1. *Immunohorizons*. 2017;1(7):133-141. doi:10.4049/immunohorizons.1700035

91. Yin H, Karayel O, Chao YY, et al. A20 and ABIN-1 cooperate in balancing CBM complex-triggered NF-κB signaling in activated T cells. *Cellular and Molecular Life Sciences*. 2022;79(2). doi:10.1007/s00018-022-04154-z

92. Swindell WR, Beamer MA, Sarkar MK, et al. RNA-seq analysis of IL-1B and IL-36 responses in epidermal keratinocytes identifies a shared MyD88-dependent gene signature. *Front Immunol*. 2018;9. doi:10.3389/fimmu.2018.00080

93. Nanda SK, Venigalla RKC, Ordureau A, et al. Polyubiquitin binding to ABIN1 is required to prevent autoimmunity. *Journal of Experimental Medicine*. 2011;208(6):1215-1228. doi:10.1084/jem.20102177

94. Fukushi M, Dixon J, Kimura T, Tsurutani N, Dixon MJ, Yamamoto N. Identification and cloning of a novel cellular protein Naf1, Nef-associated factor 1, that increases cell surface CD4 expression1. *FEBS Letters*. 1999;442(1):83-88. doi:10.1016/s0014-5793(98)01631-7

95. Gupta K, Ott D, Hope TJ, Siliciano RF, Boeke JD. A human nuclear shuttling protein that interacts with human immunodeficiency virus type 1 matrix is packaged into virions. *Journal of Virology*. 2000;74(24):11811-11824. doi:10.1128/jvi.74.24.11811-11824.2000

96. Chen S, Yang X, Cheng W, et al. Immune regulator ABIN1 suppresses HIV-1 transcription by negatively regulating the ubiquitination of Tat. *Retrovirology*. 2017;14(1). doi:10.1186/s12977-017-0338-5

97. Zhang S, Fukushi M, Hashimoto S, et al. A new ERK2 binding protein, Naf1, attenuates the EGF/ERK2 nuclear signaling. *Biochemical and Biophysical Research Communications*. 2002;297(1):17-23. doi:10.1016/s0006-291x(02)02086-7

98. Gurevich I, Zhang C, Francis N, Aneskievich BJ. TNIP1, a Retinoic Acid Receptor Corepressor and A20-binding Inhibitor of NF-κB, Distributes to Both Nuclear and Cytoplasmic Locations. *Journal of Histochemistry and Cytochemistry*. 2011;59(12):1101-1112. doi:10.1369/0022155411427728

99. Flores AM, Gurevich I, Zhang C, Ramirez VP, Devens TR, Aneskievich BJ. TNIP1 is a corepressor of agonist-bound PPARs. *Arch Biochem Biophys*. 2011;516(1):58-66. doi:10.1016/j.abb.2011.08.014

100. Ma Y, Yuan S, Tian X, et al. ABIN1 inhibits HDAC1 ubiquitination and protects it from both proteasome- and lysozyme-dependent degradation. *J Cell Biochem*. 2018;119(4):3030-3043. doi:10.1002/jcb.26428

101. le Guerroué F, Werner A, Wang C, Youle R. TNIP1 inhibits Mitophagy via interaction with FIP200 and TAX1BP1. *bioRxiv* 2022. doi:10.1101/2022.03.14.484269

102. Mirza N, Sowa AS, Lautz K, Kufer TA. NLRP10 Affects the Stability of Abin-1 To Control Inflammatory Responses. *The Journal of Immunology*. 2019;202(1):218-227. doi:10.4049/jimmunol.1800334

103. Mauro C, Pacifico F, Lavorgna A, et al. ABIN-1 binds to NEMO/IKKγ and co-operates with A20 in inhibiting NF-κB. *Journal of Biological Chemistry*. 2006;281(27):18482-18488. doi:10.1074/jbc.M601502200

104. Shamilov R, Vinogradova O, Aneskievich BJ. The anti-inflammatory protein tnip1 is intrinsically disordered with structural flexibility contributed by its ahd1-uban domain. *Biomolecules*. 2020;10(11):1-24. doi:10.3390/biom10111531

105. Vandereyken K, van Leene J, de Coninck B, Cammue BPA. Hub protein controversy: Taking a closer look at plant stress response hubs. *Front Plant Sci*. 2018;9. doi:10.3389/fpls.2018.00694

106. Dziedzic SA, Su Z, Jean Barrett V, et al. ABIN-1 regulates RIPK1 activation by linking Met1 ubiquitylation with Lys63 deubiquitylation in TNF-RSC article. *Nat Cell Biol*. 2018;20(1):58-68. doi:10.1038/s41556-017-0003-1

107. Degterev A, Ofengeim D, Yuan J. Targeting RIPK1 for the treatment of human diseases. *Proc Natl Acad Sci U S A*. 2019;116(20):9714-9722. doi:10.1073/pnas.1901179116

108. Shinkawa Y, Imami K, Fuseya Y, et al. ABIN1 is a signal-induced autophagy receptor that attenuates NF-κB activation by recognizing linear ubiquitin chains. *FEBS Lett*. 2022;596(9):1147-1164. doi:10.1002/1873-3468.14323

109. Viemann D, Goebeler M, Schmid S, et al. Transcriptional profiling of IKK2/NF-B-and p38 MAP kinase-dependent gene expression in TNF-stimulated primary human endothelial cells. Published online 2004. doi:10.1182/blood-2003

110. Imbeault M, Ouellet M, Giguère K, et al. Acquisition of Host-Derived CD40L by HIV-1 In Vivo and Its Functional Consequences in the B-Cell Compartment . *J Virol*. 2011;85(5):2189-2200. doi:10.1128/jvi.01993-10

111. Schwanhüusser B, Busse D, Li N, et al. Global quantification of mammalian gene expression control. *Nature*. 2011;473(7347):337-342. doi:10.1038/nature10098

112. Lee MJ, Yaffe MB. Protein Regulation in Signal Transduction. *Cold Spring Harb Perspect Biol*. 2016;8(6):a005918. doi:10.1101/cshperspect.a005918

113. Hlavacek WS, Faeder JR. The Complexity of Cell Signaling and the Need for a New Mechanics. *Sci Signal*. 2009;2(81). doi:10.1126/scisignal.281pe46

114. Valls PO, Esposito A. Signalling dynamics, cell decisions, and homeostatic control in health and disease. *Curr Opin Cell Biol*. 2022;75. doi:10.1016/j.ceb.2022.01.011

115. Chou WC, Rampanelli E, Li X, Ting JPY. Impact of intracellular innate immune receptors on immunometabolism. *Cell Mol Immunol*. 2022;19(3):337-351. doi:10.1038/s41423-021-00780-y

116. Zhang X, Kim TH, Thauland TJ, et al. Unraveling the mechanobiology of immune cells. *Curr Opin Biotechnol*. 2020;66:236-245. doi:10.1016/j.copbio.2020.09.004

117. Suen JY, Navlakha S. A feedback control principle common to several biological and engineered systems. *J R Soc Interface*. 2022;19(188). doi:10.1098/rsif.2021.0711

118. Naik S, Larsen SB, Gomez NC, et al. Inflammatory memory sensitizes skin epithelial stem cells to tissue damage. *Nature*. 2017;550(7677):475-480. doi:10.1038/nature24271

119. Netea MG, Domínguez-Andrés J, Barreiro LB, et al. Defining trained immunity and its role in health and disease. *Nat Rev Immunol*. 2020;20(6):375-388. doi:10.1038/s41577-020-0285-6

120. DeFelice MM, Clark HR, Hughey JJ, et al. NF-kB signaling dynamics is controlled by a dose-sensing autoregulatory loop. *Sci Signal*. 2019;12(579). doi:10.1126/scisignal.aau3568

121. O'Neill LAJ, Bird TA, Saklatvala J. Interleukin 1 signal transduction. *Immunol Today*. 1990;11:392-394. doi:10.1016/0167-5699(90)90155-3

122. Deliz-Aguirre R, Cao F, Gerpott FHU, et al. MyD88 oligomer size functions as a physical threshold to trigger IL1R myddosome signaling. *Journal of Cell Biology*. 2021;220(7). doi:10.1083/jcb.202012071

123. Rasmussen MK, Iversen L, Johansen C, et al. IL-8 and p53 are inversely regulated through JNK, p38 and NF-κB p65 in HepG2 cells during an inflammatory response. *Inflammation Research*. 2008;57(7):329-339. doi:10.1007/s00011-007-7220-1

124. Shimizu K, Nakajima A, Sudo K, et al. IL-1 Receptor Type 2 Suppresses Collagen-Induced Arthritis by Inhibiting IL-1 Signal on Macrophages. *The Journal of Immunology*. 2015;194(7):3156-3168. doi:10.4049/jimmunol.1402155

125. Shahrara S, Pickens SR, Dorfleutner A, Pope RM. IL-17 Induces Monocyte Migration in Rheumatoid Arthritis. *The Journal of Immunology*. 2009;182(6):3884-3891. doi:10.4049/jimmunol.0802246

126. Szklarczyk D, Gable AL, Nastou KC, et al. The STRING database in 2021: customizable protein–protein networks, and functional characterization of user-uploaded gene/measurement sets. *Nucleic Acids Res*. 2021;49(D1):D605-D612. doi:10.1093/nar/gkaa1074

127. Kawai T, Akira S. Regulation of innate immune signalling pathways by the tripartite motif (TRIM) family proteins. *EMBO Mol Med*. 2011;3(9):513-527. doi:10.1002/emmm.201100160

128. Zhang H, Li M, Liu Y, et al. Ubiquitin-binding domain in ABIN1 is critical for regulating cell death and inammation during development. doi:10.21203/rs.3.rs-712049/v1

129. Xia S, Chen Z, Shen C, Fu TM. Higher-order assemblies in immune signaling: supramolecular complexes and phase separation. *Protein Cell*. 2021;12(9):680-694. doi:10.1007/s13238-021-00839-6

130. Motshwene PG, Moncrieffe MC, Grossmann JG, et al. An Oligomeric Signaling Platform formed by the toll-like receptor signal transducers MyD88 and IRAK-4. *Journal of Biological Chemistry*. 2009;284(37):25404-25411. doi:10.1074/jbc.M109.022392

131. Yamin TT, Miller DK. The interleukin-1 receptor-associated kinase is degraded by proteasomes following its phosphorylation. *Journal of Biological Chemistry*. 1997;272(34):21540-21547. doi:10.1074/jbc.272.34.21540

132. Eichelbaum K, Winter M, Diaz MB, Herzig S, Krijgsveld J. Selective enrichment of newly synthesized proteins for quantitative secretome analysis. *Nat Biotechnol*. 2012;30(10):984-990. doi:10.1038/nbt.2356

133. Eichelbaum K, Krijgsveld J. Rapid temporal dynamics of transcription, protein synthesis, and secretion during macrophage activation. *Molecular and Cellular Proteomics*. 2014;13(3):792-810. doi:10.1074/mcp.M113.030916

134. Aggarwal BB, Takada Y, Shishodia S, et al. Nuclear transcription factor NF-kappa B: role in biology and medicine. *Indian J Exp Biol*. 2004;42(4):341-353.

135. Gygi SP, Rochon Y, Franza BR, Aebersold R. Correlation between Protein and mRNA Abundance in Yeast. *Mol Cell Biol*. 1999;19(3):1720-1730. doi:10.1128/MCB.19.3.1720

136. Knop J, Wesche H, Lang D, Martin MU. Effects of overexpression of IL-1 receptor-associated kinase on NFκB activation, IL-2 production and stress-activated protein kinases in the murine T cell line EL4. *Eur J Immunol*. 1998;28(10):3100-3109. doi:10.1002/(SICI)1521-4141(199810)28:10<3100::AID-IMMU3100>3.0.CO;2-7

137. Kholodenko BN. Cell-signalling dynamics in time and space. *Nat Rev Mol Cell Biol*. 2006;7(3):165-176. doi:10.1038/nrm1838

138. Lee HJ, Chung KC. PINK1 Positively Regulates IL-1β-Mediated Signaling through Tollip and IRAK1 Modulation. *J. Neuroinflammation.* 2012;9(1). doi:10.1186/1742-2094-9-271

139. Liu G, Tsuruta Y, Gao Z, Park YJ, Abraham E. Variant IL-1 Receptor-Associated Kinase-1 Mediates Increased NF-κB Activity. *The Journal of Immunology*. 2007;179(6):4125-4134. doi:10.4049/jimmunol.179.6.4125

140. Koziczak-Holbro M, Joyce C, Glück A, et al. IRAK-4 kinase activity is required for interleukin-1 (IL-1) receptor- and toll-like receptor 7-mediated signaling and gene expression. *Journal of Biological Chemistry*. 2007;282(18):13552-13560. doi:10.1074/jbc.M700548200

141. Gurung P, Fan G, Lukens JR, Vogel P, Tonks NK, Kanneganti TD. Tyrosine Kinase SYK Licenses MyD88 Adaptor Protein to Instigate IL-1α-Mediated Inflammatory Disease. *Immunity*. 2017;46(4):635-648. doi:10.1016/j.immuni.2017.03.014

142. Martin MU, Wesche H. Summary and comparison of the signaling mechanisms of the Toll:interleukin-1 receptor family. *Biochim Biophys Acta*. 2002;1592:265-280. . doi:10.1016/s0167-4889(02)00320-8

143. Verstak B, Nagpal K, Bottomley SP, Golenbock DT, Hertzog PJ, Mansell A. MyD88 adapter-like (Mal)/TIRAP interaction with TRAF6 is critical for TLR2- and TLR4-mediated NF-κB proinflammatory responses. *Journal of Biological Chemistry*. 2009;284(36):24192-24203. doi:10.1074/jbc.M109.023044

144. Miggin SM, Pålsson-McDermott E, Dunne A, et al. NF-kB Activation by the Toll-IL-1 Receptor Domain Protein MyD88 Adapter-like Is Regulated by Caspase-1.; *Proc Natl Acad Sci USA*. 2007;104(9):3372-3377. doi:10.1073/pnas.0608100104

145. Dai P, Jeong SY, Yu Y, et al. Modulation of TLR Signaling by Multiple MyD88-Interacting Partners Including Leucine-Rich Repeat Fli-I-Interacting Proteins. *The Journal of Immunology*. 2009;182(6):3450-3460. doi:10.4049/jimmunol.0802260

146. Wiese MD, Manning-Bennett AT, Abuhelwa AY. Investigational IRAK-4 inhibitors for the treatment of rheumatoid arthritis. *Expert Opin Investig Drugs*. 2020;29(5):475-482. doi:10.1080/13543784.2020.1752660

147. Bennett J, Starczynowski DT. IRAK1 and IRAK4 as emerging therapeutic targets in hematologic malignancies. *Curr Opin Hematol*. 2022;29(1):8-19. doi:10.1097/MOH.0000000000000693

148. Wu X, Yang D, Zhao F, et al. Quantification of dynamic protein interactions and phosphorylation in LPS signaling pathway by SWATH-MS. *Molecular and Cellular Proteomics*. 2019;18(6):1054-1069. doi:10.1074/mcp.RA119.001380

149. Balka KR, de Nardo D. Understanding early TLR signaling through the Myddosome. *J Leukoc Biol*. 2019;105(2):339-351. doi:10.1002/JLB.MR0318-096R

150. Lu YC, Yeh WC, Ohashi PS. LPS/TLR4 signal transduction pathway. *Cytokine*. 2008;42(2):145-151. doi:10.1016/j.cyto.2008.01.006

151. Bird TA, Gearingll AJH, Saklatvalas J. Murine Interleukin 1 Receptor. direct identification by ligand blotting and purification to homogeneity of an interleukin 1-binding glycoprotein. *J Biol Chem.* 1988;263(24):12063-12069. doi:10.1016/s0021-9258(18)37893-1

152. Cortelazzo S, Ferreri A, Hoelzer D, Ponzoni M. Lymphoblastic lymphoma. *Crit Rev Oncol Hematol*. 2017;113:304-317. doi:10.1016/j.critrevonc.2017.03.020

153. Sever R, Brugge JS. Signal transduction in cancer. *Cold Spring Harb Perspect Med*. 2015;5(4). doi:10.1101/cshperspect.a006098

154. Briskos C, Wait R, Begum S, O'Neil LAJ, Saklatvala J. Mass spectrometric analysis of the endogenous type I interlukin-1 (IL-1) receptor signaling complex formed after IL-1 binding identifies IL-1RAcP, MyD88, and IRAK-4 as the stable components. *Molecular and Cellular Proteomics*. 2007;6(9):1551-1559. doi:10.1074/mcp.M600455-MCP200

155. Wu X, Zhang W, Font-Burgada J, et al. Ubiquitin-conjugating enzyme Ubc13 controls breast cancer metastasis through a TAK1-p38 MAP kinase cascade. *Proceedings of the National Academy of Sciences*. 2014;111(38):13870-13875. doi:10.1073/pnas.1414358111

156. Park HB, Baek KH. E3 ligases and deubiquitinating enzymes regulating the MAPK signaling pathway in cancers. *Biochimica et Biophysica Acta (BBA) - Reviews on Cancer*. 2022;1877(3):188736. doi:10.1016/j.bbcan.2022.188736

157. Shi D, Grossman SR. Ubiquitin becomes ubiquitous in cancer. *Cancer Biol Ther*. 2010;10(8):737-747. doi:10.4161/cbt.10.8.13417

158. Inoue H, Takamori M, Nagata N, et al. An investigation of cell proliferation and soluble mediators induced by interleukin 1b in human synovial fibroblasts- comparative response in osteoarthritis and rheumatoid arthritis. *Inflammation Research*. 2001;50:65-72.

159. Koziczak-Holbro M, Joyce C, Glück A, et al. IRAK-4 kinase activity is required for interleukin-1 (IL-1) receptor- and toll-like receptor 7-mediated signaling and gene expression. *Journal of Biological Chemistry*. 2007;282(18):13552-13560. doi:10.1074/jbc.M700548200

160. Hein MY, Hubner NC, Poser I, et al. A Human Interactome in Three Quantitative Dimensions Organized by Stoichiometries and Abundances. *Cell*. 2015;163(3):712-723. doi:10.1016/j.cell.2015.09.053

161. Johnsson N, Johnsson K. A fusion of disciplines: Chemical approaches to exploit fusion proteins for functional genomics. *ChemBioChem*. 2003;4(9):803-810. doi:10.1002/cbic.200200603

162. Evans IM, Paliashvili K. Co-immunoprecipitation Assays. *Methods Mol Biol*: 2022;2475:125-132. doi:10.1007/978-1-0716-2217-9_8

163. Hung V, Udeshi ND, Lam SS, et al. Spatially resolved proteomic mapping in living cells with the engineered peroxidase APEX2. *Nat Protoc*. 2016;11(3):456-475. doi:10.1038/nprot.2016.018

164. Kim DI, Roux KJ. Filling the Void: Proximity-Based Labeling of Proteins in Living Cells. *Trends Cell Biol*. 2016;26(11):804-817. doi:10.1016/j.tcb.2016.09.004

165. Hughes CS, Moggridge S, Müller T, Sorensen PH, Morin GB, Krijgsveld J. Single-pot, solid-phase-enhanced sample preparation for proteomics experiments. *Nat Protoc*. 2019;14(1):68-85. doi:10.1038/s41596-018-0082-x

166. Baghirova S, Hughes BG, Hendzel MJ, Schulz R. Sequential fractionation and isolation of subcellular proteins from tissue or cultured cells. *MethodsX*. 2015;2:e440-e445. doi:10.1016/j.mex.2015.11.001

167. Saikh KU, Morazzani EM, Piper AE, Bakken RR, Glass PJ. A small molecule inhibitor of MyD88 exhibits broad spectrum antiviral activity by up regulation of type I interferon. *Antiviral Res*. 2020;181:104854. doi:10.1016/j.antiviral.2020.104854

168. Gay NJ, Gangloff M, O'Neill LAJ. What the Myddosome structure tells us about the initiation of innate immunity. *Trends Immunol*. 2011;32(3):104-109. doi:10.1016/j.it.2010.12.005

169. Narita T, Weinert BT, Choudhary C. Functions and mechanisms of non-histone protein acetylation. *Nat Rev Mol Cell Biol.* 2019;20(3):156-174. doi:10.1038/s41580-018-0081-3

170. Christensen DG, Xie X, Basisty N, et al. Post-translational Protein Acetylation: An Elegant Mechanism for Bacteria to Dynamically Regulate Metabolic Functions. *Front Microbiol*. 2019;10. doi:10.3389/fmicb.2019.01604

171. Kanakaraj P, Schafer PH, Cavender DE, et al. Interleukin (IL)-1 Receptor–associated Kinase (IRAK) Requirement for Optimal Induction of Multiple IL-1 Signaling Pathways and IL-6 Production. *Journal of Experimental Medicine*. 1998;187(12):2073-2079. doi:10.1084/jem.187.12.2073

172. Rajsbaum R, Versteeg GA, Schmid S, et al. Unanchored K48-Linked Polyubiquitin Synthesized by the E3-Ubiquitin Ligase TRIM6 Stimulates the Interferon-IKKε Kinase-Mediated Antiviral Response. *Immunity*. 2014;40(6):880-895. doi:10.1016/j.immuni.2014.04.018

173. Prior IA, Harding A, Yan J, Sluimer J, Parton RG, Hancock JF. GTP-dependent segregation of H-ras from lipid rafts is required for biological activity. *Nat Cell Biol*. 2001;3(4):368-375. doi:10.1038/35070050

174. Roy S, Wyse B, Hancock JF. H-Ras Signaling and K-Ras Signaling Are Differentially Dependent on Endocytosis. *Mol Cell Biol*. 2002;22(14):5128-5140. doi:10.1128/mcb.22.14.5128-5140.2002

175. Shearer LJ, Petersen NO. Distribution and Co-localization of endosome markers in cells. *Heliyon*. 2019;5(9):e02375. doi:10.1016/j.heliyon.2019.e02375

176. Khatri P, Sirota M, Butte AJ. Ten years of pathway analysis: Current approaches and outstanding challenges. *PLoS Comput Biol*. 2012;8(2). doi:10.1371/journal.pcbi.1002375

177. Horan K, Jang C, Bailey-Serres J, et al. Annotating Genes of Known and Unknown Function by Large-Scale Coexpression Analysis. *Plant Physiol*. 2008;147(1):41-57. doi:10.1104/pp.108.117366

178. Ramirez VP, Gurevich I, Aneskievich BJ. Emerging roles for TNIP1 in regulating post-receptor signaling. *Cytokine Growth Factor Rev*. 2012;23(3):109-118. doi:10.1016/j.cytogfr.2012.04.002

179. Nanda SK, Lopez-Pelaez M, Arthur JSC, Marchesi F, Cohen P. Suppression of IRAK1 or IRAK4 Catalytic Activity, but Not Type 1 IFN Signaling, Prevents Lupus Nephritis in Mice Expressing a Ubiquitin Binding–Defective Mutant of ABIN1. *The Journal of Immunology*. 2016;197(11):4266-4273. doi:10.4049/jimmunol.1600788

180. Zhou J, Wu R, High AA, et al. A20-binding inhibitor of NF-κB (ABIN1) controls Toll-like receptor-mediated CCAAT/enhancer-binding protein β activation and protects from inflammatory disease. *Proc Natl Acad Sci U S A*. 2011;108(44). doi:10.1073/pnas.1106232108

181. Ferrao R, Zhou H, Shan Y, et al. IRAK4 Dimerization and trans-Autophosphorylation Are Induced by Myddosome Assembly. *Mol Cell*. 2014;55(6):891-903. doi:10.1016/j.molcel.2014.08.006

182. Cheng H, Addona T, Keshishian H, et al. Regulation of IRAK-4 kinase activity via autophosphorylation within its activation loop. *Biochem Biophys Res Commun*. 2007;352(3):609-616. doi:10.1016/j.bbrc.2006.11.068

183. Kramer G, Sprenger RR, Nessen MA, et al. Proteome-wide Alterations in Escherichia coli Translation Rates upon Anaerobiosis. *Molecular & Cellular Proteomics*. 2010;9(11):2508-2516. doi:10.1074/mcp.M110.001826

184. de Godoy LMF, Olsen J v., Cox J, et al. Comprehensive mass-spectrometry-based proteome quantification of haploid versus diploid yeast. *Nature*. 2008;455(7217):1251-1254. doi:10.1038/nature07341

185. Zhang G, Bowling H, Hom N, et al. In-depth quantitative proteomic analysis of de novo protein synthesis induced by brain-derived neurotrophic factor. *J Proteome Res*. 2014;13(12):5707-5714. doi:10.1021/pr5006982

186. Ross AB, Langer JD, Jovanovic M. Proteome Turnover in the Spotlight: Approaches, Applications, and Perspectives. *Molecular & Cellular Proteomics*. 2021;20:100016. doi:10.1074/mcp.R120.002190

187. Rothenberg DA, Taliaferro JM, Huber SM, Begley TJ, Dedon PC, White FM. A Proteomics Approach to Profiling the Temporal Translational Response to Stress and Growth. *iScience*. 2018;9:367-381. doi:10.1016/j.isci.2018.11.004

188. Oeckinghaus A, Ghosh S. The NF- kB Family of Transcription Factors and Its Regulation. *Cold Spring Harb Perspect Biol*. 2009;1(4):a000034. doi:10.1101/cshperspect.a000034

189. Schuster M, Annemann M, Plaza-Sirvent C, Schmitz I. Atypical IκB proteins – nuclear modulators of NF-κB signaling. *Cell Communication and Signaling*. 2013;11(1):23. doi:10.1186/1478-811X-11-23

190. Li C, Zhu B, Son YM, et al. The Transcription Factor Bhlhe40 Programs Mitochondrial Regulation of Resident CD8+ T Cell Fitness and Functionality. *Immunity*. 2019;51(3):491-507.e7. doi:10.1016/j.immuni.2019.08.013

191. Park SL, Mackay LK. Bhlhe40 Keeps Resident T Cells Too Fit to Quit. *Immunity*. 2019;51(3):418-420. doi:10.1016/j.immuni.2019.08.016

192. Jacobs MD, Harrison SC. Structure of an IκBα/NF-κB Complex. *Cell*. 1998;95(6):749-758. doi:10.1016/S0092-8674(00)81698-0

193. Schneider-Poetsch T, Yoshida M. Along the Central Dogma—Controlling Gene Expression with Small Molecules. *Annu Rev Biochem*. 2018;87(1):391-420. doi:10.1146/annurev-biochem-060614-033923

194. Proud CG. Signalling to translation: How signal transduction pathways control the protein synthetic machinery. *Biochemical Journal*. 2007;403(2):217-234. doi:10.1042/BJ20070024

195. Aarreberg LD, Esser-Nobis K, Driscoll C, Shuvarikov A, Roby JA, Gale M. Interleukin-1β Induces mtDNA Release to Activate Innate Immune Signaling via cGAS-STING. *Mol Cell*. 2019;74(4):801-815.e6. doi:10.1016/j.molcel.2019.02.038

196. Lim PS, Hardy K, Peng K, Shannon FM. Transcriptomic analysis of mouse EL4 T cells upon T cell activation and in response to protein synthesis inhibition via cycloheximide treatment. *Genom Data*. 2016;7:148-151. doi:10.1016/j.gdata.2015.12.009

197. He Q, Shumate LT, Matthias J, et al. A G protein–coupled, IP3/protein kinase C pathway controlling the synthesis of phosphaturic hormone FGF23. *JCI Insight*. 2019;4(17). doi:10.1172/jci.insight.125007

198. Paul S, Sarraf SA, Zavar L, et al. NAP1 activates TBK1 during mitosis. *bioRxiv*. 2022. doi:https://doi.org/10.1101/2022.03.09.483647

199. Andreone BJ, Przybyla L, Llapashtica C, et al. Alzheimer's-associated PLCγ2 is a signaling node required for both TREM2 function and the inflammatory response in human microglia. *Nat Neurosci*. 2020;23(8):927-938. doi:10.1038/s41593-020-0650-6

200. Giuliano CJ, Lin A, Girish V, Sheltzer JM. Generating Single Cell–Derived Knockout Clones in Mammalian Cells with CRISPR/Cas9. *Curr Protoc Mol Biol*. 2019;128(1). doi:10.1002/cpmb.100

201. Rahighi S, Ikeda F, Kawasaki M, et al. Specific Recognition of Linear Ubiquitin Chains by NEMO Is Important for NF-κB Activation. *Cell*. 2009;136(6):1098-1109. doi:10.1016/j.cell.2009.03.007

202. Adhikari A, Xu M, Chen ZJ. Ubiquitin-mediated activation of TAK1 and IKK. *Oncogene*. 2007;26(22):3214-3226. doi:10.1038/sj.onc.1210413

203. Takeda A, Oberoi-Khanuja TK, Glatz G, et al. Ubiquitin-dependent regulation of MEKK2/3-MEK5-ERK5 signaling module by XIAP and cIAP1. *EMBO J*. 2014;33(16):1784-1801. doi:10.15252/embj.201487808

204. Kim HP, Imbert J, Leonard WJ. Both integrated and differential regulation of components of the IL-2/IL-2 receptor system. *Cytokine Growth Factor Rev*. 2006;17(5):349-366. doi:10.1016/j.cytogfr.2006.07.003

205. Muniyappa H, Das KC. Activation of c-Jun N-terminal kinase (JNK) by widely used specific p38 MAPK inhibitors SB202190 and SB203580: A MLK-3-MKK7-dependent mechanism. *Cell Signal*. 2008;20(4):675-683. doi:10.1016/j.cellsig.2007.12.003

206. Fujioka S, Niu J, Schmidt C, et al. NF-κB and AP-1 Connection: Mechanism of NF-κB-Dependent Regulation of AP-1 Activity. *Mol Cell Biol*. 2004;24(17):7806-7819. doi:10.1128/mcb.24.17.7806-7819.2004

207. Gazon H, Barbeau B, Mesnard JM, Peloponese JM. Hijacking of the AP-1 signaling pathway during development of ATL. *Front Microbiol*. 2018;8(JAN). doi:10.3389/fmicb.2017.02686

208. Papoutsopoulou S, Symons A, Tharmalingham T, et al. ABIN-2 is required for optimal activation of Erk MAP kinase in innate immune responses. *Nat Immunol*. 2006;7(6):606-615. doi:10.1038/ni1334

209. Hulsen T, de Vlieg J, Alkema W. BioVenn – a web application for the comparison and visualization of biological lists using area-proportional Venn diagrams. *BMC Genomics*. 2008;9(1):488. doi:10.1186/1471-2164-9-488

210. Cox J, Mann M. MaxQuant enables high peptide identification rates, individualized p.p.b.-range mass accuracies and proteome-wide protein quantification. *Nat Biotechnol*. 2008;26(12):1367-1372. doi:10.1038/nbt.1511

211. Tyanova S, Temu T, Sinitcyn P, et al. The Perseus computational platform for comprehensive analysis of (prote)omics data. *Nat Methods*. 2016;13(9):731-740. doi:10.1038/nmeth.3901

212. Tan Y, Kagan JC. Biochemical isolation of the myddosome from murine macrophages. In: *Methods in Molecular Biology*. Vol 1714. Humana Press Inc.; 2018:79-95. doi:10.1007/978-1-4939-7519-8_6

Appendix

App. Tab. 1: Proteins identified in MyD88-IP exclusively after 15-min of IL-1β stimulation. Proteins were included with a false discovery rate (FDR) of the peptide spectral matches (PSMs), protein, and site of 1% based on Andromeda score.

Gene name	Protein name
Abcc1	Multidrug resistance-associated protein 1
C1qbp	Complement component 1 Q subcomponent-binding protein, mitochondrial
Lsm2	U6 snRNA-associated Sm-like protein LSm2
Banf1	Barrier-to-autointegration factor; Barrier-to-autointegration factor, N-terminally processed
Eef1b	Elongation factor 1-beta
Klc1	Kinesin light chain 1
Pde8a	High affinity cAMP-specific and IBMX-insensitive 3,5-cyclic phosphodiesterase 8A
Myl1; Myl3	Myosin light chain 1/3, skeletal muscle isoform; Myosin light chain 3
Abcb1b; Abcb1a	Multidrug resistance protein 1B; Multidrug resistance protein 1A
Il1b	Interleukin-1 beta
Srgn	Serglycin
Rps6ka1	Ribosomal protein S6 kinase alpha-1
Nefh	Neurofilament heavy polypeptide
Ranbp1	Ran-specific GTPase-activating protein
Nr2f2; Nr2f1	COUP transcription factor 2; COUP transcription factor 1
Rab11a; Rab11b	Ras-related protein Rab-11A; Ras-related protein Rab-11B
Tbc1d10a	TBC1 domain family member 10A
Pafah1b1	Platelet-activating factor acetylhydrolase IB subunit alpha
Tuba1c	Tubulin alpha-1C chain
Hist1h3a	Histone H3.1
Irf3	Interferon regulatory factor 3
Smad4	Mothers against decapentaplegic homolog 4
Ccdc69	Coiled-coil domain-containing protein 69
Tfb2m	Dimethyladenosine transferase 2, mitochondrial
Uevld	Ubiquitin-conjugating enzyme E2 variant 3
Zyg11b	Protein zyg-11 homolog B
Eif3j1; Eif3j2	Eukaryotic translation initiation factor 3 subunit J-A;Eukaryotic translation initiation factor 3 subunit J-B
Agap2	Arf-GAP with GTPase, ANK repeat and PH domain-containing protein 2
Ppp1r12c	Protein phosphatase 1 regulatory subunit 12C
Usp30	Ubiquitin carboxyl-terminal hydrolase 30
Eef2kmt	Protein-lysine N-methyltransferase EEF2KMT
IRAK1	Interleukin-1 receptor-associated kinase 1
Isg15	Ubiquitin-like protein ISG15
Ptprj	Receptor-type tyrosine-protein phosphatase eta
Sec23ip	SEC23-interacting protein
Rab35	Ras-related protein Rab-35
Ccdc88c	Protein Daple
Wdr90	WD repeat-containing protein 90

Sipa1l2	Signal-induced proliferation-associated 1-like protein 2
Erbb2ip	Protein LAP2
Ube3c	Ubiquitin-protein ligase E3C
Sap130	Histone deacetylase complex subunit SAP130
Eea1	Early endosome antigen 1
Jakmip1	Janus kinase and microtubule-interacting protein 1
Obfc1	CST complex subunit STN1
Vrk3	Inactive serine/threonine-protein kinase VRK3
Alms1	Alstrom syndrome protein 1 homolog
Aagab	Alpha- and gamma-adaptin-binding protein p34
Sh3kbp1	SH3 domain-containing kinase-binding protein 1
Ssx2ip	Afadin- and alpha-actinin-binding protein
Gpn1	GPN-loop GTPase 1
Acsf2	Acyl-CoA synthetase family member 2, mitochondrial
Agap3	Arf-GAP with GTPase, ANK repeat and PH domain-containing protein 3
Tnfaip8	Tumor necrosis factor alpha-induced protein 8
Triobp	TRIO and F-actin-binding protein
Etfa	Electron transfer flavoprotein subunit alpha, mitochondrial
Yeats4	YEATS domain-containing protein 4
Tmed5	Transmembrane emp24 domain-containing protein 5
Dlst	Dihydrolipoyllysine-residue succinyltransferase component of 2-oxoglutarate dehydrogenase complex, mitochondrial
Fam45a	Protein FAM45A
Atr	Serine/threonine-protein kinase ATR
Hip1r	Huntingtin-interacting protein 1-related protein
Jmy	Junction-mediating and -regulatory protein
Actr10	Actin-related protein 10
Tnip1	TNFAIP3-interacting protein 1
Sucla2	Succinyl-CoA ligase [ADP-forming] subunit beta, mitochondrial

App. Tab. 2: Proteins identified in MyD88-IP exclusively after 30-min of IL-1β stimulation. Proteins were included with a FDR of the PSMs, protein, and site of 1% based on Andromeda score.

Gene name	Protein name
Zmym4	Zinc finger MYM-type protein 4
Chd5	Chromodomain-helicase-DNA-binding protein 5
Xpnpep3	Probable Xaa-Pro aminopeptidase 3
Krt10	Keratin, type I cytoskeletal 10
Dtnb	Dystrobrevin beta
Tom1	Target of Myb protein 1
Grap2	GRB2-related adaptor protein 2
Dhfr	Dihydrofolate reductase
Srp54	Signal recognition particle 54 kDa protein
Chd1	Chromodomain-helicase-DNA-binding protein 1
Cux1	Homeobox protein cut-like 1
Mpp1	55 kDa erythrocyte membrane protein
Aup1	Ancient ubiquitous protein 1
Erf	ETS domain-containing transcription factor ERF

Ikzf2	Zinc finger protein Helios
Mcl1	Induced myeloid leukemia cell differentiation protein Mcl-1 homolog
Ly9	T-lymphocyte surface antigen Ly-9
Cbfb	Core-binding factor subunit beta
Pag1	Phosphoprotein associated with glycosphingolipid-enriched microdomains 1
Fam117b	Protein FAM117B
Wdr62	WD repeat-containing protein 62
Tax1bp1	Tax1-binding protein 1 homolog
Hdgfrp2	Hepatoma-derived growth factor-related protein 2
Grb2	Growth factor receptor-bound protein 2
Psmb6	Proteasome subunit beta type-6
Map4k2	Mitogen-activated protein kinase kinase kinase kinase 2
Apc	Adenomatous polyposis coli protein
Irak1	Interleukin-1 receptor-associated kinase 1
Zyx	Zyxin
Wapal	Wings apart-like protein homolog
Gpalpp1	GPALPP motifs-containing protein 1
Myof	Myoferlin
Herc4	Probable E3 ubiquitin-protein ligase HERC4
Dync1li2	Cytoplasmic dynein 1 light intermediate chain 2
Picalm	Phosphatidylinositol-binding clathrin assembly protein
Huwe1	E3 ubiquitin-protein ligase HUWE1
Med23	Mediator of RNA polymerase II transcription subunit 23
Htatsf1	HIV Tat-specific factor 1 homolog
Vps13c	Vacuolar protein sorting-associated protein 13C
Tbc1d4	TBC1 domain family member 4
Tlk1	Serine/threonine-protein kinase tousled-like 1
Ikzf4	Zinc finger protein Eos
Ahctf1	Protein ELYS
Kctd5	BTB/POZ domain-containing protein KCTD5
Sfxn3	Sideroflexin-3
Pqbp1	Polyglutamine-binding protein 1
Cers2	Ceramide synthase 2
St13	Hsc70-interacting protein
Hgs	Hepatocyte growth factor-regulated tyrosine kinase substrate
Cdk5rap3	CDK5 regulatory subunit-associated protein 3
Nasp	Nuclear autoantigenic sperm protein
Vimp	Selenoprotein S
Gadd45gip1	Growth arrest and DNA damage-inducible proteins-interacting protein 1
Nup37	Nucleoporin Nup37
Rgs19	Regulator of G-protein signaling 19
Ndc80	Kinetochore protein NDC80 homolog
Pus10	Putative tRNA pseudouridine synthase Pus10
Rpap3	RNA polymerase II-associated protein 3
Srp19	Signal recognition particle 19 kDa protein

Prkar1a	cAMP-dependent protein kinase type I-alpha regulatory subunit; cAMP-dependent protein kinase type I-alpha regulatory subunit, N-terminally processed
Cyb5r3	NADH-cytochrome b5 reductase 3; NADH-cytochrome b5 reductase 3 membrane-bound form; NADH-cytochrome b5 reductase 3 soluble form
Adrm1	Proteasomal ubiquitin receptor ADRM1
Fmnl1	Formin-like protein 1
Stub1	STIP1 homology and U box-containing protein 1
Tnip1	TNFAIP3-interacting protein 1
Hdac6	Histone deacetylase 6

App. Table 3: Proteins identified in MyD88-IP exclusively after 60-min of IL-1β stimulation. Proteins were included with a FDR of the PSMs, protein, and site of 1% based on Andromeda score.

Gene name	Protein name
Bin2	Bridging integrator 2
Parp4	
Capn2	Calpain-2 catalytic subunit
Dld	Dihydrolipoyl dehydrogenase, mitochondrial
Nfil3	Nuclear factor interleukin-3-regulated protein
Eef2k	Eukaryotic elongation factor 2 kinase
Snap23	Synaptosomal-associated protein 23
Map2k3	Dual specificity mitogen-activated protein kinase kinase 3
Slc6a6	Sodium- and chloride-dependent taurine transporter
Abcc1	Multidrug resistance-associated protein 1
Psmd14	26S proteasome non-ATPase regulatory subunit 14
Scamp3	Secretory carrier-associated membrane protein 3
Pold2	DNA polymerase delta subunit 2
Syt3	Synaptotagmin-3
Sptlc1	Serine palmitoyltransferase 1
Calu	Calumenin
Reps1	RalBP1-associated Eps domain-containing protein 1
Lat	Linker for activation of T-cells family member 1
Banf1	Barrier-to-autointegration factor; Barrier-to-autointegration factor, N-terminally processed
Asna1	ATPase Asna1
Ilk	Integrin-linked protein kinase
Eef1b	Elongation factor 1-beta
Epb41l2	Band 4.1-like protein 2
Psma3	Proteasome subunit alpha type-3
Smpd2	Sphingomyelin phosphodiesterase 2
Pfdn2	Prefoldin subunit 2
Klc1	Kinesin light chain 1
Dync1i2	Cytoplasmic dynein 1 intermediate chain 2
Ikbkg	NF-kappa-B essential modulator
Cops4	COP9 signalosome complex subunit 4
Lamtor3	Ragulator complex protein LAMTOR3
Stk16	Serine/threonine-protein kinase 16
Tom1	Target of Myb protein 1
Tp63	Tumor protein 63

Gcat	2-amino-3-ketobutyrate coenzyme A ligase, mitochondrial
Cope	Coatomer subunit epsilon
Grap2	GRB2-related adaptor protein 2
Abl1	Tyrosine-protein kinase ABL1
Hba	Hemoglobin subunit alpha
Prnp	Major prion protein
Prkaca	cAMP-dependent protein kinase catalytic subunit alpha
Abcb1b; Abcb1a	Multidrug resistance protein 1B; Multidrug resistance protein 1A
Aprt	Adenine phosphoribosyltransferase
Rras; Rras2	Ras-related protein R-Ras;Ras-related protein R-Ras2
Itgb2	Integrin beta-2
Itpr1	Inositol 1,4,5-trisphosphate receptor type 1
H2-Q7; H2-Q9;H2-Q8	H-2 class I histocompatibility antigen, Q7 alpha chain; H-2 class I histocompatibility antigen, Q9 alpha chain;H-2 class I histocompatibility antigen, Q8 alpha chain
Glul	Glutamine synthetase
Atp6v0a2	V-type proton ATPase 116 kDa subunit an isoform 2
Lgals1	Galectin-1
Mthfd2	Bifunctional methylenetetrahydrofolate dehydrogenase/cyclohydrolase, mitochondrial; NAD-dependent methylenetetrahydrofolate dehydrogenase; Methenyltetrahydrofolate cyclohydrolase
Prkca	Protein kinase C alpha type
Cd3e	T-cell surface glycoprotein CD3 epsilon chain
Irf2	Interferon regulatory factor 2
Glud1	Glutamate dehydrogenase 1, mitochondrial
Gna13	Guanine nucleotide-binding protein subunit alpha-13
Xrcc5	X-ray repair cross-complementing protein 5
Cebpb	CCAAT/enhancer-binding protein beta
Adh5	Alcohol dehydrogenase class-3
Marcksl1	MARCKS-related protein
Casp1	Caspase-1; Caspase-1 subunit p20;Caspase-1 subunit p10
Map2k1	Dual specificity mitogen-activated protein kinase kinase 1
Ptpn11	Tyrosine-protein phosphatase non-receptor type 11
Rab6a; Rab6b; Rab39a	Ras-related protein Rab-6A; Ras-related protein Rab-6B; Ras-related protein Rab-39A
Ttk	Dual specificity protein kinase TTK
Ptpn12	Tyrosine-protein phosphatase non-receptor type 12
Por	NADPH--cytochrome P450 reductase
Stat1	Signal transducer and activator of transcription 1
Eps15	Epidermal growth factor receptor substrate 15
Vps4b	Vacuolar protein sorting-associated protein 4B
Aldh3a2	Fatty aldehyde dehydrogenase
Gsr	Glutathione reductase, mitochondrial
Hcls1	Hematopoietic lineage cell-specific protein
Psma2	Proteasome subunit alpha type-2
Impdh1	Inosine-5-monophosphate dehydrogenase 1
Bckdha	2-oxoisovalerate dehydrogenase subunit alpha, mitochondrial
Atp6v1a	V-type proton ATPase catalytic subunit A
Aff3	AF4/FMR2 family member 3
Adcy7	Adenylate cyclase type 7
Atp6v0d1	V-type proton ATPase subunit d 1

Slc1a5	Neutral amino acid transporter B(0)
Ccna2	Cyclin-A2
Fgd1	FYVE, RhoGEF and PH domain-containing protein 1
Cebpg	CCAAT/enhancer-binding protein gamma
Stom	Erythrocyte band 7 integral membrane protein
Atp6v1d	V-type proton ATPase subunit D
Ppp2r4	Serine/threonine-protein phosphatase 2A activator
Foxp1	Forkhead box protein P1
Ctdsp1; Ctdspl	Carboxy-terminal domain RNA polymerase II polypeptide A small phosphatase 1; CTD small phosphatase-like protein
Rab2b	Ras-related protein Rab-2B
Lman2l	VIP36-like protein
Pcmtd1	Protein-L-isoaspartate O-methyltransferase domain-containing protein 1
Rab10	Ras-related protein Rab-10
Cops2	COP9 signalosome complex subunit 2
Tbpl1	TATA box-binding protein-like protein 1
Tceb2	Transcription elongation factor B polypeptide 2
Pafah1b1	Platelet-activating factor acetylhydrolase IB subunit alpha
Gng2	Guanine nucleotide-binding protein G(I)/G(S)/G(O) subunit gamma-2
Tuba1c	Tubulin alpha-1C chain
Stx4	Syntaxin-4
Erf	ETS domain-containing transcription factor ERF
Gaa	Lysosomal alpha-glucosidase
Ikzf2	Zinc finger protein Helios
Rhog	Rho-related GTP-binding protein RhoG
Mcl1	Induced myeloid leukemia cell differentiation protein Mcl-1 homolog
Prkdc	DNA-dependent protein kinase catalytic subunit
Smarcad1	SWI/SNF-related matrix-associated actin-dependent regulator of chromatin subfamily A containing DEAD/H box 1
Anxa7	Annexin A7
Cbfb	Core-binding factor subunit beta
Slc7a1	High affinity cationic amino acid transporter 1
Npepps	Puromycin-sensitive aminopeptidase
Ppp1r21	Protein phosphatase 1 regulatory subunit 21
Pde12	2,5-phosphodiesterase 12
Exoc5	Exocyst complex component 5
Mpnd	MPN domain-containing protein
Tmem55b	Type 1 phosphatidylinositol 4,5-bisphosphate 4-phosphatase
Tbc1d2b	TBC1 domain family member 2B
Gpsm3	G-protein-signaling modulator 3
Gse1	Genetic suppressor element 1
Wdr62	WD repeat-containing protein 62
Rreb1	Ras-responsive element-binding protein 1
Ppp1r7	Protein phosphatase 1 regulatory subunit 7
Eml4	Echinoderm microtubule-associated protein-like 4
Tbc1d24	TBC1 domain family member 24
Tmem237	Transmembrane protein 237
Ccdc88b	Coiled-coil domain-containing protein 88B

Snx33	Sorting nexin-33
Ankrd28	Serine/threonine-protein phosphatase 6 regulatory ankyrin repeat subunit A
Kansl1l	KAT8 regulatory NSL complex subunit 1-like protein
Rnf20	E3 ubiquitin-protein ligase BRE1A
Tom1l2	TOM1-like protein 2
Atp13a3	Probable cation-transporting ATPase 13A3
Grb2	Growth factor receptor-bound protein 2
Lrmp	Lymphoid-restricted membrane protein;Processed lymphoid-restricted membrane protein
Ppp5c	Serine/threonine-protein phosphatase 5
P4ha1	Prolyl 4-hydroxylase subunit alpha-1
Slc30a1	Zinc transporter 1
Tnfaip3	Tumor necrosis factor alpha-induced protein 3
Dvl2	Segment polarity protein dishevelled homolog DVL-2
Sla	Src-like-adapter
Fadd	FAS-associated death domain protein
Map4k2	Mitogen-activated protein kinase kinase kinase kinase 2
Slc9a1	Sodium/hydrogen exchanger 1
Arg1	Arginase-1
Pafah1b2	Platelet-activating factor acetylhydrolase IB subunit beta
Zfhx3	Zinc finger homeobox protein 3
Pde3b	cGMP-inhibited 3,5-cyclic phosphodiesterase B
Ddx19a	ATP-dependent RNA helicase DDX19A
Atrx	Transcriptional regulator ATRX
IRAK1	Interleukin-1 receptor-associated kinase 1
Zyx	Zyxin
Actr3b	Actin-related protein 3B
Isg15	Ubiquitin-like protein ISG15
Vcl	Vinculin
Galk2	N-acetylgalactosamine kinase
Wls	Protein wntless homolog
Lemd2	LEM domain-containing protein 2
Mvb12b	Multivesicular body subunit 12B
Rcbtb1	RCC1 and BTB domain-containing protein 1
Rbfa	Putative ribosome-binding factor A, mitochondrial
Slc39a10	Zinc transporter ZIP10
Snx6	Sorting nexin-6; Sorting nexin-6, N-terminally processed
Herc4	Probable E3 ubiquitin-protein ligase HERC4
Kdm3a	Lysine-specific demethylase 3A
Pigs	GPI transamidase component PIG-S
Ubtd2	Ubiquitin domain-containing protein 2
Ankib1	Ankyrin repeat and IBR domain-containing protein 1
Picalm	Phosphatidylinositol-binding clathrin assembly protein
Cyfip1	Cytoplasmic FMR1-interacting protein 1
Fuk	
Spag5	Sperm-associated antigen 5
Huwe1	E3 ubiquitin-protein ligase HUWE1
Fbxo5	F-box only protein 5
Rpap1	RNA polymerase II-associated protein 1
Rab3gap1	Rab3 GTPase-activating protein catalytic subunit

Ints2	Integrator complex subunit 2
Cpm	Carboxypeptidase M
Lrrc1	Leucine-rich repeat-containing protein 1
Acad11	Acyl-CoA dehydrogenase family member 11
Afap1	Actin filament-associated protein 1
Klhl42	Kelch-like protein 42
Lpp	Lipoma-preferred partner homolog
Fbxo46	F-box only protein 46
Ttc7a	Tetratricopeptide repeat protein 7A
Cdc23	Cell division cycle protein 23 homolog
Sephs1	Selenide, water dikinase 1
Ano10	Anoctamin-10
Elovl5	Elongation of very long chain fatty acids protein 5
Ganab	Neutral alpha-glucosidase AB
Prune	Protein prune homolog
Cox15	Cytochrome c oxidase assembly protein COX15 homolog
Hmbox1	Homeobox-containing protein 1
Fbxo30	F-box only protein 30
Eea1	Early endosome antigen 1
Rab3gap2	Rab3 GTPase-activating protein non-catalytic subunit
Acp6	Lysophosphatidic acid phosphatase type 6
Rcn2	Reticulocalbin-2
Cc2d1b	Coiled-coil and C2 domain-containing protein 1B
Klhl7	Kelch-like protein 7
Jakmip1	Janus kinase and microtubule-interacting protein 1
Rspry1	RING finger and SPRY domain-containing protein 1
Pithd1	PITH domain-containing protein 1
Kiaa1524	Protein CIP2A
Taok3	Serine/threonine-protein kinase TAO3
Tbc1d17	TBC1 domain family member 17
Chd9	Chromodomain-helicase-DNA-binding protein 9
Arap2	Arf-GAP with Rho-GAP domain, ANK repeat and PH domain-containing protein 2
Srek1	Splicing regulatory glutamine/lysine-rich protein 1
Vps26b	Vacuolar protein sorting-associated protein 26B
Asrgl1	Isoaspartyl peptidase/L-asparaginase; Isoaspartyl peptidase/L-asparaginase alpha chain; Isoaspartyl peptidase/L-asparaginase beta chain
Slc39a6	Zinc transporter ZIP6
Thop1	Thimet oligopeptidase
Brat1	BRCA1-associated ATM activator 1
Kntc1	Kinetochore-associated protein 1
Eri3	ERI1 exoribonuclease 3
Nelfb	Negative elongation factor B
Fam126b	Protein FAM126B
Parp9	Poly [ADP-ribose] polymerase 9
Abi1	Abl interactor 1
Ufl1	E3 UFM1-protein ligase 1
Pars2	Probable proline--tRNA ligase, mitochondrial
Mboat7	Lysophospholipid acyltransferase 7
Fbxl8	F-box/LRR-repeat protein 8

Lrrc45	Leucine-rich repeat-containing protein 45
Ints4	Integrator complex subunit 4
Mical3	Protein-methionine sulfoxide oxidase MICAL3
Acad9	Acyl-CoA dehydrogenase family member 9, mitochondrial
Tldc1	TLD domain-containing protein 1
Dcun1d3	DCN1-like protein 3
Stx5	Syntaxin-5
Nek9	Serine/threonine-protein kinase Nek9
Prkd3	Serine/threonine-protein kinase D3
Otud6b	OTU domain-containing protein 6B
Kiaa1598	Shootin-1
Nmral1	NmrA-like family domain-containing protein 1
Obfc1	CST complex subunit STN1
Champ1	Chromosome alignment-maintaining phosphoprotein 1
Inpp5b	Type II inositol 1,4,5-trisphosphate 5-phosphatase
Ero1l	ERO1-like protein alpha
Mtss1	Metastasis suppressor protein 1
Zc3h10	Zinc finger CCCH domain-containing protein 10
Ap3m2	AP-3 complex subunit mu-2
Ptrh2	Peptidyl-tRNA hydrolase 2, mitochondrial
Cdc16	Cell division cycle protein 16 homolog
Irak4	Interleukin-1 receptor-associated kinase 4
Top1mt	DNA topoisomerase I, mitochondrial
Fgg	Fibrinogen gamma chain
Acsf2	Acyl-CoA synthetase family member 2, mitochondrial
Sec63	Translocation protein SEC63 homolog
Tram1	Translocating chain-associated membrane protein 1
Pqbp1	Polyglutamine-binding protein 1
Ubtd1	Ubiquitin domain-containing protein 1
Fubp1	Far upstream element-binding protein 1
Erlin1	Erlin-1
Uxs1	UDP-glucuronic acid decarboxylase 1
Atl3	Atlastin-3
Dera	Deoxyribose-phosphate aldolase
B3galt6	Beta-1,3-galactosyltransferase 6
Bmp2k	BMP-2-inducible protein kinase
Cryzl1	Quinone oxidoreductase-like protein 1
Ssfa2	Sperm-specific antigen 2 homolog
Nrif1	Neurotrophin receptor-interacting factor 1
Cic	Protein capicua homolog
Mta3	Metastasis-associated protein MTA3
Mpst	3-mercaptopyruvate sulfurtransferase
Arfgap2	ADP-ribosylation factor GTPase-activating protein 2
Rragc; Rragd	Ras-related GTP-binding protein C;Ras-related GTP-binding protein D
Tmed9	Transmembrane emp24 domain-containing protein 9
Mat2b	Methionine adenosyltransferase 2 subunit beta
Eif2b2	Translation initiation factor eIF-2B subunit beta
Park7	Protein deglycase DJ-1
Cdca3	Cell division cycle-associated protein 3
Nasp	Nuclear autoantigenic sperm protein

Pccb	Propionyl-CoA carboxylase beta chain, mitochondrial
Nuf2	Kinetochore protein Nuf2
Trim34a	Tripartite motif-containing protein 34A
Bcl11b	B-cell lymphoma/leukemia 11B
Glod4	Glyoxalase domain-containing protein 4
Myl9	Myosin regulatory light polypeptide 9
Lamtor1	Ragulator complex protein LAMTOR1
Nudcd2	NudC domain-containing protein 2
Rpa3	Replication protein A 14 kDa subunit
Leprotl1	Leptin receptor overlapping transcript-like 1
Cotl1	Coactosin-like protein
Ndufb9	NADH dehydrogenase [ubiquinone] 1 beta subcomplex subunit 9
Glrx3	Glutaredoxin-3
Ppp6c	Serine/threonine-protein phosphatase 6 catalytic subunit; Serine/threonine-protein phosphatase 6 catalytic subunit, N-terminally processed
Ykt6	Synaptobrevin homolog YKT6
Psmd9	26S proteasome non-ATPase regulatory subunit 9
Golph3	Golgi phosphoprotein 3
Dis3	Exosome complex exonuclease RRP44
Raver1	Ribonucleoprotein PTB-binding 1
Cnot11	CCR4-NOT transcription complex subunit 11
Sugt1	Suppressor of G2 allele of SKP1 homolog
Gemin6	Gem-associated protein 6
Rgs19	Regulator of G-protein signaling 19
Pmpcb	Mitochondrial-processing peptidase subunit beta
Tecr	Very-long-chain enoyl-CoA reductase
Ssbp1	Single-stranded DNA-binding protein, mitochondrial
Polr3e	DNA-directed RNA polymerase III subunit RPC5
Spc24	Kinetochore protein Spc24
Lman1	Protein ERGIC-53
Nkap;Nkapl	NF-kappa-B-activating protein
Chaf1b	Chromatin assembly factor 1 subunit B
Sec13	Protein SEC13 homolog
Bcas2	Pre-mRNA-splicing factor SPF27
Stx11	Syntaxin-11
Pus10	Putative tRNA pseudouridine synthase Pus10
Polr3c	DNA-directed RNA polymerase III subunit RPC3
Tubgcp4	Gamma-tubulin complex component 4
Exoc2	Exocyst complex component 2
Amotl1	Angiomotin-like protein 1
Cul2	Cullin-2
Drap1	Dr1-associated corepressor
Idh3a	Isocitrate dehydrogenase [NAD] subunit alpha, mitochondrial
Dnase1l1	Deoxyribonuclease-1-like 1
Hm13	Minor histocompatibility antigen H13
Prkar1a	cAMP-dependent protein kinase type I-alpha regulatory subunit; cAMP-dependent protein kinase type I-alpha regulatory subunit, N-terminally processed
Cmpk1	UMP-CMP kinase
Tmem43	Transmembrane protein 43

Hmg20a	High mobility group protein 20A
Mlst8	Target of rapamycin complex subunit LST8
Ethe1	Persulfide dioxygenase ETHE1, mitochondrial
Fancg	Fanconi anemia group G protein homolog
Cars	Cysteine-tRNA ligase, cytoplasmic
Xpo4	Exportin-4
Psmg2	Proteasome assembly chaperone 2
Zcchc17	Nucleolar protein of 40 kDa
Tm9sf3	Transmembrane 9 superfamily member 3
Stk4	Serine/threonine-protein kinase 4; Serine/threonine-protein kinase 4 37kDa subunit;Serine/threonine-protein kinase 4 18kDa subunit
Ralb	Ras-related protein Ral-B
Sh3bgrl	SH3 domain-binding glutamic acid-rich-like protein
Tuba8	Tubulin alpha-8 chain
Gnpnat1	Glucosamine 6-phosphate N-acetyltransferase
Kcnq5	Potassium voltage-gated channel subfamily KQT member 5
Mlh1	DNA mismatch repair protein Mlh1
Hyou1	Hypoxia up-regulated protein 1
Adrm1	Proteasomal ubiquitin receptor ADRM1
Rqcd1	Cell differentiation protein RCD1 homolog
Isg20	Interferon-stimulated gene 20 kDa protein
Aldh9a1	4-trimethylaminobutyraldehyde dehydrogenase
Arl6ip4	ADP-ribosylation factor-like protein 6-interacting protein 4
Usp14	Ubiquitin carboxyl-terminal hydrolase 14
Drg2	Developmentally-regulated GTP-binding protein 2
Copg2	Coatomer subunit gamma-2
Jmy	Junction-mediating and -regulatory protein
Mkrn1	E3 ubiquitin-protein ligase makorin-1
Rdh11	Retinol dehydrogenase 11
Tollip	Toll-interacting protein
Atp11c	Phospholipid-transporting ATPase 11C
Nubp1	Cytosolic Fe-S cluster assembly factor NUBP1
Nubp2	Cytosolic Fe-S cluster assembly factor NUBP2
Vav3	Guanine nucleotide exchange factor VAV3
Sec11a	Signal peptidase complex catalytic subunit SEC11A
Tmed2	Transmembrane emp24 domain-containing protein 2
Nsdhl	Sterol-4-alpha-carboxylate 3-dehydrogenase, decarboxylating
Atp6ap1	V-type proton ATPase subunit S1
6-Sep	Septin-6
Timeless	Protein timeless homolog
Tapbp	Tapasin
Trpv2	Transient receptor potential cation channel subfamily V member 2
Skp1	S-phase kinase-associated protein 1
Pus1	tRNA pseudouridine synthase A, mitochondrial
Stub1	STIP1 homology and U box-containing protein 1
Arl3	ADP-ribosylation factor-like protein 3
Uchl5	Ubiquitin carboxyl-terminal hydrolase isozyme L5
Tnip1	TNFAIP3-interacting protein 1
Xpr1	Xenotropic and polytropic retrovirus receptor 1
Slc7a5	Large neutral amino acids transporter small subunit 1
Uba2	SUMO-activating enzyme subunit 2

Atp6v1c1	V-type proton ATPase subunit C 1
Bag6	Large proline-rich protein BAG6
Mbd1	Methyl-CpG-binding domain protein 1
Sucla2	Succinyl-CoA ligase [ADP-forming] subunit beta, mitochondrial
Hdac6	Histone deacetylase 6

App. Table 4: Proteins identified in IRAK4-IP exclusively after 15-min of IL-1β stimulation. Proteins were included with a FDR of the PSMs, protein, and site of 1% based on Andromeda score.

Gene name	Protein name
Pusl1	tRNA pseudouridine synthase-like 1
Ptpro	Receptor-type tyrosine-protein phosphatase O
Bsg	Basigin
Ccna2	Cyclin-A2
Vbp1	Prefoldin subunit 3
Sycp1	Synaptonemal complex protein 1
IRAK1	Interleukin-1 receptor-associated kinase 1
Dcaf5	DDB1- and CUL4-associated factor 5
Ifitm2	Interferon-induced transmembrane protein 2
Lin37	Protein lin-37 homolog
Cyb5r3	NADH-cytochrome b5 reductase 3; NADH-cytochrome b5 reductase 3 membrane-bound form;NADH-cytochrome b5 reductase 3 soluble form
Osbpl5	Oxysterol-binding protein-related protein 5
Tnip1	TNFAIP3-interacting protein 1
Abhd16a; Abhd16b	Abhydrolase domain-containing protein 16A; Abhydrolase domain-containing protein 16B

App. Tab. 5: Proteins identified in IRAK4-IP exclusively after 30-min of IL-1β stimulation. Proteins were included with a FDR of the PSMs, protein, and site of 1% based on Andromeda score.

Gene name	Protein name
Pusl1	tRNA pseudouridine synthase-like 1
Bsg	Basigin
Ccna2	Cyclin-A2
Vbp1	Prefoldin subunit 3
IRAK1	Interleukin-1 receptor-associated kinase 1
Dcaf5	DDB1- and CUL4-associated factor 5
Med19	Mediator of RNA polymerase II transcription subunit 19
Ifitm2	Interferon-induced transmembrane protein 2
Osbpl5	Oxysterol-binding protein-related protein 5
Tnip1	TNFAIP3-interacting protein 1

App. Tab. 6: Proteins identified in IRAK4-IP exclusively after 60-min of IL-1β stimulation. Proteins were included with a FDR of the PSMs, protein, and site of 1% based on Andromeda score.

Gene name	Protein name
Gls	Glutaminase kidney isoform, mitochondrial
Chd2	Chromodomain-helicase-DNA-binding protein 2
Dld	Dihydrolipoyl dehydrogenase, mitochondrial
Pdia4	Protein disulfide-isomerase A4
Anxa1	Annexin A1

Txn	Thioredoxin
Rrm2	Ribonucleoside-diphosphate reductase subunit M2
Krt8	Keratin, type II cytoskeletal 8
Glul	Glutamine synthetase
Prdx3	Thioredoxin-dependent peroxide reductase, mitochondrial
Myd88	Myeloid differentiation primary response protein MyD88
Pcmt1	Protein-L-isoaspartate(D-aspartate) O-methyltransferase
Psmb8	Proteasome subunit beta type-8
Apex1	DNA-(apurinic or apyrimidinic site) lyase; DNA-(apurinic or apyrimidinic site) lyase, mitochondrial
Mif	Macrophage migration inhibitory factor
Hmgcl	Hydroxymethylglutaryl-CoA lyase, mitochondrial
Map2k4	Dual specificity mitogen-activated protein kinase kinase 4
Eif1b; Eif1	Eukaryotic translation initiation factor 1b; Eukaryotic translation initiation factor 1
Psma2	Proteasome subunit alpha type-2
Ripk2	Receptor-interacting serine/threonine-protein kinase 2
Eif5	Eukaryotic translation initiation factor 5
Adamts20	A disintegrin and metalloproteinase with thrombospondin motifs 20
Morf4l1	Mortality factor 4-like protein 1
Vbp1	Prefoldin subunit 3
Traf5	TNF receptor-associated factor 5
Serf2	Small EDRK-rich factor 2
Prdx5	Peroxiredoxin-5, mitochondrial
Sap30bp	SAP30-binding protein
Usp39	U4/U6. U5 tri-snRNP-associated protein 2
Uap1l1	UDP-N-acetylhexosamine pyrophosphorylase-like protein 1
Tbrg1	Transforming growth factor beta regulator 1
Pdap1	28 kDa heat- and acid-stable phosphoprotein
Mars2	Methionine-tRNA ligase, mitochondrial
Ccnl1	Cyclin-L1
Gpkow	G patch domain and KOW motifs-containing protein
Rnf20	E3 ubiquitin-protein ligase BRE1A
Taf3	Transcription initiation factor TFIID subunit 3
Eif1a	Eukaryotic translation initiation factor 1A
Wbp4	WW domain-binding protein 4
Abcb7	ATP-binding cassette sub-family B member 7, mitochondrial
Arhgdib	Rho GDP-dissociation inhibitor 2
Eif2b4	Translation initiation factor eIF-2B subunit delta
Irak1	Interleukin-1 receptor-associated kinase 1
Btf3	Transcription factor BTF3
Dnajc8	DnaJ homolog subfamily C member 8
Brd2	Bromodomain-containing protein 2
Ccnt2	
Nol12	Nucleolar protein 12
Iars2	Isoleucine-tRNA ligase, mitochondrial
Sec62	Translocation protein SEC62
Srek1	Splicing regulatory glutamine/lysine-rich protein 1
Fam204a	Protein FAM204A
Irak2	Interleukin-1 receptor-associated kinase-like 2
Snrnp27	U4/U6.U5 small nuclear ribonucleoprotein 27 kDa protein

Stx5	Syntaxin-5
Nek9	Serine/threonine-protein kinase Nek9
Vps37c	Vacuolar protein sorting-associated protein 37C
Tceanc2	Transcription elongation factor A N-terminal and central domain-containing protein 2
Ccdc59	Thyroid transcription factor 1-associated protein 26
Cbwd1	COBW domain-containing protein 1
Isoc1	Isochorismatase domain-containing protein 1
Memo1	Protein MEMO1
Usp3	Ubiquitin carboxyl-terminal hydrolase 3
Klhdc4	Kelch domain-containing protein 4
Gps2	
Macrod1	O-acetyl-ADP-ribose deacetylase MACROD1
Fam76a	Protein FAM76A
Mpst	3-mercaptopyruvate sulfurtransferase
Cstf1	Cleavage stimulation factor subunit 1
Zmat2	Zinc finger matrin-type protein 2
Fam32a	Protein FAM32A
Cactin	Cactin
Prps2	Ribose-phosphate pyrophosphokinase 2
Wbscr22	Probable 18S rRNA (guanine-N(7))-methyltransferase
Znf706	Zinc finger protein 706
Snrnp35	U11/U12 small nuclear ribonucleoprotein 35 kDa protein
Cul5	Cullin-5
Ccdc124	Coiled-coil domain-containing protein 124
Znf593	Zinc finger protein 593
Leng1	Leukocyte receptor cluster member 1 homolog
Pycard	Apoptosis-associated speck-like protein containing a CARD
Mvp	Major vault protein
Ing2	Inhibitor of growth protein 2
Ccnl2	Cyclin-L2
Edf1	Endothelial differentiation-related factor 1
Glrx	Glutaredoxin-1
Psma1	Proteasome subunit alpha type-1

App. Tab. 7: Proteins identified in IRAK1-IP exclusively after 15-min of IL-1β stimulation. Proteins were included with a FDR of the PSMs, protein, and site of 1% based on Andromeda score.

Gene name	Protein name
Ranbp10	Ran-binding protein 10
Ing5	Inhibitor of growth protein 5
Zw10	Centromere/kinetochore protein zw10 homolog
Fkbp3	Peptidyl-prolyl cis-trans isomerase FKBP3
Ranbp10	Ran-binding protein 10
Fmnl3	Formin-like protein 3
Crls1	Cardiolipin synthase (CMP-forming)
Slc38a2	Sodium-coupled neutral amino acid transporter 2
Ifitm2	Interferon-induced transmembrane protein 2
Rsl24d1	Probable ribosome biogenesis protein RLP24
Mynn	Myoneurin
S100a14	Protein S100-A14
Ppapdc2	Presqualene diphosphate phosphatase

Ing5	Inhibitor of growth protein 5

App. Tab. 8: Proteins identified in IRAK1-IP exclusively after 30-min of IL-1β stimulation. Proteins were included with a FDR of the PSMs, protein, and site of 1% based on Andromeda score.

Gene name	Protein name
Hal	Histidine ammonia-lyase
Tmem55b	Type 1 phosphatidylinositol 4,5-bisphosphate 4-phosphatase
	Uncharacterized protein C17orf62 homolog
Rasef	Ras and EF-hand domain-containing protein homolog
Mast2	Microtubule-associated serine/threonine-protein kinase 2
Rraga;Rragb	Ras-related GTP-binding protein A; Ras-related GTP-binding protein B
Mynn	Myoneurin
Ppapdc2	Presqualene diphosphate phosphatase
Habp4	Intracellular hyaluro1000-binding protein 4
Polk	DNA polymerase kappa

App. Table 9: Proteins identified in IRAK1-IP exclusively after 60-min of IL-1β stimulation. Proteins were included with a FDR of the PSMs, protein, and site of 1% based on Andromeda score.

Gene name	Protein name
Pcna	Proliferating cell nuclear antigen
Myd88	Myeloid differentiation primary response protein MyD88
Psmb8	Proteasome subunit beta type-8
Tax1bp1	Tax1-binding protein 1 homolog
Dixdc1	Dixin
Tnip2	TNFAIP3-interacting protein 2
Klb	Beta-klotho
Ikbke	Inhibitor of nuclear factor kappa-B kinase subunit epsilon
Tnip1	TNFAIP3-interacting protein 1

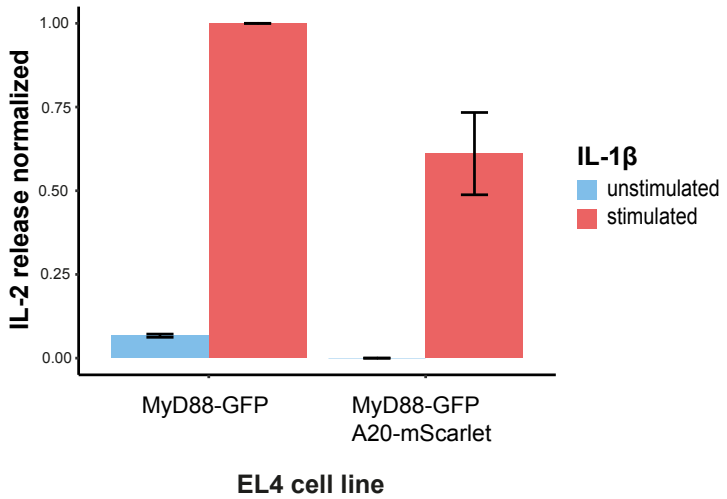

App. Fig. 1: IL-2 release of MyD88-GFP and MyD88-GFP/A20-mScarlet EL4 cells. IL-2 release was measured by ELISA after 24 h of IL-1β (10 ng/ml) stimulation. Values are shown relative to the parental MyD88-GFP cell
line. Average values were calculated from three independent experiments. Bars represent ± SEM.

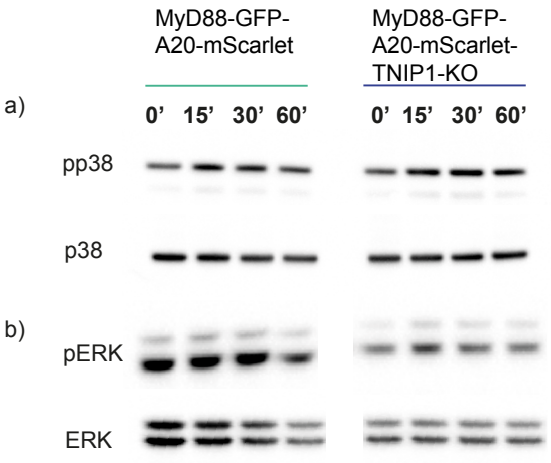

App. Fig. 2: Western blot analysis for a) phosphorylated p38 (pp38, upper panel), p38 (lower panel) and b) phosphorylated ERK (pERK, upper panel), ERK (lower panel) different gene-edited EL4 cells. MyD88-GFP/A20-mScarlet and MyD88-GFP/A20-mScarlet/TNIP1-KO EL4 cells were left untreated (0 min) or stimulated with IL-1β (10 ng/ml) for 15-, 30- and 60-min.

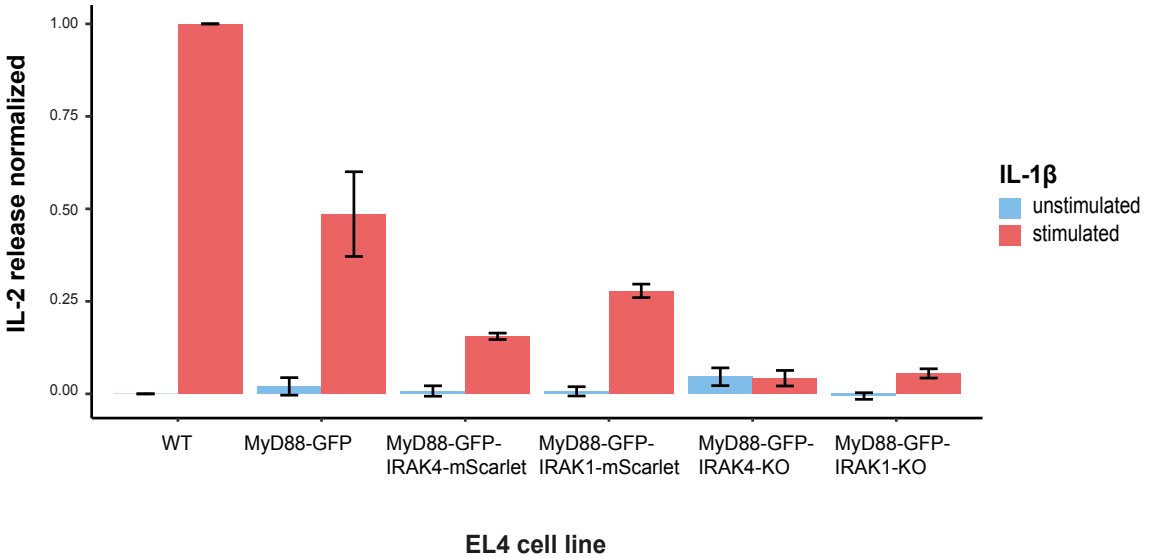

App. Fig. 3: IL-2 release of WT and endogenously tagged MyD88-GFP, MyD88-GFP/IRAK4-mScarlet, and MyD88-GFP/IRAK1-mScarlet EL4 cells. IL-2 release was measured by ELISA after 24 h of IL-1β (10 ng/ml) stimulation. Values are shown relative to the parental WT cell line. Average values were calculated from three independent experiments. Bars represent ± SEM. Results published in Deliz-Aguirre et al., 2021[122].

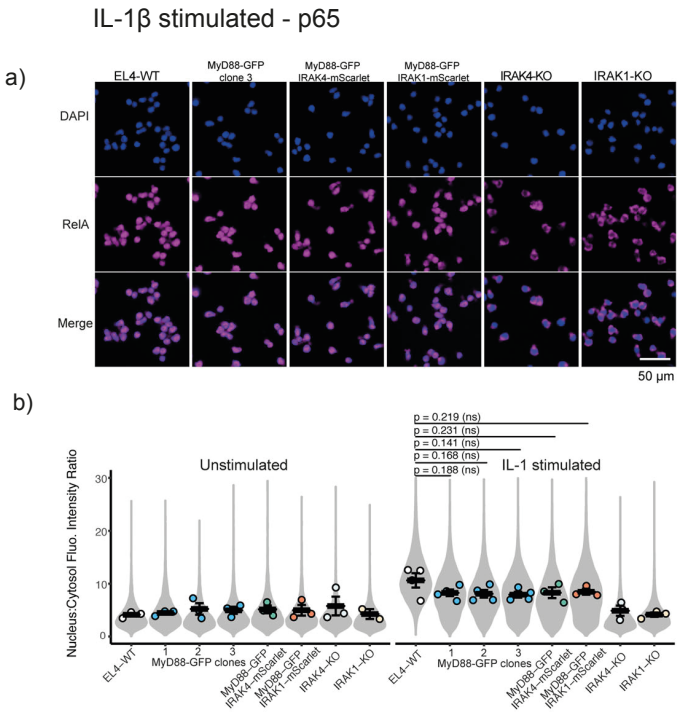

App. Fig. 4: Quantification of p65 nuclear translocation in gene-edited EL4 cells.

a) EL4 cell lines (30-min after addition to IL1β-labeled SLBs) were fixed and stained for p65 (magenta); DAPI stained nuclei (blue). Scale bar, 50 µm.

b) Quantification of p65 nucleus-to-cytoplasm staining ratio. Violin plots show the single-cell distribution p65 nucleus-to-cytoplasm staining ratio. Colored dots superimposed on violin plots correspond to the average value in the independent experiments (n = 3 or 4 experimental replicates per cell line; each replicate encompasses measurements from >2,000 cells. Bars represent mean ± SEM. P values were calculated using a two-tailed unpaired Student's t test.
(Figure and results published in Deliz-Aguirre et al., 2021[122].)

Selbstständigkeitserklärung

Hiermit erkläre ich, die Dissertation selbstständig und nur unter Verwendung der angegebenen Hilfen und Hilfsmittel angefertigt zu haben. Ich habe mich anderwärts nicht um einen Doktorgrad beworben und besitze keinen entsprechenden Doktorgrad. Ich erkläre, dass ich die Dissertation oder Teile davon nicht bereits bei einer anderen wissenschaftlichen Einrichtung eingereicht habe und dass sie dort weder angenommen noch abgelehnt wurde. Ich erkläre die Kenntnisnahme der dem Verfahren zugrunde liegenden Promotionsordnung der Lebenswissenschaftlichen Fakultät der Humboldt-Universität zu Berlin vom 5. März 2015. Weiterhin erkläre ich, dass keine Zusammenarbeit mit gewerblichen Promotionsberaterinnen/Promotionsberatern stattgefunden hat und dass die Grundsätze der Humboldt-Universität zu Berlin zur Sicherung guter wissenschaftlicher Praxis eingehalten wurden.

Berlin, September 2022

Fenja Gerpott

Acknowledgements

Completing this thesis would not have been possible with the great help and support of so many people.

Above all, thank you, Marcus, for providing the environment to grow and become an independent scientist. Your excitement about science has been truly inspiring and motivating to me. Thank you for numerous great discussions but also your patience and trust in me.

Thanks to all previous and current lab members, for your support and fun moments along the way. Namely, Fakun, you are a continuously shining star, always in a 'great' mood and willing to help – thank you. Elke and Kathrin, thank you for your assistance and teaching me so many valuable practical insights and beyond.

Thank you, Olivia, for assuming the responsibility as a co-supervisor during my last PhD year. Your support and interest in my project really kept me going.

I am deeply grateful for all your support, Christian. Thank you, not only for your patience especially when explaining statistical analytical details all over again and again, but also for experimental instructions, valuable scientific discussions, proof reading my thesis and especially for continuing support even when you were not in Berlin anymore.

Garth, thank you for reading (not only) this thesis, assisting, guiding, helping me a long this entire PhD journey with all its ups and downs and for being a true friend. You showed me how much fun biochemistry can be with 'like popcorn smelling buffers' or lab dance parties on Friday nights – I will definitely miss it and you!

Lyn and Gerben, thank you for critical reading my thesis and for always caring!

Thanks to all my friends outside the lab, which kept me going throughout this project. Thank you to numerous hours on the bike, supporting crazy running events, hours in the gym or supporting the work with 'my' refugee kids. Namely, I would like to thank Magga & Jasmin not only for being the best 'Trottel' I could have asked for, beautiful trips or eating numerous scopes of ice-cream, but especially for your unconditional support.

Last but not least, I'd like to express my gratitude for my family: my grandpa, my parents and my siblings. Too many to be all named individually, I'd like to thank my loving sister Feli for always having my back, good advice in all kind of situations and loving support not only during my PhD time.